



Virginia Commonwealth University
VCU Scholars Compass

Theses and Dissertations

Graduate School

2018

INVESTIGATING THE ROLE OF NICOTINIC ACETYLCHOLINE RECEPTORS (nAChRs) IN THE DEVELOPMENT AND MAINTENANCE OF CHEMOTHERPY-INDUCED PERIPHERAL NEUROPATHY IN MICE

Wisam B. Toma
Virginia Commonwealth University

Follow this and additional works at: <https://scholarscompass.vcu.edu/etd>



Part of the [Medical Pharmacology Commons](#)

© The Author

Downloaded from

<https://scholarscompass.vcu.edu/etd/5363>

This Dissertation is brought to you for free and open access by the Graduate School at VCU Scholars Compass. It has been accepted for inclusion in Theses and Dissertations by an authorized administrator of VCU Scholars Compass. For more information, please contact libcompass@vcu.edu.

© Wisam B. Toma

2018

All Rights Reserved

**INVESTIGATING THE ROLE OF NICOTINIC ACETYLCHOLINE RECEPTORS
(nAChRs) IN THE DEVELOPMENT AND MAINTENANCE OF CHEMOTHERPY-
INDUCED PERIPHERAL NEUROPATHY IN MICE**

**A dissertation submitted in partial fulfillment of the requirements for the degree of Doctor
of Philosophy at Virginia Commonwealth University**

By

Wisam B. Toma

Doctor of Veterinary Medicine, 2005, College of Veterinary Medicine, University of Mosul

Master of Science, 2011, College of Veterinary Medicine, University of Mosul

Director: M. Imad Damaj, Ph.D.

Professor, Department of Pharmacology and Toxicology

Virginia Commonwealth University

Richmond, Virginia

May 2018

ACKNOWLEDGEMENTS

When I arrived in the United States of America, I experienced new things, from the community, to new friends, and new methods of education. The work environment and research tools were unlike anything I had ever seen before. This period of adventure and discovery was punctuated with hard times, as well. When I learned about the troubles of my home town, I was concerned for my friends and family back home. My faith and trust in God helped me to overcome these challenges. “I can do all things through Christ who strengthens me” Philippians 4:13.

I would like to express my gratitude to my wife, Maysam. Her patience and support through the years made this possible. Maysam was with me every step of the way. Since starting my Ph.D. studies, I was blessed with two children, Princess Mariam and sweet John. I am truly lucky to have such a beautiful family by my side during my time in America. I am blessed to have a supportive extended family (parents, siblings) back home, as well. The congregation at St. Aphraim Syriac Orthodox Church at Washington, D.C made me feel welcome so far away from home. I would like to thank them for their help, support, and prayers.

It is an honor to be a part of the Damaj Lab. I learned a lot from Dr. Imad Damaj. Dr. Damaj put together a diverse lab. I enjoyed working as a member of a team in a truly collaborative environment. Without Dr. Damaj’s help, this dissertation would not be possible. More than a mentor, Dr. Damaj is a family friend. Dr. Damaj helped me and my family on a personal level. There are not words to describe the debt of gratitude I feel towards Dr. Damaj.

In addition to all of the ways that Dr. Damaj has helped me during my academic career at VCU, Dr. Damaj guided me to form a great committee: Dr. John Bigbee, Dr. Egidio Del Fabbro, Dr. Aron Lichtman, and Dr. David Gewirtz had skills in contrasting domains that complemented each other to form a strong base of knowledge for my dissertation project. Dr. Bigbee was always willing to talk with me about methods of optimizing immunohistochemistry experiments. Dr. Bigbee provided valuable feedback on my work, and most importantly, was patient with me. Dr. Del Fabbro provided unique insights on the clinical aspects of neuropathy. As a clinician, Dr. Del Fabbro's input was very useful for the development of this project, and he helped me to relate my mouse model of neuropathy back to the target population of human patients. Dr. Lichtman helped shape this project over the course of my career at VCU with thoughtful comments, ideas, and discussions. Further, Dr. Lichtman generously provided laboratory equipment that was vital to the performance of the experiments. Dr. Gewirtz' expertise in the cancer field, especially in *in vitro* studies and tumor-bearing mice, added another level of knowledge to my project. Dr. Gewirtz' thoughtful critiques and comments helped me see new angles of my research topic, which ultimately lead to comprehensive publications. Importantly, the collaboration between the Damaj Lab and the Gewirtz Lab allowed me to answer questions about if my treatments for neuropathy interfered with cancer-fighting properties of chemotherapeutics.

As I have mentioned, the Damaj Lab is an inclusive, collaborative environment that allowed me to grow as a researcher. Dr. Deniz Bagdas was the first person I met in the Damaj Lab. She trained me on many behavioral assays, experimental design, manuscript writing, statistical analysis, and critical thinking. Dr. Bagdas was like the "lab mom": always looking out for us. More than a colleague, Dr. Bagdas and her family welcomed me and my family; we have spent time together on several occasions.

My friend and colleague The Great Julie Meade was very helpful and funny, too. Julie helped me a lot in many experiments, especially optimizing immunohistochemistry and real-time PCR. Julie and I discussed articles at length and had many critical thinking discussions. As a friend to me and my family, I am very grateful for her help, support, and positivity.

I would like to thank all the other past and present lab members: Dr. Asti Jackson, Dr. Shakir AlSharari, Yasmin Alkhlaif, Rabha Younis, Bradley Neddenriep, Moriah Carper, Bryan McKiver, Faria Rahman, Abigail Parker, Tie Han, Ali Saeed, and Saunder McClain.

I would like to thank the members of Dr. Lichtman's lab, as well: Dr. Giulia Donvito, Dr. Zach Curry, Lesley Schurman, Mohammed Mustafa, Dr. Allen Owens, and Dr. Rehab Abdullah.

I worked closely with my friend Lauren Kyte to develop this project. Lauren was very helpful and kind. I am thankful for her comments, edits, scientific ideas, and performing *in vitro* experiments and *in vivo* experiments in tumor-bearing mice to complement my studies. More than collaborators, these people are close friends of mine. During my time at VCU, I have made several friends outside of my research. Dr. Sri Lakshmi Chalasani has been a close friend of my family for years.

I would like to thank our collaborators at other institutes. Dr. Ganesh Thakur and Dr. Roger Papke provided the silent agonists. I would like to express my gratitude to the Department of Pharmacology & Toxicology. The Department Chair, Dr. Dewey, and the Director of the Graduate Program, Dr. Akbarali, gave me the opportunity to pursue my graduate studies at VCU. I would like to thank my US-based funding source, the National Institutes of Health and the Massey Cancer Center. Further, I would like to thank my scholarship sponsor, The Higher Committee for

Education Development in Iraq (HCED), the Ministry of Higher Education & Scientific Research in Iraq, and the College of Veterinary Medicine at the University of Mosul.

Table of Contents

ACKNOWLEDGEMENT.....	ii
LIST OF TABLES.....	viii
LIST OF FIGURES.....	ix
LIST OF ABBREVIATIONS.....	xiii
ABSTRACT.....	xv
CHAPTER ONE.....	1
GENERAL INTRODUCTION.....	1
A-Chemotherapy-Induced Peripheral Neuropathy (CIPN).....	1
A.1 Prevalence and Symptoms of CIPN.....	1
A.2 Paclitaxel-Induced CIPN in Rodents.....	2
A.3 Potential Neurotoxicity Mechanisms of Paclitaxel.....	3
A.4 Role of Non-neuronal Cells in the Peripheral Neuropathy.....	6
A.5 CIPN Beyond Sensory Measures.....	9
B- Nicotinic Acetylcholine Receptors.....	10
B.1 Overview of Nicotinic Acetylcholine Receptors (nAChRs): Structure and Function.....	10
B.2 Nicotine and Nicotinic Receptors as Potential Targets for the Treatment of Pain.....	11
B.3 The Role of $\alpha 7$ nAChR Subtype as a Putative Target to Treat Painful Neuropathy.....	13
B.4 Intracellular Signalling Anti-inflammatory Pathway of $\alpha 7$ nAChR in Immune Cells.....	14
B.5 Pharmacological Modulation of $\alpha 7$ nAChR.....	14
C. Dissertation Aims.....	18

CHAPTER TWO.....	20
<i>Effects of Paclitaxel on the Development of Neuropathy and Affective Behaviors in the Mouse</i>	<i>20</i>
A. Introduction.....	21
B. Materials and Methods.....	22
C. Results.....	30
D. Discussion.....	45
 CHAPTER THREE.....	 53
<i>Nicotine Prevents and Reverses Paclitaxel-Induced Mechanical Allodynia in a Mouse Model of CIPN.....</i>	<i>53</i>
A. Introduction.....	54
B. Materials and Methods.....	56
C. Results.....	62
D. Discussion.....	77
 CHAPTER FOUR.....	 83
<i>The Regulatory Role of the $\alpha 7$ Nicotinic Acetylcholine Receptor (nAChR) Subtype in the Initiation and Maintenance of Paclitaxel-Induced Peripheral Neuropathy in Mice.....</i>	<i>83</i>
A. Introduction.....	84
B. Materials and Methods.....	87
C. Results.....	94
D. Discussion.....	111
 CHAPTER FIVE.....	 117
GENERAL DISCUSSION.....	117
A. Paclitaxel Induces CIPN – Overview.....	117
B. Establishment of a CIPN Model in Mice.....	118
C. Paclitaxel Induces Affective Changes in Mice.....	120
D. Nicotinic Acetylcholine Receptors as a Putative Target in CIPN.....	120
E. Future Directions.....	124
LITERATURE CITED.....	126
VITA.....	149

LIST OF TABLES

Table 1. Paclitaxel treatment does not interfere with entry into the light compartment of the light/dark box apparatus.....	41
Table 2. Summary of onset and duration of nociceptive, natural, and affective behaviors.....	45

LIST OF FIGURES

Figure 1: Proposed mechanisms of chemotherapy-induced peripheral neuropathy.....	5
Figure 2: Neuron-glia interactions in the spinal cord which lead to central sensitization.....	8
Figure 3. Proposed binding sites for multiple ligands of $\alpha 7$ nAChR.....	15
Figure 4. Paclitaxel induces nociceptive behaviors.....	31
Supplementary Figure 1. Paclitaxel has no effect on body weight and spontaneous activity in mice.....	32
Figure 5. Paclitaxel induces a reduction in intra-epidermal nerve fiber (IENF) density at 28 days post-paclitaxel injection.....	33
Figure 6. Mice are sensitized to cutaneous stimulation after second cycle of paclitaxel treatment.....	34
Supplementary Figure 2. Paclitaxel sensitizes mice to cutaneous stimulation after second cycle.....	35
Supplementary Figure 3. Carboplatin alone does not induce mechanical allodynia.....	36
Figure 7. Paclitaxel does not influence the nesting behavior of mice.....	37
Figure 8. Paclitaxel induces anxiety-like behavior in the novelty suppressed feeding assay.....	39

Figure 9. Paclitaxel induces anxiety-like behavior in the light/dark box test.....	40
Figure 10. Paclitaxel induces depression-like behavior in the forced swim test.....	42
Figure 11. Paclitaxel induces anhedonia-like behavior in the sucrose preference test.....	43
Supplementary Figure 4. Paclitaxel treatment does not interfere with total fluid intake.....	44
Figure 12. Antinociceptive and preventative effect of nicotine in a mouse model of paclitaxel-induced peripheral neuropathy.....	64
Supplemental Figure 5. Acute administration of nicotine at doses of 0.3, 0.6, and 0.9 mg/kg i.p. does not affect mechanical threshold in vehicle-treated mice.....	65
Supplemental Figure 6. Nicotine at doses of 6 and 12 mg/kg/day do not prevent paclitaxel-induced mechanical allodynia.....	65
Figure 13. The antinociceptive effect of nicotine is mediated by nicotinic acetylcholine receptors.....	66
Figure 14. Paclitaxel induces a decrease in IENF density at 35 days post-paclitaxel injection, which is prevented by nicotine administration at a dose of 24 mg/kg/day s.c.....	68
Figure 15. Nicotine fails to enhance NSCLC viable cell number under normal and serum-deprivation conditions.....	69
Supplemental Figure 7. Nicotine fails to enhance viable lung cancer cell number.....	70
Figure 16. Nicotine fails to stimulate NSCLC colony formation alone or following paclitaxel treatment.....	71

Figure 17. Nicotine fails to stimulate NSCLC cell proliferation alone or interfere with paclitaxel-induced growth inhibition of NSCLC cells.....	72
Figure 18. Nicotine fails to interfere with paclitaxel-induced apoptosis (A) and sub-G1 DNA content (B) of NSCLC cells.....	74
Supplemental Figure 8. Nicotine fails to stimulate ovarian cancer cell proliferation.....	75
Figure 19. Nicotine fails to enhance Lewis lung carcinoma tumor growth <i>in vivo</i>	76
Figure 20. The chemical structure of R-47.....	88
Figure 21. The $\alpha 7$ nAChR subtype regulates the development and maintenance of mechanical hypersensitivity.....	95
Figure 22. Paclitaxel alters the expression of Chrna7 mRNA in peripheral and spinal nervous tissues.....	96
Figure 23. Reversal and prevention of CIPN in mice.....	98
Supplemental Figure 9. Acute administration of R-47 at doses of 1, 5, and 10 mg/kg p.o. does not alter mechanical threshold in vehicle-treated mice.....	98
Figure 24. The $\alpha 7$ nAChR subtype mediates the antinociceptive effect of R-47.....	99
Figure 25. No tolerance develops following sub chronic R-47 injection.....	100
Supplementary figure 10. No motor deficits are seen following R-47 injection.....	101
Figure 26. Prevention of IENFs reduction with R-47.....	102
Figure 27. Paclitaxel alters the morphology of microglia in the dorsal horn, however, R-47 prevents the changes in microglia morphology.....	105

Figure 28. R-47 shows a CPP in mice developed neuropathy induced by paclitaxel.....	107
Supplementary Figure 11. Paclitaxel induces mechanical hypersensitivity.....	108
Figure 29. The chemical structure of paclitaxel.....	118
Figure 30. The $\alpha 7$ nAChR Plays A Regulatory Role Through Endogenous Cholinergic Anti-Inflammatory Pathway.....	122

LIST OF ABBREVIATIONS

5-HT	5-Hydroxy Tryptamine
ago-PAMs	Agonist-Allosteric Modulators
ANOVA	Analysis of Variance
ATP	Adenosine Triphosphate
AUC	Area Under the Curve
BBB	Blood Brain Barrier
BNB	Blood Nerve Barrier
CCI	Chronic Constriction Injury
CFA	Complete Freund's Adjuvant
CGRP	Calcitonin Gene Related Peptide
CIA	Collagen-Induced Arthritis
CIPN	Chemotherapy-Induced Peripheral Neuropathy
CNS	Central Nervous System
CPN	Common Peroneal Nerve
CPP	Conditioned Place Preference
DW	Distilled Water
DH	Dorsal Horn
Di	Desensitized Insensitive
DMEM	Dulbecco's Modified Eagle's Medium
DMSO	Dimethylsulfoxide
DRG	Dorsal Root Ganglia
Ds	Desensitized Sensitive
DSS	Dextran Sodium Sulfate
FBS	Fetal Bovine Serum
FST	Forced Swim Test
HO-1	Heme Oxygenase-1
i.p.	Intraperitoneally
Iba1	Ionized Calcium Binding Adaptor Molecule 1
IENFs	Intra-Epidermal Nerve Fibers
IL-1 β	Interleukin-1 β
IL-6	Interleukin-6

I κ -B	Inhibitor kappa B
Jak-2	Janus Kinase-2
KO	Knockout
LDB	Light/Dark Box
LLC	Lewis Lung Carcinoma
MCP-1	Monocyte Chemoattractant Protein-1
mGPCRs	metabotropic G-Protein Coupled Receptors (GPCRs)
MLA	Methyllycaconitine
MTS	3-(4,5-dimethylthiazol-2-yl)-5-(3-carboxymethoxyphenyl)-2-(4-sulfophenyl)-2H-tetrazolium
MTT	3-(4,5-dimethylthiazol-2-yl)-2,5-diphenylte-trazolium bromide
nAChRs	Nicotinic Acetylcholine Receptors
NF- κ B	Nuclear Factor-kappaB
NGF	Nerve Growth Factor
Nrf2	Nuclear Factor [Erythroid-Derived 2]-Like 2
NSCLC	Non-Small Cell Lung Cancer
NSF	Novelty Suppressed Feeding
OCT	Optimum Cutting Temperature
p.o.	Per Os
PAMs	Positive Allosteric Modulators
PBS	Phosphate-Buffered Saline
PGE2	Prostaglandin E2
PI	Propidium Iodide
PI3K	Phosphatidylinositol 3 Kinase
PKC	Protein Kinase C
PNS	Peripheral Nervous System
PPAR- α	Peroxisome Proliferator-Activated Receptor-alpha
PSNL	Partial Sciatic Nerve Ligation (PSNL)
qRT-PCR	Real-Time Reverse Transcription Polymerase Chain Reaction
ROS	Reactive Oxygen Species
SCI	Spinal Cord Injury
SN	Sciatic Nerve
SNC	Sciatic Nerve Constriction
SNT	Spinal Nerve Transection
SOCS3	Suppressor of Cytokine Signaling 3
STAT3	Signal Transducer and Activators of Transcription
TNF- α	Tumor Necrosis Factor- α
TNT	Tibial Nerve Transection
WT	Wildtype

ABSTRACT

INVESTIGATING THE ROLE OF NICOTINIC ACETYLCHOLINE RECEPTORS (nAChRs) IN THE DEVELOPMENT AND MAINTENANCE OF CHEMOTHERPY- INDUCED PERIPHERAL NEUROPATHY IN MICE

By Wisam B. Toma, DVM, M.Sc.

**A dissertation submitted in partial fulfillment of the requirements for the degree of
Doctor of Philosophy at Virginia Commonwealth University**

Virginia Commonwealth University, 2018

Director: M. Imad Damaj, Ph.D.

Professor, Pharmacology and Toxicology

Chemotherapy-Induced Peripheral Neuropathy (CIPN) is a major dose-limiting side effect of several anticancer drugs. The prevalence of CIPN ranges from one-third to two-thirds of cancer patients. CIPN can persist for months to years after completion of chemotherapy. Despite the efficacious use of paclitaxel in the treatment of tumors, it can induce many sensory symptoms, such as paresthesia, numbness, tingling and burning pain, and mechanical and cold allodynia, which typically are present in the hands and feet. Similar to other types of chronic pain, paclitaxel-

induced CIPN is comorbid with depression and anxiety in cancer survivors, and paclitaxel induces changes in affect-like behavior in cancer-free animal models, suggesting that paclitaxel can cause long-lasting changes in mood, reducing the quality of life. While adjuvant therapies, such as duloxetine, tricyclic antidepressants, and gabapentin are prescribed to treat CIPN symptoms, none of these compounds can consistently reverse or prevent the development of CIPN. With no FDA-approved medication to treat CIPN, the purpose of the dissertation was to: i) characterize and develop a mouse model of paclitaxel-induced CIPN, ii) identify putative targets for CIPN treatment, and iii) test novel compounds for their ability to prevent and reverse CIPN in C57BL/6J mice. In the first Aim, we demonstrate that paclitaxel induces time- and dose-dependent hypersensitivity (mechanical and cold), which is potentiated by combination therapy with the chemotherapeutic carboplatin. In addition, paclitaxel-treated mice show changes in affect-like behaviors (anxiety-like, depression-like). In the second Aim, we used the prototypic nicotinic receptor (nAChR) agonist nicotine to reverse or prevent paclitaxel-induced mechanical hypersensitivity and degeneration of Intra-Epidermal Nerve Fibers (IENFs). Further, we discovered that nicotine's antinociceptive effects in this mouse model of CIPN are mediated by the nicotinic receptor subtype $\alpha 7$. The third Aim used genetic and pharmacological approaches to dissect the role of $\alpha 7$ on the development and maintenance of paclitaxel-induced CIPN. Null mutant $\alpha 7$ mice (KO) hastens the onset, increases the magnitude, and delays the recovery of paclitaxel-induced mechanical hypersensitivity, as compared to littermate wildtype controls, whereas the selective $\alpha 7$ silent agonist R-47 reverses and prevents paclitaxel-induced CIPN in C57BL/6J mice. We also examined the impact of R-47 on the paclitaxel-induced reduction of intraepidermal nerve fiber (IENF), as well as microglial morphology in the dorsal horn of the spinal cord. The data show that R-47 prevents paclitaxel-induced changes in microglial

morphology and mechanical hypersensitivity behavior, without producing tolerance upon repeated administration. Finally, R-47 induces preference using the conditioned place test in paclitaxel-treated mice but vehicle-treated animals, suggesting that R-47 is a viable candidate for ongoing, spontaneous pain, with limited risk of abuse potential. Overall, these results support that the $\alpha 7$ nAChR subtype is an important target for the treatment and prevention of CIPN.

CHAPTER ONE

GENERAL INTRODUCTION

A-Chemotherapy-Induced Peripheral Neuropathy (CIPN)

A.1 Prevalence and Symptoms of CIPN

One of the major dose-limiting side effects of several anticancer drugs is Chemotherapy-Induced Peripheral Neuropathy (CIPN). The prevalence of CIPN has been reported to be 68.1% at first month after treatment, 60% within 3 months, and 30% within 6 months or longer in cancer patients treated with many chemotherapeutics that have a different mechanism of action such as taxanes and platinum compounds (Seretny et al., 2014). In particular, 97 % of breast cancer patients treated with paclitaxel experience neuropathy symptoms during a median follow-up time of 57 months (Tanabe et al., 2013). According to American Cancer Society, over 600,000 newly diagnosed cancer patients will receive paclitaxel as first-line treatment (Siegel et al., 2018). Paclitaxel is a taxane based chemotherapeutic which can be extracted from the bark of the Pacific yew tree (Wani et al., 1971). Paclitaxel induces its anticancer effects through the promotion of polymerization of tubulin, which disrupts microtubule dynamics, preventing depolymerization of the microtubule during cell division, leading to apoptosis (Long and Fairchild, 1994; Jordan and Wilson, 2004). Clinically, paclitaxel is used to treat many types of solid tumors including breast, ovarian, non-small cell lung, head/neck, gastric, and prostatic cancers (Qin et al., 2012; Miltenburg

and Boogerd, 2014). Despite the efficacious use of paclitaxel in the treatment of tumors, it can induce many sensory symptoms due to peripheral neuropathy, which typically presents in patients with a “stocking and glove” distribution in the feet and hands, respectively (Boyette-davis et al., 2015). CIPN symptoms commonly include paresthesia, numbness, tingling and burning pain, and mechanical and cold allodynia (Kerckhove et al., 2017). At higher doses, paclitaxel may lead to motor or autonomic dysfunction. Unfortunately, these symptoms may lead to dose reduction of chemotherapeutic agent or discontinuation of treatment (Han and Smith, 2013). While adjuvant therapies, such as duloxetine, tricyclic antidepressants, and gabapentin are prescribed to treat CIPN symptoms, none of these compounds can consistently reverse or prevent the development of CIPN (Hershman et al., 2014). Thus, there is no currently FDA approved medication to treat CIPN.

A.2 Paclitaxel-Induced CIPN in Rodents

The use of animal (rodent) models of CIPN allow us to understand the mechanisms of the disease better, and to perform studies under controlled conditions. Additionally, rodent studies permit us to explore novel therapies for the treatment and prevention of CIPN. A review by (Hoke and Ray, 2014) discussed the use of rodents as a preclinical model of CIPN. The authors describe the importance of including multiple outcome measures in rodents to validate and represent the clinical symptoms seen in human patients experiencing CIPN induced by paclitaxel. These outcome measures may include reflexive measures such as thermal, mechanical and cold hypersensitivity, which frequently used in literature as behavioral-sensory assays. Additionally, histopathologic techniques can be used to examine further the nerve degeneration such as intra-epidermal nerve fibers (IENFs) and alteration in the neuronal cell bodies which could be impacted by paclitaxel. Furthermore, electrophysiological studies such as nerve conduction velocity and amplitude assess the integrity of large myelinated axons which can be disrupted by chemotherapy

treatment. Moreover, choosing dose, route of administration, frequency of delivery (acute or repeated), rodent strain, and sex that correlate with the human dosing regimen and length of treatment should be considered during animal studies. For example, a recent study by (Wozniak et al., 2018) shows that administration of paclitaxel at a dose of 30 mg/kg i.v. to BALB/c female mice in a six-dose regimen induced prolonged (until six months post paclitaxel injection) and a significant reduction in the nerve conduction velocity and amplitude in the sciatic nerve. Also, a significant reduction of IENFs developed in paclitaxel-treated mice compared to vehicle-treated mice lasted until three months post paclitaxel injection. Furthermore, paclitaxel level was detectable up to 6 months in the sciatic nerve (SN) and in the dorsal root ganglia (DRG), along with degeneration of sciatic nerve and abnormalities of neuronal cell bodies in the DRG. Similarly, administration of paclitaxel at doses of 2, 4, and 8 mg/kg i.p. every other day for a total of 4 injections (one cycle) to C57 BL/6 J mice significantly developed both mechanical and cold hypersensitivity in a time and dose-dependent manner. Additionally, paclitaxel-treated mice reveal a significant reduction of IENFs (Toma et al., 2017). Likewise, rats treated with paclitaxel at a dose of 2 mg/kg i.p. every other day for one cycle show long-lasting, significant mechanical hypersensitivity compared to vehicle-treated rats (Duggett et al., 2016; Griffiths and Flatters, 2015) and an enhanced release of Reactive Oxygen Species (ROS) in the DRG neurons. A similar paclitaxel treatment regimen in rats results in a significant reduction of IENFs (Jin et al., 2008).

A.3 Potential Neurotoxicity Mechanisms of Paclitaxel

The primary target of paclitaxel neurotoxicity is the Peripheral Nervous System (PNS), specifically, the peripheral axons along with the skin nerve fibers and the (DRG) where paclitaxel accumulates. One reason for paclitaxel peripheral neurotoxicity is because the Blood-Nerve Barrier (BNB) is considered more “deficient” than the Blood Brain Barrier (BBB) primarily due

to lack of P-glycoprotein transporter activity, which decrease the effectiveness of chemotherapeutics removal (Balayssac et al., 2005; Balayssac et al., 2011). The primary nociceptive afferent neurons that are responsible for the transmission of pain signals are the unmyelinated C and thinly myelinated A δ fibers in which their activation could lead to peripheral sensitization processes thereby worsening the development of neuropathic pain (Baron, 2006). There are several mechanisms proposed to cause the neurotoxicity; these mechanisms may involve mitochondrial dysfunction, neuroinflammation, microtubule damage, neuron apoptosis, ion channel modulation, and oxidative stress in both DRG and Dorsal Horn (DH) of the spinal cord (see Figure 1), (Areti et al., 2014; Kerckhove et al., 2017). One of the important features of CIPN induced by paclitaxel is the reduction or degeneration of the IENFs, the remainder of which become hyperexcitable (Jaggi and Singh, 2012). Reduction of IENFs is an indicator of morphological changes. Thus, several studies in rats (Bennett et al., 2011; Liu et al., 2010; Ko et al., 2014) and mice (Krukowski et al., 2015; Toma et al., 2017) suggest that paclitaxel induces the reduction of IENFs. Additionally, paclitaxel causes axonopathy through perturbation of anterograde axonal transport (Smith et al., 2016), alteration in nerve conductance velocity (Wozniak et al., 2016; Boehmerle et al., 2014), and axon degeneration (Benbow et al., 2016). The neuroinflammatory aspect of CIPN induced by paclitaxel is an essential feature for the development of CIPN. It involves activation of glial cells in the CNS such as astrocytes and microglia, and in PNS such as Schwann and satellite glial cells that surround DRG, as well as infiltration of macrophages and T-cells into DRG (Zhang et al., 2016). The neuroinflammatory process leads to the release of pro-inflammatory cytokines such as Tumor Necrosis Factor (TNF)- α , Interleukin (IL)-1 β , and chemokines such as Monocyte Chemoattractant Protein (MCP)-1. Cytokines and chemokines increase the sensitivity of nociceptors' neurogenic inflammation (Zaks-zilberman et al., 2001; Ji

et al., 2013). Also, paclitaxel indirectly enhances the release of inflammatory mediators such as substance P, bradykinin, serotonin, and histamine (McMahon et al., 2005; Costa et al., 2011).

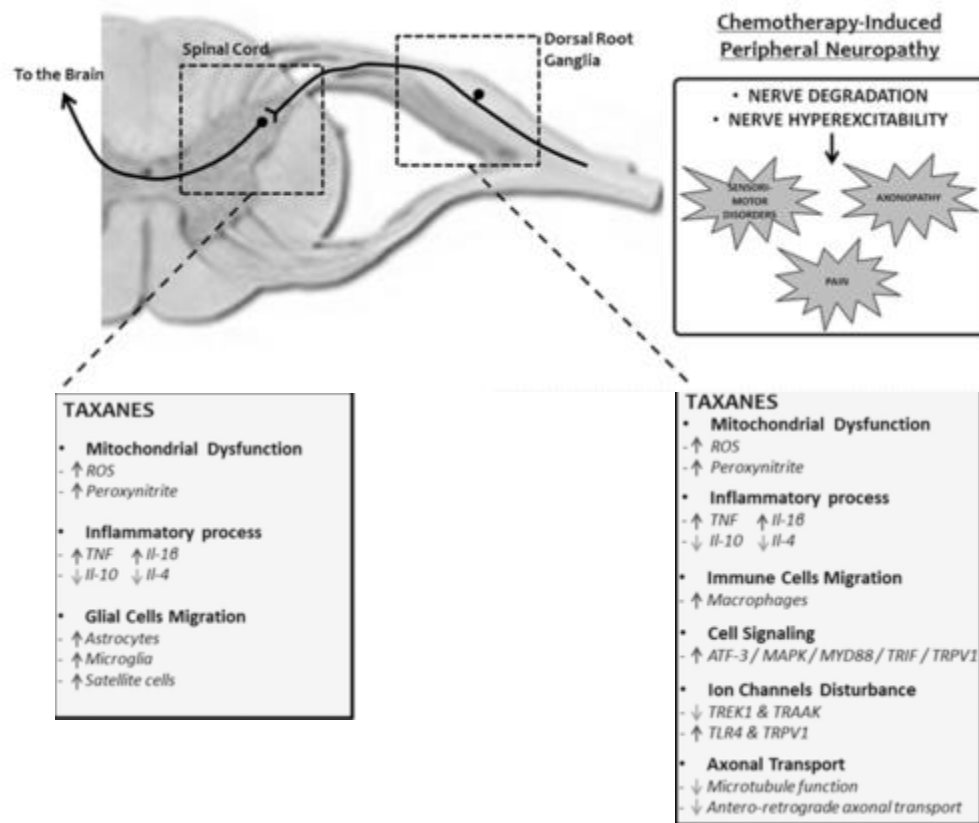


Figure 1: Proposed mechanisms of chemotherapy-induced peripheral neuropathy. Different targets of taxanes induced neurotoxicity including peripheral nerves, DRG, and spinal cord. ATF-3, cyclic AMP-dependent transcription factor 3; IL-1 β , interleukin-1 β ; IL-10, interleukin-10; IL-4, interleukin-4; MAPK, mitogen-activated protein kinase; MYD88, myeloid differentiation primary response gene 88; ROS, reactive oxygen species; TLR4, toll-like receptor 4; TNF, tumor necrosis factor; TRAAK, TWIK-related arachidonic acid activated K⁺ channel; TREK1, TWIK1-related K⁺ channel 1; TRIF, TIR-domain-containing adapter-inducing interferon- β ; TRPV1, transient receptor potential vanilloid 1. Adapted and modified from (Kerckhove et al., 2017).

A.4 Role of Non-neuronal Cells in the Peripheral Neuropathy

A growing body of evidence suggests the involvement of non-neuronal (immune and glial) cells in the pathogenesis of nerve injury and subsequently changing the functionality of neurons in the PNS and CNS (Scholz and Woolf, 2007). Repeated injection of paclitaxel into mice results in accumulated levels in the sciatic nerve, and DRG for at least 30 days (Wozniak et al., 2016). Once paclitaxel accumulates, it triggers the peripheral immune cells to react fast enough to induce an inflammatory reaction. Thus, the inflammatory cascade involves the attraction of Langerhans cells, keratinocytes cells, mast cells, and neutrophils which leads to the release of inflammatory mediators such as 5-Hydroxy Tryptamine (5-HT), Histamine, Nerve Growth Factor (NGF), IL-1 β , IL-6, Prostaglandin E2 (PGE2). The accumulation of inflammatory fluid is so-called “Inflammatory soup” (Baliki and Apkarian, 2015). Following that, the injured nociceptive fiber will further release neurotransmitters and neuropeptides, for instance, adenosine triphosphate (ATP), histamine, substance P, and Calcitonin Gene Related Peptide (CGRP). Also, the fiber will exhibit upregulation of ion channel expression, including Na⁺, K⁺, and Ca²⁺ channels with altered firing properties. Collectively, these sequences of events produce the peripheral sensitization (Pinho-Ribeiro et al., 2017). Additionally, paclitaxel causes the infiltration of macrophages and T-cells into the DRG which will further augment the release of inflammatory cytokines (Peters et al., 2007; Liu et al., 2014). Consequently, central sensitization develops following multiple pathological changes in the dorsal horn of the spinal cord. The central terminals of primary afferent nociceptors are already hyperexcitable and release neurotransmitters, chemokines, enzymes that stimulate or activate the microglia, astrocytes, and oligodendrocytes along with infiltrated T-cells, where they “cross-talk” with each other and with the nociceptors. Once they become activated, the

spinal glial cells release the inflammatory mediators like the cytokines, chemokines, and neurotrophic factors. This process will further stimulate the projection neurons and interneurons that eventually lead to persistent pain (see Figure 2), (Ji et al., 2016). Several studies suggest that neuropathy induced by chemotherapy or chronic nerve injury activates the glial cells. For example, a study by (Zhang et al., 2008) shows that mice that underwent common peroneal nerve (CPN) ligation develop microglial phenotypic changes in the spinal cord but not in higher areas of the brain. Furthermore, spinal nerve transection (SNT) as a model of peripheral neuropathy results in spinal microgliosis and these microglial cells are required for the pain hypersensitivity (Gu et al., 2016). Additionally, (Echeverry et al., 2017) supports the previous finding that spinal microglial cells are necessary for the long-term maintenance of neuropathic pain where rats underwent partial sciatic nerve ligation (PSNL), a model of peripheral neuropathy. Astrocytes activation occurs following oxaliplatin, bortezomib, and vincristine models of CIPN in rats (Yoon et al., 2013; Robinson et al., 2014; X. T. Ji et al., 2013).

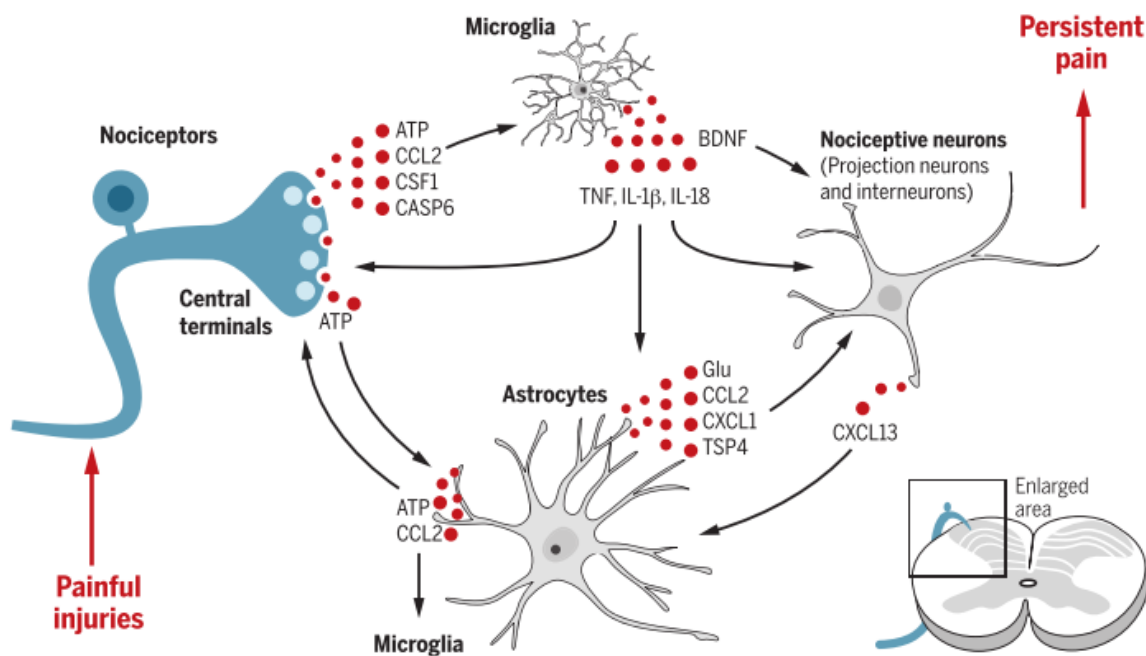


Figure 2: Neuron-glia interactions in the spinal cord which lead to central sensitization.

Chemotherapy can induce hyperexcitability of nociceptors which in turn leads to the release of glial modulators from their central terminals. Thus, this process leads to “activation” of both microglia and astrocytes which in turn release the inflammatory mediators that leads to pain chronification. ATP, Adenosine Tri Phosphate; CCL2, C-C motif ligand 2; CSF1, Colony-Stimulating Factor-1; CASP6, caspase-6; GLU, Glutamate; BDNF, Brain-Derived Neurotrophic Factor; CXCL1, C-X-C motif ligand 1; CXCL13, C-X-C motif ligand 13; TSP4, thrombospondin-4. Adapted and modified from Ji et al., 2016.

A.5 CIPN Beyond Sensory Measures

Following chemotherapy treatment, clinical studies suggest that anxiety and depression develop in cancer patients and survivors which impact their quality of life. For instance, (So et al., 2009) demonstrate that breast cancer patients experience a cluster of symptoms including pain (77%), anxiety (21%), and depression (36%). Another study by (Bao et al., 2016) shows that breast cancer survivors who have CIPN, develop a higher level of insomnia, anxiety, and depression compared to the patients who did not develop CIPN. Additionally, (Thornton et al., 2008) reveals that taxane-based treatment group reports higher and significantly worse emotional distress and mental quality of life in a randomized clinical trial in patients who had stage II/III breast cancer. In preclinical studies, C57 BL/6 J mice treated with paclitaxel at a dose of 8 mg/kg i.p. every other day for a total of 4 injections develop anxiety-like behavior in novelty suppressed feeding (NSF) and light/dark box tests (Toma et al., 2017). Moreover, paclitaxel-treated mice display signs of depression-like behavior in forced swim test and an anhedonia-like state in the sucrose preference test. Similarly, Swiss albino mice that underwent PSNL show significant allodynic response associated with anxiety and depression-like behaviors. (La Porta et al., 2016). Likewise, (Yalcin et al., 2011) suggests that C57 BL/6 J mice that underwent right sciatic nerve ligation display anxiety-like behavior four weeks after the initiation of peripheral neuropathy and depression-like behavior after 6-8 weeks following the development of peripheral neuropathy.

Clinically, patients experience pain in multidimensional aspects, including sensory, affective, and cognitive aspects (Navratilova et al., 2013). To evaluate the affective-motivational component of pain in a preclinical model of neuropathy, the conditioned place preference (CPP) test is a tool that can be used to assess the ability of candidate drugs to show “pain relief” in animals experiencing ongoing, spontaneous pain. The CPP test also has the benefit of revealing if such

candidate drugs produce reward in control animals. Ideally, analgesics would only produce CPP in animal models of neuropathy (Park et al., 2016). The CPP test is a pavlovian conditioning paradigm where the antinociceptive treatment is considered the unconditioned stimulus and the “pain relief” is considered the unconditioned response. Additionally, the chamber paired with the treatment is considered the conditioned stimulus and the preference to the side that was paired with the treatment is considered the conditioned response. The CPP test boxes consist of two main chambers equipped with two different colors and textures, and a neutral middle chamber. The animal is conditioned to receive the vehicle in one chamber and the candidate analgesic in the other chamber. Baseline or preconditioning time is measured before the conditioning shifts start. On the test day, the animal freely moves between all three chambers in a drug-free state. The preference score is calculated by determining the difference between the time spent on the drug-paired side during test day minus the time in the drug-paired side during the baseline day. In rats that underwent spinal nerve ligation, pregabalin at a dose of 300 mg/kg i.p. shows CPP in neuropathic rats but not in sham rats, suggesting that pregabalin reverses the aversive or “painful” state of rats during the early stage of neuropathic pain (Asaoka et al., 2018). Additionally, cisplatin-treated mice show CPP with gabapentin. A gabapentin dose of 100 mg/kg i.p. produces a significant preference for the drug-associated treatment chamber, but not in non-cisplatin treated mice (Park et al., 2013), suggesting that gabapentin does not show intrinsic rewarding properties.

B- Nicotinic Acetylcholine Receptors

B.1 Overview of Nicotinic Acetylcholine Receptors (nAChRs): Structure and Function

The nicotinic acetylcholine receptors (nAChRs) are pentameric ligand-gated ion channels. nAChRs belong to the superfamily of Cys-loop ligand-gated ion channels and arrange in a form to create a central pore (Albuquerque et al., 2009). The subunits are classified as either alpha (α -

$\alpha 10$) or non-alpha ($\beta 2$ - $\beta 4$) containing nAChRs (Hurst et al., 2013). nAChRs are permeable to both Na^+ and Ca^{2+} ions. nAChRs are present in two primary forms, either heteromeric such as $\alpha 4\beta 2^*$ nAChR subtype, or homomeric such as $\alpha 7$ nAChR subtype (the asterisk refers to other α or β subunits that could be co-assembled), (Millar and Gotti, 2009; Hendrickson et al., 2013; Zoli et al., 2015). The nAChRs are activated endogenously by the neurotransmitter acetylcholine or exogenously by nicotine, a prototypic nAChRs agonist (Albuquerque et al., 2009). Also, nAChRs present in three conformational states; closed, open, and desensitized (Dani and Bertrand, 2007).

B.2 Nicotine and Nicotinic Receptors as Potential Targets for the Treatment of Pain

Several studies report the involvement of nicotinic receptors and drugs targeting these receptors in pain treatment. For instance, nicotine shows analgesic and/or antinociceptive properties in both human and animal experimental pain studies (Flood and Damaj, 2014). For example, a randomized, placebo-controlled crossover design shows nicotine exposure to spinal cord injury (SCI) related pain in non-smokers. Nicotine administration results in a significant reduction of pain sites that had characteristics of both neuropathic and musculoskeletal symptoms (Richardson et al., 2012). Likewise, several preclinical studies demonstrate the antinociceptive effect of nicotine in multiple pain assays. For instance, nicotine shows a significant antinociceptive activity in acute pain assays (tail flick and hot plate) and reduces significantly the time spent in paw licking in both phase I and phase II of formalin test in mice (AlSharari et al., 2012). In addition, a low oral dose of nicotine results in significant reduction of disease severity, histologic damage scores, and colonic level of $\text{TNF-}\alpha$ in a dextran sodium sulfate (DSS) colitis mouse model (AlSharari et al., 2013a). In another study, wild-type mice with PNSL received bone marrow (BM) cells from green fluorescent protein (EGFP)-transgenic mice. These labeled bone marrow-derived cells, which are present on macrophage and neutrophils, infiltrated into the injury site, resulting in

the development of mechanical and thermal hypersensitivity. Administration of nicotine perineurally once daily for four days produces significant prevention of both mechanical and thermal hypersensitivity and reduction of upregulated cytokines and chemokines in injured mice as well (Kiguchi et al., 2012). Furthermore, (Di Cesare Mannelli et al., 2013) shows that i.p. injection of 1.5 mg/kg nicotine results in reversal of allodynia in rats treated with oxaliplatin. Also, rats that underwent tibial nerve transection (TNT) as a model of peripheral neuropathy show that intrathecal administration of nicotine significantly alleviates mechanical hypersensitivity (Abdin et al., 2006). Moreover, our recent work shows acute administration of nicotine reverses substantially mechanical hypersensitivity induced by paclitaxel in a dose-dependent manner. Nicotine at a dose of 24 mg/kg/ day s.c. via minipumps for seven days results in complete prevention of mechanical hypersensitivity. Additionally, nicotine prevents the degeneration of IENFs (Kyte et al., 2017).

There might be limitations for using nicotine or some nicotinic analogs as a potential treatment for CIPN. For example, nausea, vomiting, dizziness, and headache (Dutta et al., 2012; Rowbotham et al., 2009), were reported with nicotine and some non-selective $\alpha 4\beta 2^*$ agonists. Another important limitation is the potential pro-survival and/or carcinogenic effects of nicotine that may enhance the proliferation of both tumor and healthy cells (Catassi et al., 2008). These potential pro-tumor effects could be mediated by multiple nAChRs subtypes and through various signalling pathways. For example, janus-activated kinase/STAT, and phosphoinositide 3-kinase/AKT pathways (Schaal and Chellappan, 2014; Grando, 2014). However, our recent work shows that nicotine failed to promote the proliferation of A549 and H460 non-small cell lung cancer cells. Furthermore, chronic nicotine administration does not increase the growth of Lewis lung carcinoma tumors in C57 BL/6J mice (Kyte et al., 2018).

B.3 The Role of $\alpha 7$ nAChR Subtype as a Putative Target to Treat Painful Neuropathy

One of the putative important targets for pain and inflammation is the $\alpha 7$ nicotinic acetylcholine receptor ($\alpha 7$ nAChR) subtype. The $\alpha 7$ nAChR distributes throughout the pain transmission pathway: centrally (on neuronal cells) and peripherally (on neuronal and non-neuronal cells, such as macrophages, and T-cells) (Kawashima et al., 2007; Cordero-Erausquin et al., 2004). The $\alpha 7$ nAChR subtype is highly permeable to Ca^{2+} ions, has a low probability of channel opening, and can desensitize rapidly (Williams et al., 2011). The roles of $\alpha 7$ nAChR subtype involve in numerous physiological processes throughout the body. For instance, memory, learning, cognition, neuroprotection (specifically in the treatment of Alzheimer's, Parkinson's and other neurodegenerative diseases), and neuronal survival (Egea et al., 2015). Additionally, the presence of the $\alpha 7$ nAChR subtype on the surface of the immune cells, specifically macrophages and microglia, makes this receptor subtype an essential component of the cholinergic anti-inflammatory pathway (defined as neural signals transmitted via the vagus nerve that inhibit cytokine release through a mechanism that requires the $\alpha 7$ subunit-containing $\alpha 7$ nAChR (Pavlov and Tracey, 2015)). For example, in a mouse model of colitis, where mice were administered 2.5% of DSS orally, the $\alpha 7$ knockout (KO) mice show substantially enhanced colitis severity scores and elevated TNF- α level as compared to wild-type (WT) mice (AlSharari et al., 2016). Similarly, in a mouse model of endotoxemia, the $\alpha 7$ nAChR subtype is required for the inhibitory action of acetylcholine to TNF- α release from macrophages. Thus, electrical stimulation of the vagus nerve inhibits the TNF- α synthesis in $\alpha 7$ nAChR, wild-type mice but fails to inhibit TNF- α synthesis in $\alpha 7$ nAChR knockout mice (Wang et al., 2003). Furthermore, $\alpha 7$ nAChR KO mice show a significant increase in edema, hyperalgesia, and allodynia in the complete Freund's adjuvant (CFA) test compared with the WT littermates (AlSharari et al., 2013b).

B.4 Intracellular Signalling Anti-inflammatory Pathway of $\alpha 7$ nAChR in Immune Cells

The $\alpha 7$ nAChR has several intracellular signaling pathways following their activation. For example, once classical agonists (acetylcholine, choline) bind to the receptor and activate it, the channel opens allowing calcium ions influx. The tyrosine kinase, Janus kinase (Jak-2) phosphorylation leads to phosphorylation of Signal Transducer and Activators of Transcription (STAT3). The Jak/STAT pathway leads to inhibition of the translocation of nuclear factor-kappaB (NF- κ B) into the nucleus. Thus, blockade the production of proinflammatory cytokines (Corradi and Bouzat, 2016). Calcium ions influx activates protein kinase C (PKC). Phosphorylation of PKC activates phosphatidylinositol 3 kinase (PI3K)/Akt pathway. This activation promotes the translocation of the transcription factor nuclear factor [erythroid-derived 2]-like 2 (Nrf2) which results in overexpression of heme oxygenase-1 (HO-1). Thus, promoting anti-inflammatory effects (Egea et al., 2015). Additionally, phosphorylation of inhibitor kappa B (I κ -B) through the STAT3 pathway results in further inhibition of NF- κ B translocation (Yoshikawa et al., 2006). Furthermore, the STAT3 pathway negatively regulates NF- κ B through increasing the activity of suppressor of cytokine signaling 3 (SOCS3) proteins (de Jonge et al., 2005). Moreover, cross-talk between $\alpha 7$ nAChR and metabotropic G-protein Coupled Receptors (GPCRs) further mediates intracellular signaling (Kabbani et al., 2013). Another interaction is between $\alpha 7$ nAChR- and peroxisome proliferator-activated receptor alpha (PPAR- α). The antinociceptive effects of $\alpha 7$ nicotinic agonists in the formalin test was reported to be mediated by activation of spinal PPAR- α in the mouse (Donvito et al., 2017).

B.5 Pharmacological Modulation of $\alpha 7$ nAChR

Various selective ligands (such as agonists, positive allosteric modulators (PAMs), agonist-allosteric modulators (ago-PAMs), and silent agonists) for the $\alpha 7$ nAChR were identified

and were found to induce pharmacological effects following different conformational changes of the receptor. This section will discuss the pharmacology of these ligands in pain and inflammation studies. Figure 3 shows the multiple and distinct binding sites for several $\alpha 7$ nAChR ligands. While agonist binds to classical orthosteric agonist binding site (A), the silent agonist site (S) is distinct but seems to overlap the agonist binding site. Conventional PAMs bind to the positive allosteric modulatory site (P), located in the transmembrane domain. Ago-PAMs can bind to a distinct direct allosteric activation binding site (D) located in the extracellular domain to induce receptor activation and a pharmacological effect on its own without needing the classical agonist binding (Horenstein et al., 2016). Ago-PAMs can also bind to the (P) site located in the transmembrane domain (Papke et al., 2017).

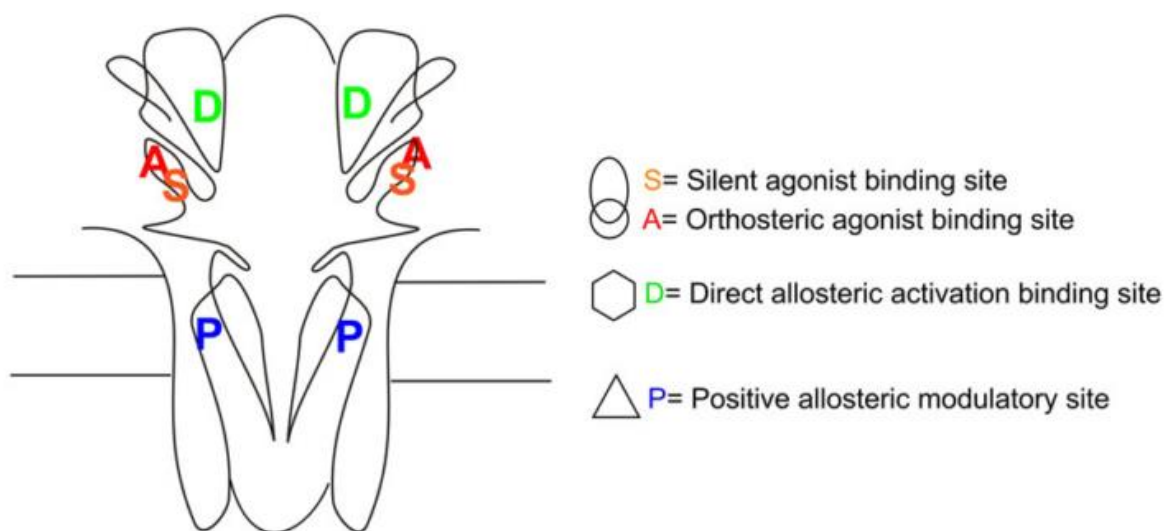


Figure 3. Proposed binding sites for multiple ligands of $\alpha 7$ nAChR. Adapted from (Papke et al., 2017)

Administration of selective $\alpha 7$ nAChR agonists choline and PHA-543613 result in significant reduction of colitis severity score in DSS colitis mouse model (AlSharari et al., 2016). Similarly, choline and PHA-543613 show significant reduction in the paw licking time in phase I

and II of the formalin test (Freitas et al., 2013a; Freitas et al., 2013b). Additionally, chronic administration of TC-2020, a selective $\alpha 7$ nAChR agonist into rats results in significant attenuation of chronic constriction injury (CCI)-induced mechanical hypersensitivity (Loram et al., 2012).

There are possible limitations on the use of direct $\alpha 7$ nicotinic agonists. For instance, the low probability of channel opening and rapid receptor desensitization (Williams et al., 2012) after activation by agonists. Also, inverted U shape dose-response curve after *in vivo* administration in many pain and inflammation models (AlSharari et al., 2016) (Freitas et al., 2013b), and possible gastrointestinal disturbances (Kem et al., 2018).

PAMs are one type of $\alpha 7$ nAChR pharmacological modulators. PAMs bind to their distinctive binding site in the transmembrane domain of the receptor, which leads to enhancing the effectiveness of an orthosteric agonist by increasing the apparent affinity for agonist (Manetti et al., 2018; Bertrand et al., 2008; Young et al., 2008). PAMs are of two types, Type I and Type II. While Type I PAMs act by enhancing the amplitude of the $\alpha 7$ nAChR transient current (this occurs by lowering the energy barriers into the open state). Type II PAMs increase the amplitude of the current, prolonging the channel opening time by reducing the desensitization, and reactivating the channel (possibly by lowering the free energy of the conducting states and changing the conformation of the receptor to conduct ions) (Papke, 2014). Additionally, the $\alpha 7$ nAChR have two desensitized states, with one being sensitive (Ds), and the other one being insensitive (Di) to conversion to open states by Type II PAMs, which reduce desensitization of the $\alpha 7$ nAChR (Williams et al., 2011). In the carrageenan model of inflammatory pain, administration of the selective Type II PAM PNU-120596 reduces paw edema, which corresponds with increased paw withdrawal latency in thermal hypersensitivity assays. Similarly, PNU-120596 reverses mechanical hypersensitivity in CCI, a model of neuropathic pain (Freitas et al., 2013c).

Our recent work on GAT107, a new selective dual allosteric agonist-PAM (ago-PAM) for $\alpha 7$ nAChR, adds support for the idea of modulation of the nicotinic acetylcholine system as a viable treatment for the inflammatory aspects of chronic and neuropathic pain. GAT107 shows dose-dependent anti-inflammatory and anti-nociceptive properties in the formalin and CFA chronic inflammatory pain tests, as well as an anti-allodynic effect in neuropathic pain models. In addition, GAT 107 attenuated the increased activation of spinal astrocyte GFAP and phosphorylated p38MAPK which are inflammatory markers (Bagdas et al., 2016).

A new class of selective $\alpha 7$ nAChR ligands called silent agonists act by binding to the receptors at a very low efficacy (< 2%) and do not induce a current, but instead, stabilize a non-conducting state associated with desensitization. Also, they inhibit the response of $\alpha 7$ nAChR to ACh and appear as an agonist when a type II PAM is used (Briggs et al., 2009; Chojnacka et al., 2013). Administration of the silent agonist NS6740 reduces the time spent in paw licking in the formalin test and attenuates mechanical hypersensitivity in CCI neuropathic pain model (Papke et al., 2015). Additionally, NS6740 suppresses LPS-stimulated secretion of TNF- α in cultured rat microglia, suggesting a modulatory role in the inflammation (Thomsen and Mikkelsen, 2012). Furthermore, R-47 (PMP-072), another silent agonist for the $\alpha 7$ nAChR, significantly inhibits the cellular infiltration in a model of allergic lung inflammation (Clark et al., 2014). Likewise, R-47 at a dose of 10 mg/kg orally reduces synovitis significantly and shows 48% attenuation of arthritis score in murine collagen-induced arthritis (CIA) model (van Maanen et al., 2015).

C. Dissertation Aims

The central hypothesis of the current work is that the $\alpha 7$ nAChR subtype plays a regulatory role in pathogenesis (development and maintenance) of paclitaxel-induced CIPN. To test this hypothesis, the following aims were conducted:

Aim 1: Characterization of paclitaxel-induced CIPN in a mouse model. As stated in section A.2, studying CIPN in rodents gives us a better understanding of possible underlying basic mechanisms and possible targets with potential translational value. Additionally, animal models of CIPN allow us to investigate mechanisms underlying the pathophysiology of the disease. Thus, rodent models of CIPN present or show similar pathological and electrophysiological characteristics, and symptoms noticed in human patients experiencing CIPN (Authier et al., 2009). For that, we assessed whether the effects of paclitaxel on cold and mechanical hypersensitivity, as well as IENFs degeneration were dose-dependent. Additionally, we tested the impact of multiple cycles of paclitaxel on peripheral neuropathy development and recovery. Combination of paclitaxel and carboplatin treatments were administered in order to determine if co-administration causes sensitization in any of the behavioral measures. Additionally, anxiety and depression occur as comorbidities following chemotherapy treatment in human patients already suffering from painful neuropathy. However, preclinical data involved in studying anxiety- and depression-like behaviors with CIPN are sparse. For that, we used a battery of tests to address the development of affective changes. For example, we used novelty suppressed feeding and light/dark box tests to

evaluate anxiety-like behavior. Furthermore, we used the forced swim test and the sucrose preference test to determine depression-like and anhedonia-like behaviors, respectively.

Aim 2: Investigation of nicotine as an antinociceptive drug in a mouse model of paclitaxel-induced CIPN. Using the characterized model in Aim 1, we used nicotine, the prototypical agonist of nicotinic receptors, to determine its potential to prevent and reverse mechanical hypersensitivity and IENFs degeneration. Also, we validated nAChRs as the target of nicotine using a pharmacological approach. Furthermore, we identified that the $\alpha 7$ nAChR is playing an important role in nicotine's effects in the CIPN mouse model. Moreover, we utilized multiple cancer cell lines with different assays *in vitro*, and tumor-bearing mice infused with nicotine to address the potential proliferative effect of nicotine.

Aim 3: Exploration of R-47 as an antinociceptive drug in a mouse model of paclitaxel-induced CIPN. Our initial data in Aim 2 suggested that $\alpha 7$ nAChRs may represent an important target for the treatment of CIPN. Therefore, we first determined if $\alpha 7$ nAChRs play a modulatory role in paclitaxel-induced CIPN. For that, $\alpha 7$ WT and KO mice treated with a low dose of paclitaxel (1 mg/kg i.p. for one cycle) demonstrated that $\alpha 7$ KO mice develop significant mechanical hypersensitivity compared to WT mice, and they also exhibited prolonged maintenance of mechanical hypersensitivity. Furthermore, our preliminary data showed that paclitaxel treatment caused a downregulation of $\alpha 7$ nAChRs in the DRG and spinal cords of mice. These findings suggest that $\alpha 7$ nAChRs might modulate the development of CIPN. In addition to the methods used in Aim 2 studies, Aim 3 included in-depth examination of the effects of the selective $\alpha 7$ nAChR silent agonist R-47 in the paclitaxel-induced CIPN mouse model after acute and chronic administration, as well its effects on IENFs and microglia morphology.

CHAPTER TWO

Effects of Paclitaxel on the Development of Neuropathy and Affective Behaviors in the Mouse

Wisam Toma^{a†}, S. Lauren Kyte^{a†}, Deniz Bagdas ^{a,b}, Yasmin Alkhlaif^a, Shakir D. Alsharari^c,
Aron H. Lichtman^a, Zhi-Jian Chen^d, Egidio Del Fabbro^e, John W. Bigbee^f, David A. Gewirtz^a,
and M. Imad Damaj^a

Virginia Commonwealth University, School of Medicine, ^aDepartment of Pharmacology and Toxicology, ^dDepartment of Neurology, ^eDepartment of Internal Medicine, and ^fDepartment of Anatomy and Neurobiology, Richmond, VA, 23298, USA; ^bUludag University, Experimental Animals Breeding and Research Center, Faculty of Medicine, Bursa, Turkey; King Saud University, College of Pharmacy, ^cDepartment of Pharmacology and Toxicology, Riyadh, Kingdom of Saudi Arabia

†These authors contributed equally to this work.

Disclosure: the present work published in *Neuropharmacology* 117:305-315; 2017

A. Introduction

Various neoplastic diseases, such as breast, lung, and ovarian cancer, are commonly treated with paclitaxel, a chemotherapeutic drug in the taxane class. The anti-tumor effect of paclitaxel is mediated through its binding to microtubules of the cytoskeleton and enhancement of tubulin polymerization, thereby resulting in cell cycle arrest, and ultimately apoptotic cell death (Jordan and Wilson, 2004). Although paclitaxel effectively increases both progression-free survival and overall survival in cancer patients, it also produces painful sensory and emotional deficits (Dranitsaris et al., 2015; Seretny et al., 2014). Specifically, paclitaxel causes chemotherapy-induced peripheral neuropathy (CIPN), a result of peripheral nerve fiber dysfunction or degeneration, acutely in 59-78% of cancer patients and chronically in 30% of cancer patients (Beijers et al., 2012). CIPN is characterized by sensory symptoms such as numbness, tingling, cold and mechanical allodynia, as well as an overall decrease in quality of life. In addition, cancer patients receiving chemotherapy experience behavioral symptoms including fatigue, anxiety, and depression. For example, approximately 58% of cancer patients suffer from depression, while anxiety is prevalent in approximately 11.5% of the cancer patient population (Massie, 2004; Mehnert et al., 2014). Importantly, patients with comorbidities of depression and anxiety suffer from increased severity of symptoms and experience delayed recovery, which may interfere with positive outcomes (Massie, 2004). In comparison, 34% and 25% of the general population of patients experiencing neuropathic pain report respective feelings of depression and anxiety (Gustorff et al., 2008).

It is clear that there is a critical need to determine the mechanisms underlying these behavioral symptoms elicited by cancer chemotherapy drugs, as well as to identify new targets to prevent or treat these side effects. A necessary requisite to accomplish these aims is to establish relevant

preclinical models of chemotherapy-induced side effects. However, to our knowledge there are presently no published preclinical studies that have characterized paclitaxel-induced affective-like behaviors. Thus, the objectives of the current study were to develop a mouse model of paclitaxel-induced side effects. Multiple assessments of nociceptive and affective-related behaviors were performed in mice treated with one cycle of paclitaxel (i.p., every other day for a total of four injections). After determining the dose-response curve and time-course of paclitaxel-induced mechanical and cold allodynia following systemic administration in mice, the impact of paclitaxel was assessed on multiple affective behavioral phenotypes in individual cohorts of mice, such as nest building, anxiety- (light/dark box test, novelty suppressed feeding), depression- (forced swim test), and anhedonia- (sucrose preference test) related behaviors. In addition, studies investigated the nociceptive effect of carboplatin treatment alone and in combination with paclitaxel due to the use of the carboplatin-paclitaxel combination in the clinic.

B. Materials and Methods

Animals

Adult male C57BL/6J mice (8 weeks at beginning of experiments, 20-30 g) were purchased from The Jackson Laboratory (Bar Harbor, ME). A total of 197 mice were used, with 84 used to assess nociceptive effects and 113 used to assess affective-like behaviors. Mice were housed in an AAALAC-accredited facility in groups of four, then individually housed for the duration of the nesting, novelty suppressed feeding (NSF), and sucrose preference assays in order to accurately assess the ability of each individual mouse to nest, and to measure the food or sucrose consumed by each individual mouse. Mice were group-housed for all other behavioral assays. Food and water were available ad libitum, except when under the food restrictions of the NSF assay. The mice in each cage were randomly allocated to different treatment groups. All behavioral testing on

animals was performed in a blinded manner; behavioral assays were conducted by an experimenter blinded to the treatment groups. Experiments were performed during the light cycle (7:00 am to 7:00 pm) and were approved by the Institutional Animal Care and Use Committee of Virginia Commonwealth University and followed the National Institutes of Health Guidelines for the Care and Use of Laboratory Animals. Animals were euthanized via CO₂ asphyxiation, followed by cervical dislocation. Any subjects that showed behavioral disturbances unrelated to chemotherapy-induced pain were excluded from further behavioral testing. Animal studies are reported in compliance with the ARRIVE guidelines (Kilkenny et al., 2010).

Drugs

Paclitaxel and carboplatin were purchased from Tocris (Bristol, United Kingdom). Paclitaxel was dissolved in a mixture of 1:1:18 [1 volume ethanol/1 volume Emulphor-620 (Rhone-Poulenc, Inc., Princeton, NJ)/18 volumes distilled water]. Carboplatin was dissolved in 0.9% saline. All injections were administered intraperitoneally (i.p.) in a volume of 1 ml/100 g body weight.

Induction of CIPN model

In the clinic, low-dose paclitaxel therapy consists of administering 80 mg/m² intravenously once every week; the duration of treatment is dependent upon disease progression and limiting toxicity (Seidman et al., 2008). To mimic this low-dose regimen, our studies involved i.p. injections of 2, 4, or 8 mg/kg paclitaxel every other day for a total of four injections (1 cycle), resulting in a cumulative human equivalent dose of 28.4-113.5 mg/m² (Reagan-Shaw et al., 2007). A low-dose regimen (8 mg/kg, 1 cycle) results in long-term mechanical allodynia, which better represents the clinical manifestation of peripheral neuropathy, and allows for affective-related

behavioral measures to not be obscured by severe motor deficits and weight loss. When referring to the time at which affective behavioral assays were conducted, “post-paclitaxel injection” refers to the time after the first of four paclitaxel injections.

Immunohistochemistry and quantification of intra-epidermal nerve fibers (IENFs)

The staining procedure was based on a previously described method of Bennett et al., (2011) with modifications. The glabrous skin of the hind paw was excised, placed in freshly prepared 4% paraformaldehyde in 0.1 M PBS (pH 7.4), and stored overnight at 4°C in the same fixative. The samples were embedded in paraffin and sectioned at 25 µm. Sections were deparaffinized, washed with PBS, and incubated at room temperature for 30 min in blocking solution (5% normal goat serum and 0.3% Triton X-100 in PBS). Sections were incubated with a 1:1000 dilution of the primary antibody, PGP9.5 (Fitzgerald - cat# 70R-30722, MA, USA) overnight at 4°C in a humidity chamber. Following phosphate buffer saline (PBS) washes, sections were incubated for 90 min at room temperature with a 1:250 dilution of goat anti-rabbit IgG (H+L) secondary antibody conjugated with Alexa Fluor® 594 (Life Technologies - cat# A11037, OR, USA). Sections were mounted in Vectashield (Vector Laboratories, Burlingame, CA, USA) and examined using a Zeiss Axio Imager A1 – Fluorescence microscope (Carl Zeiss, AG, Germany). Sections were examined in a blinded fashion under 63x magnification. The IENFs in each section were counted in a blinded fashion and the density of fibers is expressed as fibers/mm. An individual cohort consisting of 6 mice per group was used.

Cycles of paclitaxel

To investigate the impact of paclitaxel treatment on peripheral sensitization following repeated cycles, we used the lowest paclitaxel dose in this study for a total of two cycles. Mice

were injected with vehicle or paclitaxel (2 mg/kg) for each cycle. Mechanical thresholds were evaluated between the days of injection and subsequently once per week. The second cycle of treatment began one week after the first cycle. An individual cohort consisting of 6 mice per group was used.

Carboplatin-paclitaxel treatment

In this study, we first investigated if carboplatin, which is often used in combination with paclitaxel for chemotherapeutic intervention, would induce allodynia in mice on its own after systemic administration. To explore the effect of carboplatin on changes in nociceptive behavior, mice were injected with carboplatin (0, 5, or 20 mg/kg) for 1 cycle and tested for 7 days. In a separate experiment, we studied the impact the carboplatin treatment on paclitaxel-induced allodynia using the sequence of carboplatin-paclitaxel administration. Mice were first injected with carboplatin (5 mg/kg, 1 cycle), then another cycle of injections was administered with a low dose of paclitaxel (1 mg/kg). The second cycle of treatment (paclitaxel, 1 mg/kg) began one week following the first cycle (carboplatin, 5 mg/kg). Mechanical thresholds were evaluated between the days of injection. An individual cohort consisting of 6 mice per group was used.

Assessment of nociceptive behavior

An individual cohort consisting of 6 mice per group was used for the assessment of mechanical and cold allodynia; the mice had a resting period of 24 hours between assays. An additional cohort consisting of 6 mice per group was used for the locomotor activity test to assess potential paclitaxel-induced motor deficits.

Mechanical allodynia evaluation (von Frey test)

Mechanical allodynia thresholds were determined using von Frey filaments according to the method suggested by Chaplan et al. (1994) and as described in our previous report (Bagdas et al., 2015). The mechanical threshold is expressed as \log_{10} (10 \times force in [mg]).

Cold allodynia evaluation (acetone test)

This test was conducted as previously described (Otrubova et al., 2013), but with slight modifications. Briefly, mice were placed in a Plexiglas cage with mesh metal flooring and allowed to acclimate for 30 min before testing. 10 μ l of acetone was projected via air burst from the pipette onto the plantar surface of each hind paw. Time spent licking, lifting, and/or shaking the hind paw was recorded by a stopwatch over the course of 60 s.

Locomotor activity test

The test was performed as described previously in Bagdas et al. (2015). Briefly, mice were placed into individual Omnitech (Columbus, OH) photocell activity cages (28 x 16.5 cm) containing two banks of eight cells each. Interruptions of the photocell beams, which assess walking and rearing, were then recorded for the next 30 min. Data are expressed as the number of photocell interruptions.

Assessment of affective behaviors

Nesting procedure

The nesting procedure was adapted as previously described by Negus et al. (2015) with some modifications. Briefly, mice were housed individually in cages containing corn cob bedding and all previous nesting material was removed from the home cage prior to conducting the nesting

assay. For each cage, one compressed cotton nestlet was weighed and cut into 6 rectangular pieces of equal size. The mice were then relocated to a quiet, dark room. After an acclimation period of approximately 30 min, the nestlet pieces were then placed on top of the wire cage lid, parallel to the wire and evenly spaced. The mice were allowed 120 min to nest, after which the weight of the nestlet pieces remaining on the cage lid and the nest quality (0-2; 0 = no nest formed, 1 = some nesting activity, 2 = established nest) was recorded. The percentage of animals that did nest, the amount of nesting material acquired (percent weight used), and the ability to participate in innate murine nesting behavior (nest quality) were determined. The nesting assay was conducted with three individual cohorts of mice: one at 1 week (n = 6 per group), one at 2 weeks (n = 6 per group), and another at both 8 and 11 weeks (n = 6 Veh, n = 7 PAC) post-paclitaxel (8 mg/kg, i.p) or vehicle injection. These specific cohorts were used for both the nesting and NSF assays, since nesting is not thought to be a stress-inducing task. The mice had a resting period of one week between assays.

Novelty suppressed feeding (NSF)

The NSF test measures a rodent's aversion to eating in a novel environment. It assesses stress-induced anxiety by measuring the latency of an animal to approach and eat a familiar food in an aversive environment (Bodnoff et al, 1988). Mice were housed individually in cages with wood-chip bedding and were deprived of food for 24 h. At the end of the deprivation period, the mice were relocated to a quiet, dark room. After an acclimation period of approximately 30 min, the mice were allowed access to an unused, pre-weighed food pellet in a clean test cage containing fresh wood-chip bedding, which was placed directly under a bright light. Each mouse was placed in a corner of the test cage, and a stopwatch was immediately started. The latency to eat (s), defined as the mouse sitting on its haunches and biting the pellet with the use of forepaws, was recorded. The amount of food (g) consumed by the mouse in 5 min was measured, serving as a control for

change in appetite as a possible confounding factor. The NSF assay was conducted with two individual cohorts of mice, one at 3 weeks (n = 6 per group) and another at both 9 and 11 weeks (n = 6 Veh, n = 7 PAC) post-paclitaxel (8 mg/kg, i.p.) or vehicle injection. These specific cohorts were used for both the nesting and NSF assays, since nesting is not thought to be a stress-inducing task. The mice had a resting period of one week between assays.

Light/dark box (LDB) test

The light/dark box test is based upon a conflict between the innate aversion to brightly illuminated areas and spontaneous exploratory activity (Crawley and Goodwin, 1980). The test was adapted as previously described (Wilkerson et al., 2016) with minor modifications. Briefly, the LDB apparatus consisted of a small, enclosed dark box (36 x 10 x 34 cm) with a passage way (6 x 6 cm) leading to a larger, light box (36 x 21 x 34 cm). The mice were acclimated to the testing room for 30 min prior to testing. Mice were placed in the light compartment and allowed to explore the apparatus for 5 min. The number of entries into the light compartment and the total time spent (s) in the light compartment were recorded for 5 min by a video monitoring system and measured by ANY-MAZE software (Stoelting Co., Wood Dale, IL). Individual cohorts of mice (n = 6 per group) were tested at 3, 6, and 9 weeks post-paclitaxel (8 mg/kg, i.p.) or vehicle injection.

Forced swim test (FST)

The forced swim test was performed as described previously by Damaj et al. (2004), the common method for assessing depression-like behavior in mice (Bogdanova et al., 2013). Briefly, mice were gently placed into individual glass cylinders (25 x 10 cm) containing 10 cm of water, maintained at 24°C, and left for 6 min. Immobility was recorded (s) during the last 4 min. A mouse was considered to be immobile when floating in an upright position and only making small

movements to keep its head above water, but not producing displacements. An individual cohort of mice ($n = 6$ per group) was tested throughout the FST study at 1, 2, 3, and 4 weeks post-paclitaxel (8 mg/kg, i.p) or vehicle injection.

Sucrose preference

The sucrose preference test is used as a measure of anhedonia-like behavior (Thompson and Grant, 1971). Mice had access to two, 25 ml sipper tubes, one containing normal drinking water and the other containing a 2% sucrose solution. Mice were housed individually, with access to food, water, and 2% sucrose 24 h per day. Mice were acclimated to the cages with sipper tubes for 3 days prior to injection (days 1-3), during which baseline measurements were taken. Paclitaxel (8 mg/kg, i.p.) or vehicle injections started on day 4. Water and sucrose intake were measured on days 1, 2, 3, 4, 5, and 6, as well as on days 10, 11 and 12. The location of both sipper tubes was switched daily to avoid place preference. Sucrose preference was calculated as a percentage of the volume of 2% sucrose consumed over the total fluid intake volume. An individual cohort of mice ($n = 8$ per group) was tested during the vehicle/paclitaxel treatment.

Statistical analyses

In the current study, a power analysis calculation was performed with the Lamorte's Power Calculator (Boston University Research Compliance) to determine the sample size of animals for each group (Charan and Kantharia, 2013). For assessing the nociceptive behaviors, the calculation showed that an n of 5 was required to achieve a power of 90% with an alpha error of 0.05; we used 6 mice per group. For the behavioral assays, the calculations showed that an n of 5 for novelty suppressed feeding, an n of 5 for nesting, an n of 8 for the light/dark box test, an n of 6 for the forced swim test, and an n of 8 for sucrose preference was required to achieve a power of 90%

with an alpha error of 0.05; we used 6 to 8 mice per group. The data were analyzed with GraphPad Prism software, version 6 (GraphPad Software, Inc., La Jolla, CA) and are expressed as mean \pm SEM. Before conducting statistical analyses, normality and variance tests were performed; normality of residuals was determined by the Shapiro-Wilk test for $n > 6$ or the Kolmogorov-Smirnov test for $n \leq 6$, and equal variance was determined by the F test. Data that did not pass the normality test were analyzed by non-parametric tests, and data that did not have equal variance were analyzed without the assumption of equal standard deviations. Data were normalized to initial vehicle measurements when appropriate. Unpaired t tests were performed to compare behaviors of vehicle- and paclitaxel-treated mice at a single time point. Two-way repeated measure analysis of variance (ANOVA) tests were conducted, and followed by the Bonferroni post hoc test, when behavioral outcomes of vehicle- and paclitaxel-treated mice were being compared over multiple time points. Differences were considered to be significant at $P < 0.05$.

C. Results

Paclitaxel induced changes in nociceptive behaviors in mice

Initial experiments determined the effect of paclitaxel on the development of mechanical and cold allodynia as a function of the drug dose. As anticipated, increased nociceptive responses and duration of effects were related to dose of paclitaxel. However, no significant changes in body weight gain or spontaneous activity were observed. As seen in Figures 4A and B, paclitaxel induced both mechanical allodynia [$F_{\text{dose} \times \text{time}} (21, 105) = 9.481, P < 0.0001$] and cold allodynia [$F_{\text{dose} \times \text{time}} (9, 45) = 14.76, P < 0.0001$] in dose- and time-related manners, respectively. At 8 mg/kg paclitaxel, mechanical allodynia was observed on day 1 post-paclitaxel injection, and this effect was sustained for more than 90 days (data not shown). On the other hand, 2 and 4 mg/kg paclitaxel induced mechanical allodynia beginning on day 3, and the effects did not differ in terms of

magnitude or time to recover. With regard to cold allodynia, paclitaxel presented a clear dose-dependent induction on day 8 post-paclitaxel injection. However, mice that received 2 or 4 mg/kg paclitaxel recovered by day 22, whereas the 8 mg/kg group continued to exhibit cold allodynia. In regard to general body condition, even the highest dose of paclitaxel (8 mg/kg) did not significantly alter body weight [$F_{\text{dose} \times \text{time}} (5, 25) = 1.093, P > 0.05$; Supplementary Fig. 1A], or motor coordination [$F_{\text{dose} \times \text{time}} (4, 40) = 0.5204, P > 0.05$; Supplementary Fig. 1B].

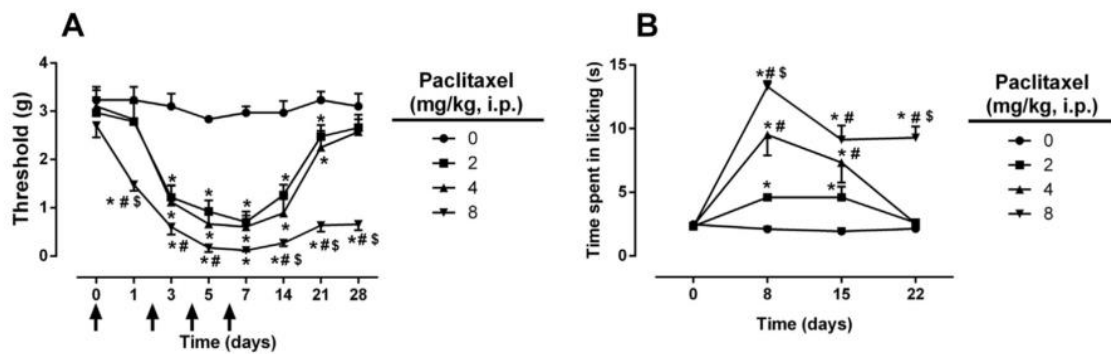
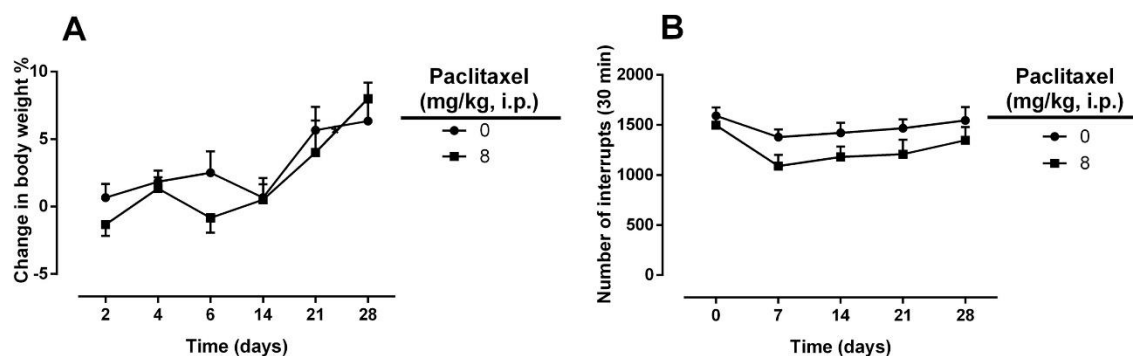


Figure 4. Paclitaxel induces nociceptive behaviors. Paclitaxel doses of 2, 4, and 8 mg/kg (i.p., every other day for a total of 4 injections) induce both mechanical (A) and cold (B) allodynia in a dose and time dependent manner. Arrows indicate vehicle/paclitaxel injections on days 0, 2, 4, and 6. Baseline measurements were taken before vehicle/paclitaxel administration on day 0. The same cohort was tested for both mechanical and cold allodynia; $n = 6$ per group (data expressed as mean \pm SEM). * $P < 0.05$ vs vehicle; # $P < 0.05$ vs paclitaxel (2 mg/kg); \$ $P < 0.05$ vs paclitaxel (4 mg/kg). BL, baseline.



Supplementary Figure 1. Paclitaxel has no effect on body weight and spontaneous activity in mice.

One cycle of paclitaxel (8 mg/kg, i.p., every other day for a total of 4 injections) did not cause significant loss of body weight (A) or alteration in motor coordination (B) compared to vehicle-treated mice. Vehicle/paclitaxel injections were administered on days 0, 2, 4, and 6. Baseline measurements were taken before vehicle/paclitaxel administration on day 0. One cohort was tested (n = 6 per group); data expressed as mean \pm SEM.

Paclitaxel decreased the density of intra-epidermal nerve fibers (IENFs)

Because changes in the density of peripheral nerve fibers represent a hallmark of CIPN, we studied the changes in peripheral nerve fiber density following paclitaxel treatment using immunohistochemistry. At 28 days post-paclitaxel injection, mice treated with paclitaxel (8 mg/kg, 1 cycle) demonstrated significant reductions in the density of IENFs when compared to vehicle-treated mice [$t = 3.736$, $df = 10$, $P < 0.01$; Fig. 5A]. Representative immunostained sections of foot pads from vehicle- (Fig. 5B; upper panel) and paclitaxel-treated mice (Fig. 5B; lower panel) show the reduction in IENFs following paclitaxel treatment.

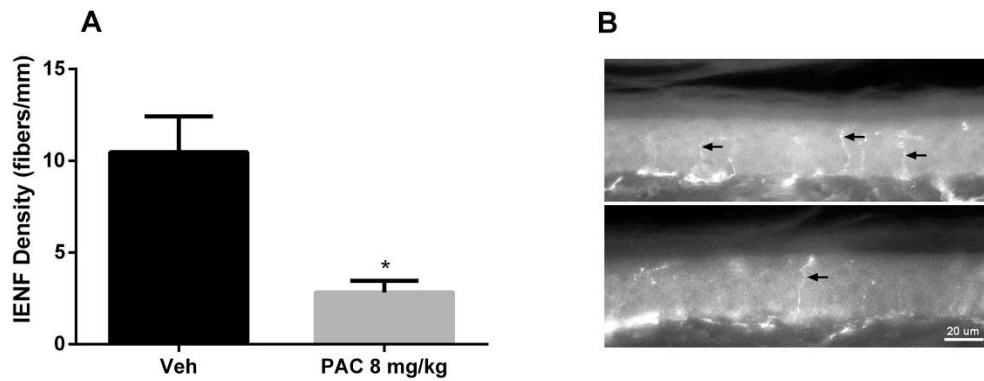


Figure 5. Paclitaxel induces a reduction in intra-epidermal nerve fiber (IENF) density at 28 days post-paclitaxel injection. A) Quantification of IENF density in mice treated with one cycle of paclitaxel (8 mg/kg, i.p., every other day for a total of 4 injections) shows a significant reduction compared to vehicle. One cohort was tested; $n = 6$ per group (data expressed as mean \pm SEM). * $P < 0.05$ vs vehicle. Veh, vehicle; PAC, paclitaxel. B) Immunostained sections of vehicle- (upper panel) and paclitaxel-treated (lower panel) hind foot pad skin showing the reduction of IENFs (arrows) following paclitaxel treatment. Bar represents 20 microns in both images.

Impact of repeated drug cycles on paclitaxel-induced mechanical allodynia

To investigate the effect of repeated cycles of paclitaxel on mechanical allodynia, mice were injected with two cycles of a low dose of paclitaxel (2 mg/kg). As expected, the first cycle of paclitaxel (2 mg/kg) was capable of inducing mechanical allodynia. Indeed, paclitaxel (2 mg/kg) induced a significant reduction in mechanical threshold that lasted for at least 14 days after the first injection of paclitaxel [$F_{\text{dose} \times \text{time}} (7, 35) = 8.436, P < 0.0001$; Fig 6A]. After a one-week wash-out period, mice received another cycle of paclitaxel (2 mg/kg). Surprisingly, the effects of paclitaxel were significantly enhanced in the mice subjected to a second cycle, which was demonstrated by a further decrease in mechanical threshold [$F_{\text{dose} \times \text{time}} (3, 15) = 48.61, P < 0.0001$; Supplementary Fig. 2]. In addition, mice that received a second cycle of paclitaxel treatment (2 mg/kg) displayed a much longer duration of allodynia (Fig. 6B) compared to one cycle of treatment (Fig. 6A) [$F_{\text{dose} \times \text{time}} (13, 65) = 10.97, P < 0.0001$; Fig. 6B]. Whereas mice given one cycle

recovered by day 21 post-paclitaxel injection, mice given two cycles recovered by day 63 after the first injection of paclitaxel. Calculation of the area under the curve (AUC) threshold for the initial 28 days of both the first and second cycles of paclitaxel treatment revealed significant differences (2.5-fold difference) between cycles [$F_{\text{treatment}}(3, 20) = 60.35$, $P < 0.0001$; Fig. 6C].

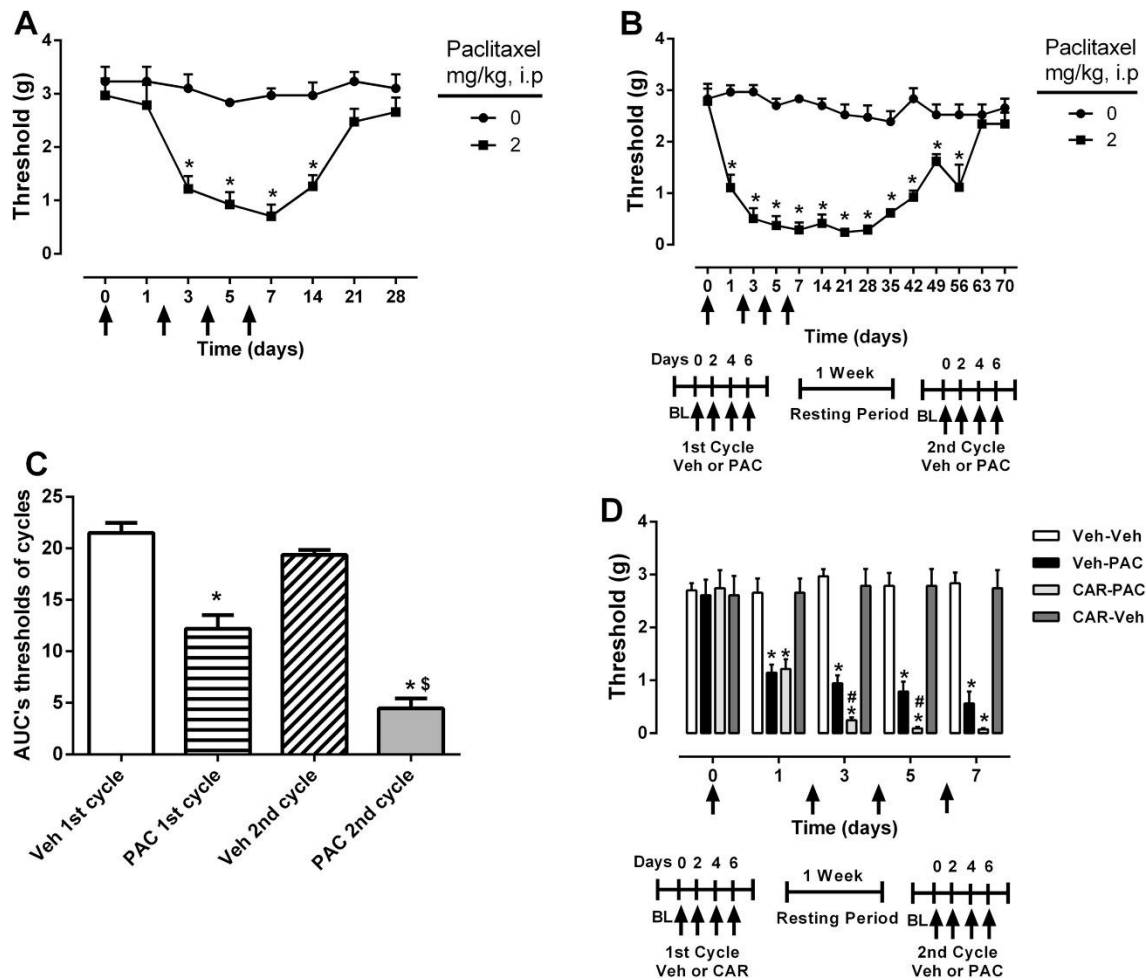
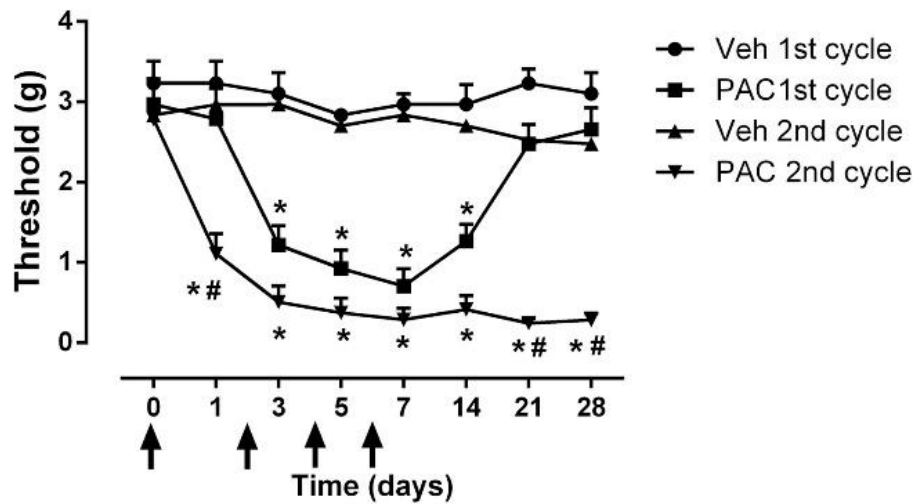


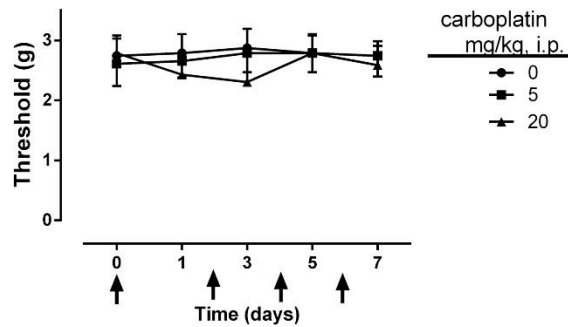
Figure 6. Mice are sensitized to cutaneous stimulation after second cycle of paclitaxel treatment. A) Mice treated with one cycle of paclitaxel (2 mg/kg) or vehicle (i.p., every other day for a total of 4 injections). B) Mice from 3A treated with a second cycle of paclitaxel (2 mg/kg) or vehicle (i.p., every other day for a total of 4 injections). C) AUC mechanical threshold for initial 28 days of first and second cycles of paclitaxel treatment. D) Comparison of mechanical thresholds during the second cycle of treatment between mice treated with carboplatin (5 mg/kg) alone and with carboplatin followed by a low dose of paclitaxel (1 mg/kg). Arrows indicate vehicle/paclitaxel/carboplatin injections on days 0, 2, 4, and 6 of each cycle. Baseline measurements were taken before vehicle/paclitaxel/carboplatin administration on day 0. One cohort was tested; $n = 6$ per group (data expressed as mean \pm SEM). * $P < 0.05$ vs vehicle; § $P < 0.05$ vs first cycle of paclitaxel (2 mg/kg), # $P < 0.05$ vs carboplatin (5 mg/kg). Veh, vehicle; PAC, paclitaxel; CAR, carboplatin.



Supplementary Figure 2. Paclitaxel sensitizes mice to cutaneous stimulation after second cycle. Comparison of mechanical threshold during the initial 28 days of one- or two-cycle paclitaxel (2 mg/kg, i.p.) or vehicle treatment. Arrows indicate vehicle/paclitaxel injections on days 0, 2, 4, and 6. Baseline measurements were taken before vehicle/paclitaxel administration on day 0. One cohort was tested ($n = 6$ per group); data expressed as mean \pm SEM. * $P < 0.05$ vs vehicle; # $P < 0.05$ vs first cycle of paclitaxel (2 mg/kg). Veh, vehicle; PAC, paclitaxel.

Paclitaxel induced allodynia following carboplatin treatment

We further investigated the impact of carboplatin treatment on paclitaxel-induced allodynia. Mice given one cycle of carboplatin alone did not demonstrate significant mechanical nociceptive changes. As shown in Supplementary Figure 3, one cycle of 5 or 20 mg/kg carboplatin did not significantly reduce the mechanical threshold [$F_{\text{dose} \times \text{time}} (8, 40) = 0.4526$, $P > 0.05$]. However, in a separate cohort of mice, a low-dose paclitaxel (1 mg/kg) cycle administered one week following the completion of the carboplatin (5 mg/kg) cycle led to a significant reduction of mechanical threshold compared to the vehicle-paclitaxel group [$F_{\text{dose} \times \text{time}} (12, 60) = 16.65$, $P < 0.0001$; Fig. 6D].



Supplementary Figure 3. Carboplatin alone does not induce mechanical allodynia. Dose-response curve for mice treated with one cycle of carboplatin at doses of 0, 5, and 20 mg/kg, i.p., every other day for a total of 4 injections. Arrows indicate vehicle/carboplatin injections on days 0, 2, 4, and 6. Baseline measurements were taken before vehicle/carboplatin administration on day 0. One cohort was tested (n = 6 per group); data expressed as mean \pm SEM.

Paclitaxel induced changes in affective-related behaviors in mice

To assess whether paclitaxel interferes with the natural behavior of mice, a nesting assay was conducted at various time points after paclitaxel treatment was initiated. However, paclitaxel did not interfere with nesting activity [$z = 0.856$, $P > 0.05$; $z = 1.000$, $P > 0.05$], the quantity of nesting material used [$t = 0.08655$, $df = 10$, $P > 0.05$; $t = 0.03402$, $df = 10$, $P > 0.05$], or nest quality [$t = 0.4152$, $df = 10$, $P > 0.05$; $t = 0.2033$, $df = 10$, $P > 0.05$] at 1 and 2 weeks post-paclitaxel injection, respectively (Fig. 7). Similar results were observed at 8 and 11 weeks post-paclitaxel injection, in which nesting activity was not significantly affected by paclitaxel [$z = 0.926$, $P > 0.05$; Fig. 7A]. The use of nesting material [$F_{\text{treatment} \times \text{time}}(1,11) = 1.157$, $P > 0.05$] and nest quality

$[F_{\text{treatment} \times \text{time}} (1,11) = 0.0094, P > 0.05]$ were also not found to be significantly altered (Fig. 7B and C).

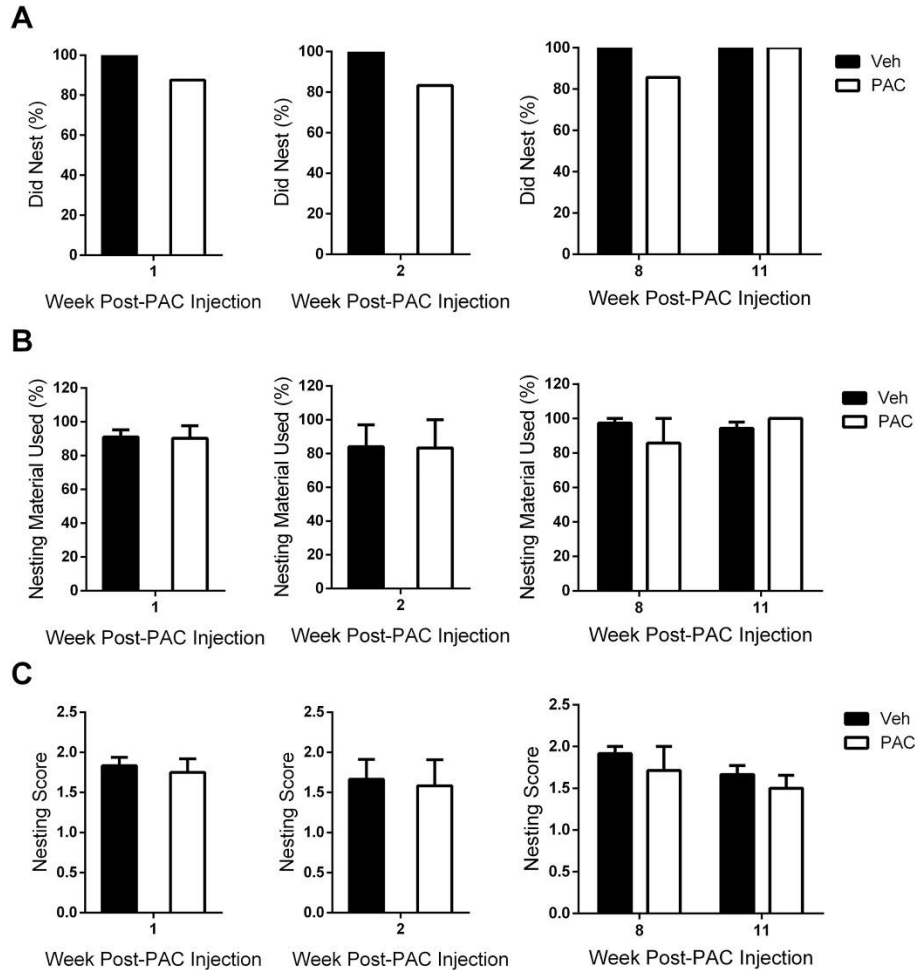


Figure 7. Paclitaxel does not influence the nesting behavior of mice. Mice were allowed 120 minutes to nest at weeks 1, 2, 8, and 11 post-paclitaxel (8 mg/kg, i.p.) or vehicle injection. A) It was determined that mice had participated in nesting activity if at least one nestlet piece had been chewed or pulled into the home cage. A comparison of proportions via z-tests between vehicle- and paclitaxel-treated mice was not significant at any time point. B) The percentage of nesting material used was determined by the following equation: (weight of initial nestlet pieces – weight of remaining nestlet pieces)/weight of initial nestlet pieces. C) The quality of each nest was evaluated on a scale ranging from 0 to 2 (0 = no nest formed, 1 = some nesting activity, 2 = established nest). Individual cohorts were tested at 1 week (n = 6 per group), 2 weeks (n = 6 per group), 8 and 11 weeks (n = 6 Veh, n = 7 PAC) post-paclitaxel (8 mg/kg, i.p.) or vehicle injection; data expressed as mean \pm SEM. Post-PAC injection refers to the time following the first of four paclitaxel injections. Veh, vehicle; PAC, paclitaxel.

With regard to affective-related changes, we assessed anxiety-, depression-, and anhedonia-like behaviors at various time points in mice treated with paclitaxel, according to the aforementioned treatment regimen. Alterations in anxiety were assessed utilizing the novelty suppressed feeding (NSF) assay. Paclitaxel significantly increased the latency to eat in a novel environment at 3 and 9 weeks post-paclitaxel injection (Fig. 8A). A significant increase in latency to eat occurred at 3 weeks post-paclitaxel treatment [$t = 2.224$, $df = 12$, $P < 0.05$, Fig. 8A]. In addition, significant differences in latency to eat between vehicle- and paclitaxel-treated mice occurred at 9 weeks post-paclitaxel injection ($P < 0.05$), which dissipated by week 11. The amount of food consumed in the test cage was not impacted by paclitaxel treatment (Fig. 8B).

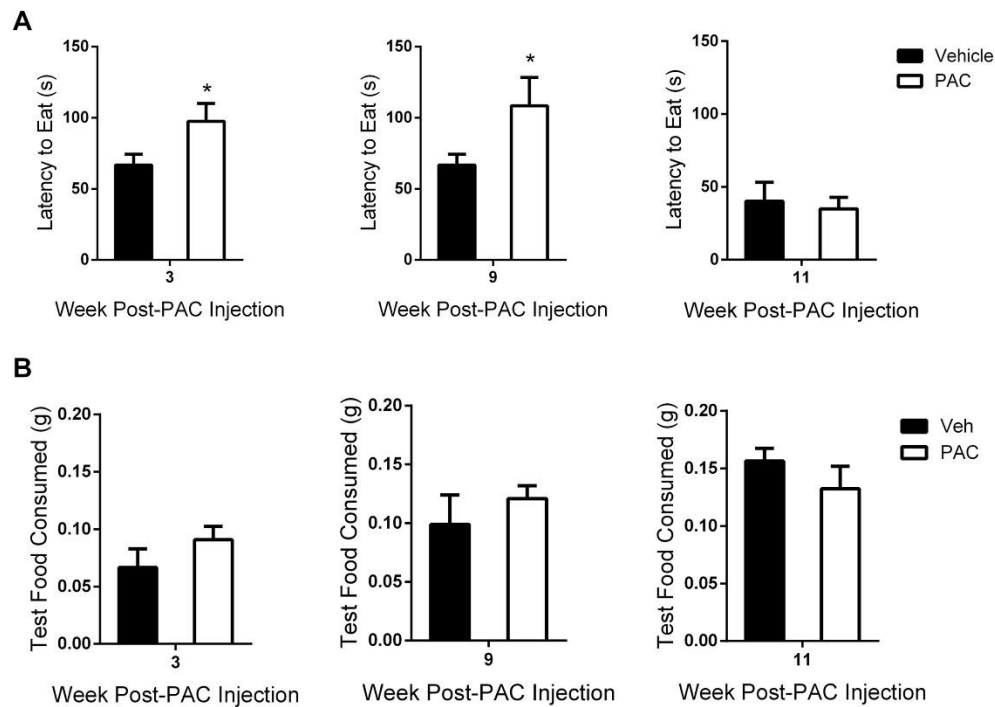


Figure 8. Paclitaxel induces anxiety-like behavior in the novelty suppressed feeding assay. (A) Latency to eat test cage food was determined as the time in seconds from the when the mouse was placed inside the test cage until the mouse sat on its haunches while holding and biting the food pellet. (B) Consumption of test cage food was calculated with the following equation: (initial weight of food pellet – weight of food pellet after 5 min eating period in test cage). Individual cohorts were tested at 3 weeks (n = 6 per group), 9 and 11 weeks (n = 6 Veh, n = 7 PAC) post-paclitaxel (8 mg/kg, i.p.) or vehicle injection; data expressed as mean \pm SEM. * P < 0.05 vs vehicle. Post-PAC injection refers to the time following the first of four paclitaxel injections. Veh, vehicle; PAC, paclitaxel.

Paclitaxel was also found to induce anxiety-like behavior in the light/dark box (LDB) test, in which time spent in the light compartment of the LDB apparatus was significantly decreased at 3 weeks [$t = 2.277$, $df = 14$, $P < 0.05$], 6 weeks [$t = 2.350$, $df = 14$, $P < 0.05$], and 9 weeks [$t = 2.309$, $df = 14$, $P < 0.05$] post-paclitaxel treatment (Fig. 9). Importantly, the *number* of entries into the light compartment was not significantly decreased at any time point for the paclitaxel-treated mice (Table 1), suggesting that the decrease in time spent in the light compartment is not due to motor deficits (Supplementary Fig. 1B).

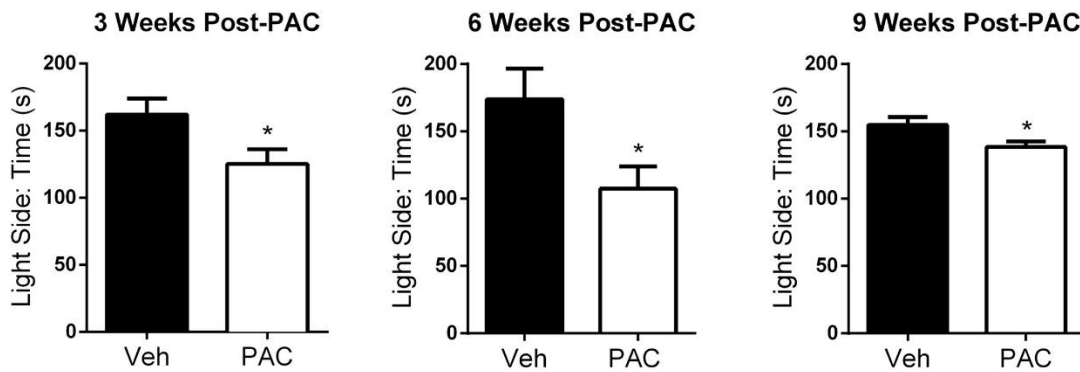


Figure 9. Paclitaxel induces anxiety-like behavior in the light/dark box test. Mice were free to explore both light and dark compartments for 5 min. The study was conducted with individual cohorts of mice ($n = 8$ per group) at 3, 6, and 9 weeks post-paclitaxel (8 mg/kg, i.p.) or vehicle injection; data expressed as mean \pm SEM. * $P < 0.05$ vs vehicle. Post-PAC injection refers to the time following the first of four paclitaxel injections. Veh, vehicle; PAC, paclitaxel.

Light Side: Number of Entries

	3 Weeks Post-PAC	6 Weeks Post-PAC	9 Weeks Post-PAC
Vehicle	16 ± 1.7	15 ± 2.0	14 ± 1.7
Paclitaxel	14 ± 1.9	13 ± 1.9	12 ± 1.7

Table 1. Paclitaxel treatment does not interfere with entry into the light compartment of the light/dark box apparatus. Unpaired *t* tests revealed no significant differences between vehicle- and paclitaxel-treated mice at any time point. One experiment was conducted with individual cohorts of mice (*n* = 8 per group) at each time point. Post-PAC injection refers to the time following the first of four paclitaxel injections. Data are expressed as mean ± SEM.

The mice were then evaluated for depression-like behavior in FST, an experimental paradigm that assesses immobility when placed in a container of water. Within the same cohort of mice, paclitaxel treatment induced an emotional-like deficit during FST [$F_{\text{treatment} \times \text{time}} (3,15) = 6.200$, $P < 0.01$; Fig. 10]. The time spent immobile during FST was significantly increased at 2 and 3 weeks post paclitaxel-injection ($P < 0.01$), an effect that dissipated by week 4 (Fig. 10).

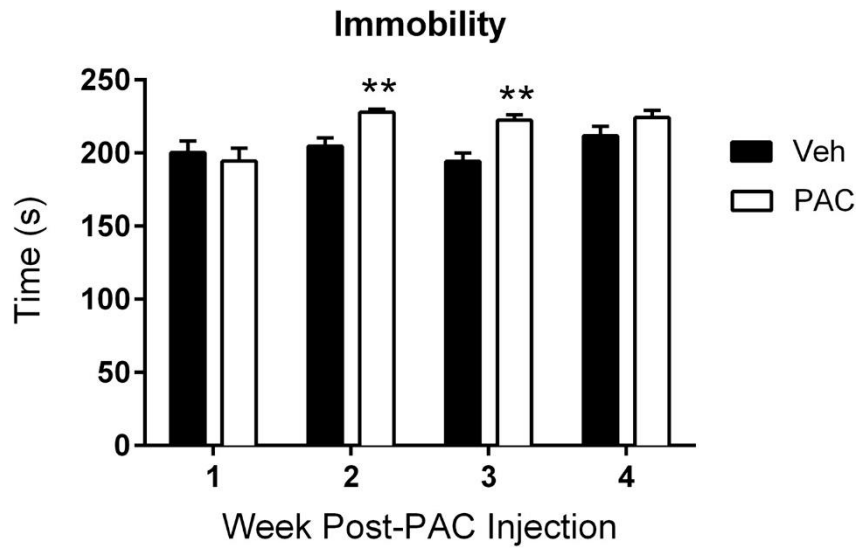


Figure 10. Paclitaxel induces depression-like behavior in the forced swim test. Time represents the number of seconds the mouse was immobile when placed in water; the cut-off time was 240 seconds. The same cohort of mice ($n = 6$ per group) was tested at weeks 1, 2, 3, and 4 post-paclitaxel (8 mg/kg, i.p.) or vehicle injection; data expressed as mean \pm SEM. ** $P < 0.01$ vs vehicle. Post-PAC injection refers to the time following the first of four paclitaxel injections. Veh, vehicle; PAC, paclitaxel.

Lastly, anhedonia-like behavior was assessed using the sucrose preference test. The interaction between paclitaxel treatment and time was significant within the same cohort of mice [$F_{\text{treatment} \times \text{time}}(8,112) = 9.424$, $P < 0.0001$, Fig. 11]. Paclitaxel produced a significant decrease in sucrose preference during ($P < 0.0001$) and shortly after ($P < 0.01$, $P < 0.05$) completion of the treatment regimen when compared to vehicle-treated mice (Fig. 11). To ensure that the decrease in consummatory behavior was not due to a decrease in overall consumption, we assessed total fluid intake between vehicle- and paclitaxel-treated mice, which was found to not differ significantly between the two groups (Supplementary Fig. 4).

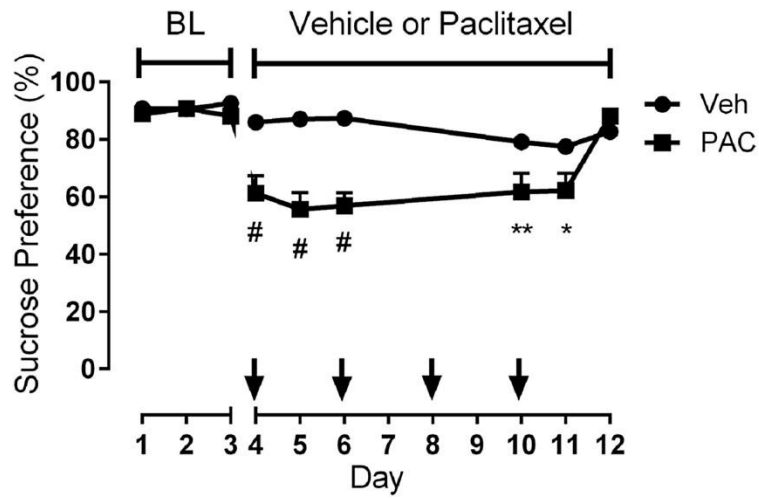
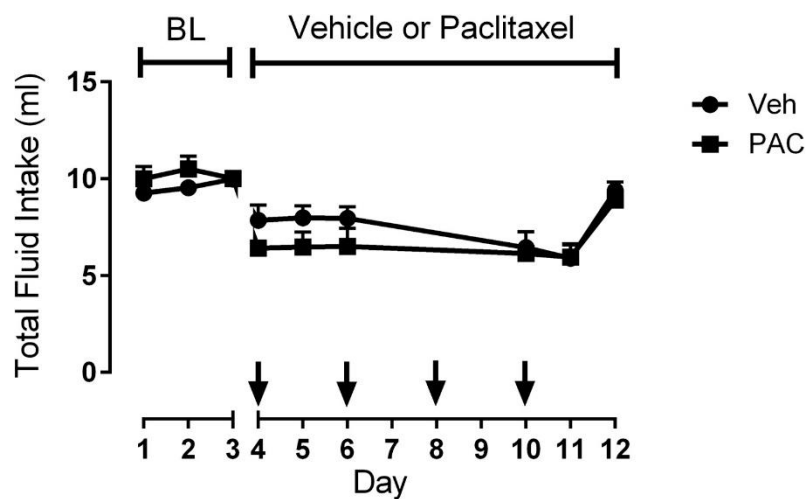


Figure 11. Paclitaxel induces anhedonia-like behavior in the sucrose preference test. Mice were provided with two sipper tubes, one containing normal drinking water and the other containing a 2% sucrose solution, for 24 h per day. Sucrose preference was determined as the percentage of 2% sucrose volume consumed over the total fluid intake volume. Arrows indicate the time of each paclitaxel (8 mg/kg, i.p.) or vehicle injection. The study was conducted with the same cohort of mice ($n = 8$ per group) during paclitaxel (8 mg/kg, i.p.) or vehicle injections; data expressed as mean \pm SEM. $*P < 0.05$, $**P < 0.01$, $\#P < 0.0001$ vs vehicle. BL, baseline; Veh, vehicle; PAC, paclitaxel.



Supplementary Figure 4. Paclitaxel treatment does not interfere with total fluid intake. The total fluid intake is the sum of volumes of water and 2% sucrose consumed by each mouse. Arrows indicate the time of each paclitaxel (8 mg/kg, i.p.) or vehicle injection (n = 8 per group); data expressed as mean \pm SEM. A two-way ANOVA was performed, followed by the Bonferroni post hoc test; no significant differences between vehicle- and paclitaxel-treated mice were found at any time point. BL, baseline; Veh, vehicle; PAC, paclitaxel.

Weeks Post-PAC Injection							
Behavior	Assay	1	2-3	4-5	6-7	8-9	10-11
Nociceptive	Mechanical Allodynia	+	+	+	+	+	+
	Cold Allodynia	+	+	ND	ND	ND	ND
Natural	Nesting	-	-	ND	ND	-	-
Anxiety-like	NSF	ND	+	ND	ND	+	-
	LDB	ND	+	ND	+	+	ND
Depression-like	FST	-	+	-	ND	ND	ND
	Sucrose Preference	+	-	ND	ND	ND	ND

Table 2. Summary of onset and duration of nociceptive, natural, and affective behaviors. Post-PAC injection refers to the time following the first of four paclitaxel injections. NSF, novelty suppressed feeding; LDB, light/dark box; FST, forced swim test; (-), no phenotype; (+), nociceptive/affective behavior; ND, not determined.

D. Discussion

The results of the present study demonstrate that a clinically relevant dosing regimen of paclitaxel given systemically to male C57BL/6J mice causes the induction and long-term maintenance of mechanical and cold allodynia, as well as negative affective-related symptoms,

including anxiety- and depression-like behaviors of shorter duration. These changes occurred without significant decreases in body weight or impairment of locomotion following paclitaxel treatment (Supplementary Fig.1), findings that are in accordance with other studies showing that various doses of paclitaxel do not alter body weight (Boehmerle et al., 2014) or locomotor activity (Deng et al., 2015; Neito et al., 2008).

Few studies have been performed under similar experimental conditions examining the effect of various doses of paclitaxel on the development of mechanical and cold allodynia, especially during the early period of injection and regarding the magnitude of that allodynia. Our results are consistent with other reports showing that paclitaxel induces both mechanical and cold allodynia in male mice (Deng et al., 2015; Slivicki et al., 2016; Naji-Esfahani et al., 2016). Interestingly, Ward et al. (2011) reported that a cycle of low-dose paclitaxel (1 or 2 mg/kg) elicited a considerably greater magnitude of cold allodynia in female mice than in male mice. Importantly, it has been noted in the clinic that neuropathic pain is more prevalent in women than in men (Fillingim et al., 2009). Therefore, it is possible that sex differences may arise in affective-like behaviors, along with nociceptive behaviors, following paclitaxel treatment.

With regard to morphological changes, our experiments show that 8 mg/kg paclitaxel produces a robust decrease in the density of intra-epidermal nerve fibers (IENFs), which is consistent with the results of Krukowski et al. (2015) that demonstrate significant reductions in IENF density following repeated administrations of paclitaxel in mice. Additional studies in rats have shown a dose-dependent decrease in IENFs following a wide range of paclitaxel doses (0.5 - 32 mg/kg), as well as a correlation between paclitaxel-induced loss of IENFs and allodynia (Bennett et al., 2011; Ko et al., 2014). Also, it is known that the polymodal C and A δ fibers are retracted following paclitaxel administration (Basbaum et al., 2009; Landowski et al., 2016;

Vichaya et al., 2015). Despite the decrease in IENF density, the remaining nociceptive fibers can become hyperactive and/or sensitized due to their release of chemical mediators of inflammation, such as substance P and calcitonin gene-related peptide (CGRP), as well as exposure to pro-inflammatory cytokines released by infiltrating immune cells, such as macrophages (Carozzi et al., 2015).

The present study also revealed that two cycles of 2 mg/kg paclitaxel (cumulative dose of 16 mg/kg) causes mice to exhibit lower mechanical thresholds than mice that received the same cumulative dose following one cycle of 4 mg/kg paclitaxel (Supplementary Fig. 2; Fig. 4A). This finding suggests that sensitization occurs during the first cycle of paclitaxel treatment. The observed sensitization may be due to the accumulation of paclitaxel in the periphery, as detectable concentrations of paclitaxel have been measured in the dorsal root ganglia and the sciatic nerve up to 26 days post-paclitaxel dosing (Wozniak et al., 2016).

In the clinic, paclitaxel has been administered in combination with cisplatin in non-small cell lung cancer patients. The combination produces additional neurotoxicity, and even two cycles of the treatment can result in neuropathy (Arrieta et al., 2010). In an attempt to avoid this toxicity, paclitaxel and carboplatin have been used in combination. Carboplatin is considered to be less neurotoxic than cisplatin and only 4–6% of patients who receive carboplatin may develop peripheral neuropathy (McWhinney et al., 2009). Furthermore, a study in ovarian cancer patients revealed that the carboplatin-paclitaxel treatment induced significantly less peripheral neuropathy than that produced by the cisplatin-paclitaxel treatment (Neijt et al., 2000). Clinical studies have shown that administration of carboplatin before paclitaxel is feasible in patients (Markman et al., 2003; Davidson et al., 2016). Our data show that in contrast to paclitaxel, mice treated with carboplatin (5 or 20 mg/kg) alone failed to show significant allodynia. However, when a low dose

of carboplatin (5 mg/kg) was followed by a low dose of paclitaxel (1 mg/kg), mice develop more severe mechanical allodynia when compared to paclitaxel alone, suggesting that carboplatin sensitized the mice to subsequent paclitaxel treatment. To our knowledge, studies of carboplatin- or carboplatin-paclitaxel-induced mechanical allodynia in mice have not been reported previously.

This work also investigated the affective-related consequences of paclitaxel treatment. Using a paclitaxel regimen that caused a long-lasting allodynia (8 mg/kg, 1 cycle), we observed an increase in the latency to eat during the NSF assay and aversion to the light compartment of the LDB apparatus. These effects in two tests of anxiety suggest that, under the present experimental conditions, paclitaxel induces an anxiety-like state. We also found that paclitaxel-treated mice exhibit increased immobility time during FST and anhedonia-like behavior in the sucrose preference test. The observed decrease in sucrose preference could also indicate that an alteration in taste (dysgeusia), a phenomenon seen in some patients receiving paclitaxel (Turcott et al., 2016), is occurring during paclitaxel treatment; yet, we cannot make that conclusion from a single oral consumption assay. The possible taste alteration may produce decreased appetite, but no significant changes in body weight were detected. Collectively, these results indicate that in addition to peripheral neuropathy signs, paclitaxel induces a deficit in the emotional-like state of the mice. Conversely, paclitaxel did not affect nesting behavior, an assay that has been shown to reflect pain-depressed behavior when lactic acid and complete Freund adjuvant (CFA) are used as noxious stimuli (Negus et al., 2015). The lack of an effect in this assay is consistent with the hypothesis that the value of a habit-like survival task does not alter depending on the motivational state (Rock, et al. 2014). Thus, the necessity of establishing a nest for thermoregulation, fitness, and shelter may overcome the nociceptive and negative affective symptoms of paclitaxel.

To increase our understanding of paclitaxel-induced toxicity, the relationship between nociceptive and affective symptoms needs to be considered, as well as the temporal order in which these side effects develop. Studies have shown that the pathology of a tumor itself can cause emotional disturbances in rodents (Pyter et al., 2009), but our experiments in non-tumor-bearing mice reveal that paclitaxel alone is also capable of inducing anxiety- and depression-like behaviors. At 1-week post-paclitaxel injection, we observed the development of both mechanical and cold allodynia, as well as anhedonia-like behavior (Table 2). Anxiety- and depression-like behaviors arise in the subsequent weeks following paclitaxel treatment. The immediate appearance of nociceptive symptoms is consistent with paclitaxel acting directly on the peripheral nervous system, but there may be a separate central mechanism of the drug. While paclitaxel seems to accumulate in peripheral organs such as the peripheral nervous system, it has been detected in the brain of mice following tail vein injection, even at low concentrations (Gangloff et al., 2005; Kemper et al., 2003), suggesting that it crossed the blood brain barrier. Therefore, the presence of paclitaxel in the central nervous system and/or paclitaxel-induced peripheral neuropathy itself may be causing changes in affective behaviors through neuroinflammation mechanisms and/or an induction of central neurotoxicity. It is also possible that paclitaxel-induced sensitization of immune responses may have played a role in the development of peripheral neuropathy, and perhaps of affective-like behaviors. Indeed, hypersensitivity to stimuli, not only in neuropathic pain but also in inflammatory pain, can be explained by both peripheral and central sensitization of sensory nerve fibers (Fornasari, 2012). In regard to the neuroimmune interface, glial responses have also been shown to play a role in central and peripheral nervous system function during neuropathic pain (Scholz and Woolf, 2007).

The differences between the onset, duration, and resolution of these affective behaviors should also be considered. Although changes in nociceptive behavior, such as mechanical allodynia, occur immediately following paclitaxel administration, there appears to be a delay in the initiation of emotional-like deficits. Clinically, somatic and affective symptoms can occur simultaneously. Breast cancer patients often experience a cluster of symptoms including pain (77%), anxiety (21%), and depression (36%), indicating that they may share a common mechanism (So et al., 2009). Those patients receiving chemotherapy experience the cluster symptoms to a greater degree and are at a higher risk for decreased quality of life.

The time-dependent development of both anxiety- and depression-like behaviors has also been observed in other mouse neuropathic pain models. La Porta et al. (2016) reported ipsilateral mechanical and cold allodynia from day 3 to day 27 post-partial sciatic nerve ligation (PSNL) in Swiss albino male mice, with enhanced anxiety-like behavior in the elevated plus maze from 1 to 3 weeks post-PSNL and increased depressive-like behavior during FST, but only at 3 weeks post-PSNL. Also, a significant decrease in sucrose preference was observed from day 1 to day 20 post-PSNL. Although this study utilized a different model of neuropathic pain, alterations in nociceptive behaviors were also induced immediately and persisted for approximately four weeks. However, we found that anxiety-like behavior can be maintained for 9 weeks following nerve exposure to a noxious stimulus. Consistent findings were made in regard to depression-like behavior, in which increased immobility during FST did not appear until 2-3 weeks. We recognize that repeated testing of the same cohort during FST could be a limitation, however, vehicle-treated mice did not express adaptation to the assay. The development of anhedonia-like behavior was also similar, during which a decrease in sucrose preference was observed the day following PSNL or paclitaxel

treatment, but the effect only persisted for 11 days post-paclitaxel injection, whereas PSNL induced this behavior until day 20.

Similarly, using sciatic nerve constriction (SNC) in male C57BL/6J mice, Yalcin, et al. (2011) reported that ipsilateral mechanical allodynia persisted for 90 days, and increased anxiety-like behavior in the light/dark box test was observed at 4, 7, and 8 weeks post-SNC, a time-dependent effect similar to that seen in the present study. Latency to first contact and bite the food pellet during the NSF assay was observed at 5 and 8 weeks post-SNC, an effect that appeared earlier in paclitaxel-induced neuropathic pain. Increased immobility in neuropathic mice was observed at 8 and 9 weeks post-SNC during FST, whereas paclitaxel-induced neuropathic pain caused immobility at 2 and 3 weeks post-paclitaxel injection. The differences and similarities amongst these studies illustrate the importance of establishing a clinically relevant model specific to the type of neuropathic pain of interest in order to best determine the responsible mechanisms. Also, these data suggest that multiple pathways and/or brain regions are involved in the manifestation of affective-related behaviors. Yet it remains plausible that paclitaxel administration and models of nerve injury share common mechanisms for the induction of affective-related behaviors.

In conclusion, this work characterizes a preclinical mouse model of both the nociceptive and negative affective symptoms of paclitaxel treatment, which can be utilized to test the efficacy of potential therapeutics for the treatment of paclitaxel-induced side effects, as well as investigate mechanisms of action. In addition, this study allows for the separate investigation of chemotherapy-induced pain-related behaviors in a tumor-free environment, which cannot be ethically accomplished in a clinical setting.

Conflicts of interest

The authors declare no conflicts of interest.

Acknowledgements

This study was supported by NIH grant R01-CA206028 to MID and DAG, and partly supported by pilot funding from the VCU Massey Cancer Center supported, in part, with funding from NIH-NCI Cancer Center Support Grant P30 CA016059.

CHAPTER THREE

Nicotine Prevents and Reverses Paclitaxel-Induced Mechanical Allodynia in a Mouse

Model of CIPN

S. Lauren Kyte¹, Wisam Toma¹, Deniz Bagdas, Julie A. Meade, Lesley D. Schurman, Aron H. Lichtman, Zhi-Jian Chen, Egidio Del Fabbro, Xianjun Fang, John W. Bigbee, M. Imad Damaj, and David A. Gewirtz

Departments of Pharmacology and Toxicology (S.L.K., W.T., D.B., J.A.M., L.D.S., A.H.L., M.I.D., D.A.G.), Neurology (Z.C.), Internal Medicine (E.D.), Biochemistry and Molecular Biology (X.F.), Anatomy and Neurobiology (J.W.B.), and Massey Cancer Center (D.A.G.), Virginia Commonwealth University, Richmond, Virginia; Experimental Animals Breeding and Research Center (D.B.), Uludag University, Bursa, Turkey

¹These authors contributed equally to this work.

Disclosure1: the present work published in Journal of Pharmacology and Experimental Therapeutics 364:110-119

Disclosure2: the *in vitro* experiments regarding the use of nicotine, paclitaxel in different cell lines and assays, and tumor-bearing mice experiments were conducted in Dr. David Gewirtz laboratory, primarily by S. Lauren Kyte

Abbreviations: ANOVA, analysis of variance; CIPN, chemotherapy-induced peripheral neuropathy; DMEM, Dulbecco's modified Eagle's medium; DMSO, dimethylsulfoxide; FBS, fetal bovine serum; IENF, intraepidermal nerve fiber; LLC, Lewis lung carcinoma; MLA, methyllycaconitine; MTS, 3-(4,5-dimethylthiazol-2-yl)-5-(3-carboxymethoxyphenyl)-2-(4-sulfophenyl)-2H-tetrazolium; MTT, 3-(4,5-dimethylthiazol-2-yl)-2,5-diphenyltetrazolium bromide; nAChR, nicotinic acetylcholine receptor; NSCLC, non-small cell lung cancer; PBS, phosphate-buffered saline; PI, propidium iodide.

A. Introduction

Chemotherapy continues to play a significant role in the treatment and survival of cancer patients. However, a number of cancer chemotherapeutic drugs can promote either transient or prolonged tissue and organ toxicities, including chemotherapy-induced peripheral neuropathy (CIPN). CIPN, a result of peripheral nerve fiber dysfunction or degeneration, is characterized by sensory symptoms including: numbness, tingling, burning, hyperalgesia, allodynia, and in some cases neuropathic pain. Approximately 68% of cancer patients experience CIPN within a month following the completion of their treatment, whereas 30% suffer from symptoms of CIPN for 6 months or longer after chemotherapy (Seretny et al., 2014). When CIPN manifests during the administration of chemotherapy, it can become dose-limiting and/or delay treatment, thereby interfering with the full course of treatment that may be required for a positive clinical outcome (Hama and Takamatsu, 2016).

Cancer chemotherapeutic drugs and drug classes associated with peripheral neuropathy include the taxanes (paclitaxel), platinum-based compounds (cisplatin, oxaliplatin), vinca alkaloids (vincristine), and bortezomib. Paclitaxel, a taxane commonly used to treat breast, lung,

and ovarian cancers, increases both progression-free and overall survival in cancer patients (Dranitsaris et al., 2015). Unfortunately, paclitaxel has been found to cause CIPN both acutely and chronically in 59-78% and 30% of cancer patients, respectively (Beijers et al., 2012).

There are currently no effective preventative or therapeutic treatments for CIPN. Opioids, anti-convulsants, anti-depressants, anesthetics, and muscle relaxants either perform modestly in relieving CIPN-induced neuropathic pain, do not show consistent efficacy in the majority of patients, and/or produce intolerable side effects (Majithia et al., 2016; Hershman et al., 2014; Kim et al., 2015).

Nicotine and nicotine analogues have demonstrated potential utility as analgesic and/or antinociceptive drugs, as well as anti-inflammatory agents in both human and experimental pain studies (Umana et al., 2013; Alsharari et al., 2013a; Flood and Damaj, 2014). For example, nicotine elicits analgesic effects in non-smokers suffering from spinal cord injury in a randomized, placebo-controlled, cross-over design experiment (Richardson et al., 2012). Additionally, a recent preclinical study demonstrated that intraperitoneal administration of nicotine at a dose of 1.5 mg/kg reverses allodynia induced by oxaliplatin, a chemotherapeutic agent used to induce peripheral neuropathy in rats (Di Cesare Mannelli et al., 2013).

The studies described in this report characterize the antinociceptive and/or neuroprotective effects of nicotine in a CIPN mouse model, while further evaluating the influence of nicotine on lung tumor cell proliferation and sensitivity to the anti-tumor properties of paclitaxel.

B. Materials and Methods

Animals. Adult male C57BL/6J mice (8 weeks at the beginning of experiments, 20-30 g) were purchased from The Jackson Laboratory (Bar Harbor, ME). Mice were housed in an AAALAC-accredited facility in groups of four; the mice in each cage were randomly allocated to different treatment groups. Food and water were available *ad libitum*. Experiments were performed during the light cycle (7:00 am to 7:00 pm) and were approved by the Institutional Animal Care and Use Committee of Virginia Commonwealth University and followed the National Institutes of Health Guidelines for the Care and Use of Laboratory Animals. Animals were euthanized via CO₂ asphyxiation followed by cervical dislocation. Any subjects that showed behavioral disturbances unrelated to chemotherapy-induced pain were excluded from further behavioral testing.

Drugs. Paclitaxel was purchased from Tocris (1097, Bristol, United Kingdom) and dissolved in a mixture of 1:1:18 [1 volume ethanol/1 volume Emulphor-620 (Rhone-Poulenc, Inc., Princeton, NJ)/18 volumes distilled water]. Paclitaxel injections were administered intraperitoneally (i.p.) every other day for a total of four injections to induce neuropathy, as previously described by Toma et al., (2017). (-)-Nicotine hydrogen tartrate salt and mecamlamine HCl were purchased from Sigma-Aldrich (St. Louis, MO, USA) and dissolved in 0.9% saline. For acute administration, nicotine was injected i.p. at doses of 0.3, 0.6, or 0.9 mg/kg (Bagdas et al., 2017; Di Cesare Mannelli et al., 2013). Nicotine at doses of 6, 12, or 24 mg/kg/day was also administered chronically via 7-day subcutaneous (s.c.) osmotic minipumps (Alzet, Model 1007D, Cupertino, CA), which were implanted 2 days prior to paclitaxel treatment (Alsharari et al., 2015). Mecamlamine was administered at a dose of 2 mg/kg s.c. 15 minutes before administration of nicotine or saline (Bagdas et al., 2014). Methyllaconitine (MLA) was purchased from RBI (Natick, MA, USA)

and administered at a dose of 10 mg/kg s.c. 10 minutes before administration of nicotine (Freitas et al., 2013). All doses were chosen based on previous works that demonstrated which dose, time of exposure, and route of administration for each drug effectively acted upon the appropriate receptor and was not toxic to the animal. All i.p. or s.c. injections were given in a volume of 1 ml/100 g body weight, whereas the osmotic minipumps released 0.5 µl/hour.

Immunohistochemistry and quantification of intra-epidermal nerve fibers. The hind paw epidermis was collected from the following groups of mice: vehicle-saline, vehicle-nicotine (24 mg/kg/day), paclitaxel (8 mg/kg)-saline, and paclitaxel (8 mg/kg)-nicotine (24 mg/kg/day). The staining procedure was performed as previously described (Toma et al., 2017). Briefly, the glabrous skin of the hind paw was excised, placed in freshly prepared 4% paraformaldehyde in 0.1 M PBS (pH 7.4), and stored overnight at 4 °C in the same fixative. The samples were embedded in paraffin, sectioned at 25 µm, and stained with PGP9.5 (Fitzgerald - 70R-30722, MA, USA) and goat anti-rabbit IgG (H+L) secondary antibody conjugated with Alexa Fluor® 594 (Life Technologies - A11037, OR, USA). Sections were examined using a Zeiss Axio Imager A1 – Fluorescence microscope (Carl Zeiss, AG, Germany) in a blinded fashion under 63x magnification, but imaged under 40x magnification; the density of fibers is expressed as fibers/mm.

Mechanical allodynia evaluation (von Frey test). Mechanical allodynia thresholds were determined using von Frey filaments according to the method suggested by Chaplan et al. (1994) and as described previously (Bagdas et al., 2015). The mechanical threshold is expressed as log₁₀ (10 £ force in [mg]). For the nicotine-mediated reversal of CIPN experiment, paclitaxel-treated

mice were tested for mechanical allodynia following acute nicotine administration on days 7-14 following the initial paclitaxel injection. All behavioral testing on animals was performed in a blinded manner.

Minipump Implantation. The procedure was performed as previously described in Alsharari et al. (2013) with minor modifications. Mice were anesthetized with 2.5% isoflurane/ 97.5% oxygen. The anesthetized mice were prepared by shaving of the back and swabbing with betadine, followed by 70% ethanol pads. Sharp, sterile scissors was used to make a 1 cm incision in the skin of the upper back/neck. The sterile, preloaded minipump (Alzet, Model 1007D, Cupertino, CA) with different doses of nicotine or saline was inserted with sterile forceps by a technician wearing sterile gloves. The wound was closed with sterile 9 mm stainless steel wound clips. The mice were allowed to recover on heated pads and were monitored before returning to their home cages.

Cell culture. All lung cancer cells were maintained in DMEM supplemented with 10% (v/v) fetal bovine serum (FBS, Serum Source International, FB22-500HI, NC, USA) and 1% (v/v) combination of 10,000 U/ml penicillin and 10,000 µg/ml streptomycin (Pen/Strep, ThermoFisher Scientific, 15140-122, Carlsbad, CA), unless stated otherwise. Cells were incubated at 37°C under a humidified, 5% CO₂ atmosphere. The H460 non-small cell lung cancer (NSCLC) cell line was generously provided by the laboratory of Dr. Richard Moran at Virginia Commonwealth University (VCU), the A549 NSCLC cell line was a gift from the laboratory of Dr. Charles Chalfant at VCU, and the Lewis lung carcinoma (LLC) cells were provided by Dr. Andrew Larner at VCU. In order to establish the T1 primary lung cancer cell line, tissues were obtained from adenocarcinoma tumors in accordance with the VCU IRB protocol. Tissues were minced well and

washed multiple times by centrifugation in sterile PBS. Thereafter, the tissues were resuspended in DMEM. Tissue homogenates were layered on collagen (Sigma-Aldrich, C3867, St. Louis, MO)-coated plates. Cell colonies started to appear after 2-3 weeks. Upon confluence, the cells were trypsinized and passaged. The ovarian cancer cell lines, SKOV-3/DDP and OVCAR-3, were generously provided by the laboratory of Dr. Xianjun Fang at VCU and were cultured in RPMI160 supplemented with 10% (v/v) FBS and 1% (v/v) Pen/Strep.

Paclitaxel was dissolved in DMSO, diluted with sterile PBS, and added to the medium in order to obtain the desired concentration. Staurosporine (Sigma-Aldrich, S6942, St. Louis, MO) was purchased as 1 mM in DMSO. Cells were not exposed to greater than 0.1% DMSO in any experiment. (-)-Nicotine hydrogen tartrate salt was dissolved in sterile PBS. All experiments involving these light-sensitive drugs were performed in the dark.

Assessment of cell viability. Cell viability was measured by either the 3-(4,5-dimethylthiazol-2-yl)-2,5-diphenyltetrazolium bromide (MTT)/3-(4,5-dimethylthiazol-2-yl)-5-(3-carboxymethoxyphenyl)-2-(4-sulfophenyl)-2H-tetrazolium (MTS) colorimetric assay or trypan blue exclusion. For the MTT/MTS assay, cells were seeded in 96-well plates and treated with various concentrations of nicotine for 24 hours, at which time the drug was removed and replaced with fresh medium. Depending on the replication rate of the cell line, the cells were allowed 24 or 48 hours to proliferate following drug exposure. For the serum deprivation study, cells were seeded in DMEM (10% FBS) for 24 hours, then the medium was removed and replaced with DMEM supplemented with various concentrations of FBS (0-10%) with or without nicotine (1 μ M); cell viability was assessed at either 48 or 96 hours post-treatment without drug removal. At the time of

testing, the medium was removed, then the cells were washed with PBS and stained with thiazolyl blue tetrazolium bromide (MTT, 2 mg/ml; Sigma-Aldrich, M2128, St. Louis, MO) in PBS for 3 hours. The MTT solution was aspirated and replaced with DMSO. The color change was measured by a spectrophotometer (ELx800UV, BioTek, VT) at 490 nm. To avoid potentially aspirating cells, the CellTiter 96[®] Aqueous One Solution Cell Proliferation Assay (MTS; Promega, G358C, Madison, WI) was utilized for less adherent cell lines (A549, LLC, and T1); the use of MTS rather than MTT eliminates washing steps before and after staining.

For trypan blue exclusion, cells were incubated with trypsin (0.25% trypsin-EDTA) for 3 minutes, stained with trypan blue (Invitrogen, 15250, Carlsbad, CA), and the viable, unstained cells were counted using a hemocytometer with bright-field microscopy.

Assessment of colony formation. Cells were seeded at a low density in DMEM (10% FBS). After 24 hours, the paclitaxel and paclitaxel + nicotine samples were exposed to paclitaxel (50 nM) for 24 hours, after which the medium was replaced with fresh, drug-free medium. After 24 hours, the nicotine and paclitaxel + nicotine samples were exposed to nicotine (1 μ M) for 24 hours, after which the medium was replaced with fresh, drug-free medium. Once the control colonies reached a size of 50 cells per colony (approximately 8-10 days after seeding), the samples were fixed with methanol, stained with crystal violet, and quantified (ColCount, Discovery Technologies International).

Assessment of apoptosis and DNA content. Flow cytometry analyses were performed using BD FACSCanto II (BD Biosciences, San Jose, CA) and BD FACSDiva software at the Virginia

Commonwealth University Flow Cytometry Core facility. For all studies, 10,000 cells per replicate within the gated region were analyzed. When collecting samples, both adherent and floating cells were harvested with 0.1% trypsin-EDTA and neutralized with medium after 48 hours of drug exposure. For quantification of apoptosis, cells were centrifuged and washed with PBS, then resuspended in 100 μ l of 1x binding buffer with 5 μ l of Annexin V and 5 μ l of propidium iodide (BD Biosciences, FITC Annexin V Apoptosis Detection Kit, 556547, San Jose, CA). The samples were then incubated at room temperature while protected from light for 15 minutes. The suspension solution was then brought up to 500 μ l using the 1x binding buffer and analyzed by flow cytometry. For quantification of DNA content, the cells were resuspended in 500 μ l of a propidium iodide (PI) solution (50 μ g/ml PI, 4 mM sodium citrate, 0.2 mg/ml DNase-free RNase A, and 0.1% Triton-X 100) for 1 hour at room temperature, while being protected from light (Tate et al., 1983). Before flow cytometry analysis, NaCl was added to the cell suspensions to achieve a final concentration of 0.20 M.

Assessment of tumor growth *in vivo*. Male C57BL/6J adult mice were subcutaneously injected with 1.5×10^6 Lewis lung carcinoma (LLC) cells in both flanks. The LLC cells were collected via trypsinization, then neutralized with medium, centrifuged, and washed with PBS. Pellets of 1.5×10^6 LLC cells were then resuspended in 30 μ l of 80% basement membrane extract (Trevigen, 3632-010-02, Gaithersburg, MD)/20% PBS. Mice were anesthetized with isoflurane via inhalation during tumor cell injection. Palpable tumors formed at approximately 7 days post-tumor cell injection, and on day 11 tumor volumes ($l \times w \times h$) were sufficient to be assessed with calipers; subsequent tumor volume measurements were collected every other day. Subcutaneous osmotic minipumps (Alzet, Model 1007D, Cupertino, CA) were implanted as previously described at 13

days post-tumor cell injection to release 24 mg/kg nicotine daily for a total of 7 days. Body weight and tumor volume were observed until humane endpoints were reached, at which time mice were euthanized via CO₂ asphyxiation followed by cervical dislocation.

Statistical analyses. A power analysis calculation was performed with the Lamorte's Power Calculator (Boston University Research Compliance) to determine the sample size of animals for each group (Charan and Kantharia, 2013). For assessing nociceptive behavior and tumor volume, the calculations showed that an n of 5 was required to achieve a power of 90% with an alpha error of 0.05; we used 8 mice per group for the nociceptive assay and 5-6 mice per group for the *in vivo* cancer study. The data were analyzed with GraphPad Prism software, version 6 (GraphPad Software, Inc., La Jolla, CA) and SPSS, version 24, and are expressed as mean \pm SEM. One- and two-way analysis of variance (ANOVA) tests were conducted and followed by the Bonferroni post hoc test, three-way mixed factor ANOVAs were performed and followed by the Sidak post hoc test, and linear mixed models were conducted to account for the loss of tumor-bearing mice (Little and Rubin, 1987); repeated measures were considered for all *in vivo* studies. Differences were determined to be significant at $P < 0.05$.

C. Results

Nicotine reverses and prevents paclitaxel-induced mechanical allodynia. Initial experiments were designed to determine if acute administration of nicotine reverses paclitaxel-induced mechanical allodynia. **Fig. 12A** demonstrates that nicotine reversed mechanical allodynia in paclitaxel-treated mice in a time- and dose-dependent manner [$F_{\text{time} \times \text{dose}}(18, 126) = 17.10, P < 0.0001$], with full reversal (mechanical threshold values restored to baseline levels) following administration of 0.9 mg/kg and partial reversal with 0.6 mg/kg. Nicotine did not alter mechanical

thresholds in vehicle-treated mice [$F_{\text{time} \times \text{dose}} (18, 126) = 0.6122, P = 0.88$] (**Supplemental Fig. 5**).

Having demonstrated that nicotine reversed the allodynic effect of paclitaxel, the next series of experiments was designed to investigate whether nicotine also *prevents* the development of paclitaxel-induced nociceptive (allodynic) responses. Seven days of nicotine (24 mg/kg/day) administration prevented the development of mechanical allodynia throughout the entire duration of the experiment, up to 35 days post-paclitaxel injection [$F (9, 252) = 6.703, P < 0.001$; **Fig. 12B**]. As shown in **Supplemental Figure 6**, 6 mg/kg/day and 12 mg/kg/day nicotine did not prevent the development of paclitaxel-induced mechanical allodynia.

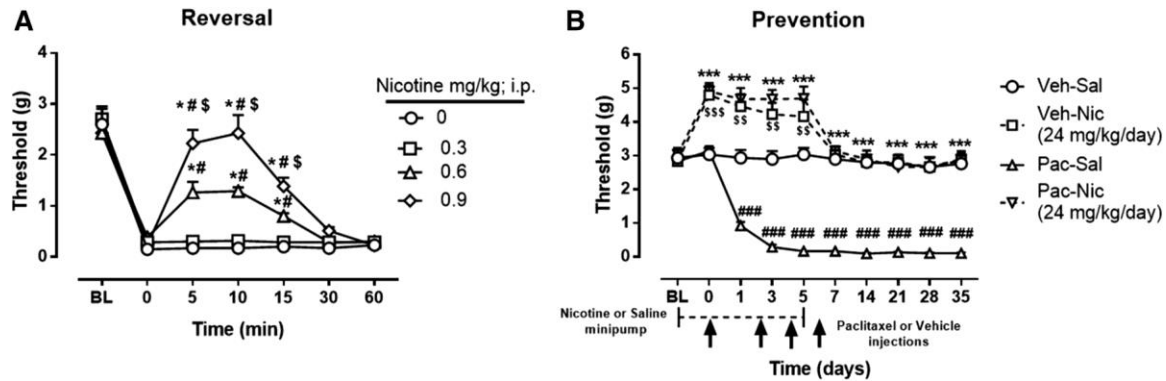
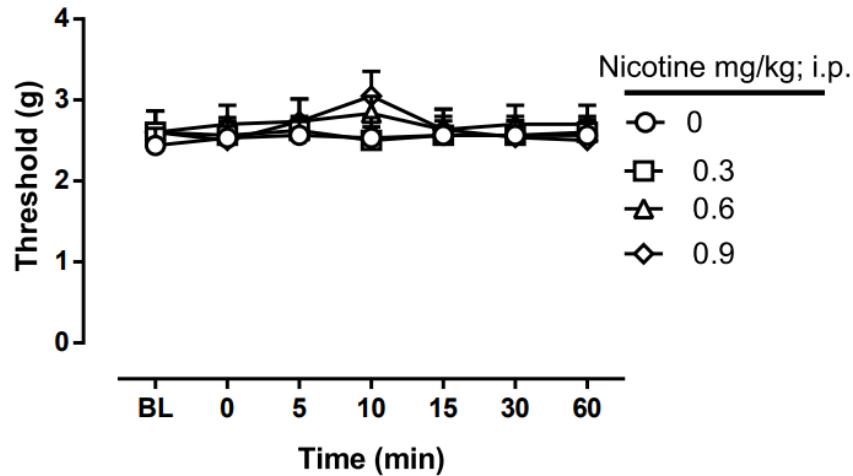
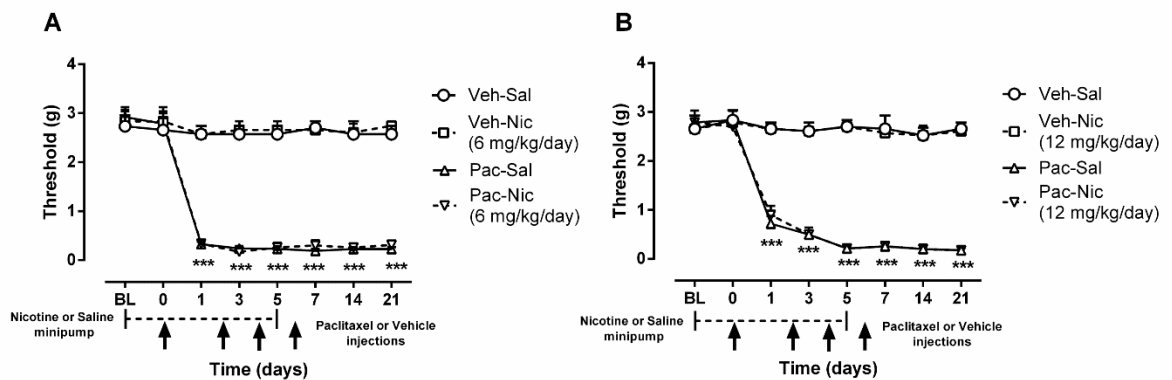


Figure 12. Antinociceptive and preventative effect of nicotine in a mouse model of paclitaxel-induced peripheral neuropathy. Reversal of mechanical allodynia by acute administration of nicotine at doses of 0.3, 0.6, and 0.9 mg/kg i.p. in paclitaxel-treated mice at day 7-14 post-initial paclitaxel injection (A). $^{*}P < 0.0001$ vs Saline (0 mg/kg); $^{*}P < 0.0001$ vs nicotine (0.3 mg/kg); $^{*}P < 0.0001$ vs nicotine (0.6 mg/kg). Prevention of mechanical allodynia by chronic administration of nicotine at a dose of 24 mg/kg/day (B). Arrows indicate vehicle/paclitaxel injections on days 0, 2, 4, and 6. Minipumps with nicotine were implanted s.c. in the mouse, starting 2 days before the vehicle/paclitaxel treatment cycle and ending on day 5. Baseline measurements were taken at BL before saline/nicotine minipump implantation and on day 0 before paclitaxel/vehicle administration. $^{***}P < 0.001$ Pac-Nic vs Pac-Sal; $^{###}P < 0.001$ Pac-Sal vs Veh-Sal; $^{$$$}P < 0.001$, $^{$$}P < 0.01$ Veh-Nic vs Veh-Sal. BL, baseline; Veh, vehicle; Sal, saline; Nic, nicotine; Pac, paclitaxel. $n = 8$ per group; data expressed as mean \pm SEM. *Statistical analysis:* For mice treated with 24 mg/kg nicotine, a $2 \times 2 \times 10$ Mixed Factor ANOVA of chemotherapy drug (paclitaxel or vehicle) in nicotine- or saline-treated mice by day showed a significant 3-way interaction [$F(9, 252) = 7.851$, $P < 0.001$]. A subsequent 2×10 Mixed Factor ANOVA of paclitaxel or vehicle treatment by day was calculated for each level of treatment (nicotine or saline). Saline-treated mice demonstrated a significant interaction of chemotherapy drug (paclitaxel or vehicle) by day [$F(9, 252) = 15.054$, $P < 0.001$], where a Sidak post hoc test revealed lower threshold responding in paclitaxel-treated mice compared to vehicle-treated mice on days 0 - 35 ($P < 0.001$). A separate 2×10 Mixed Factor ANOVA calculated where nicotine or saline treatment by day differed at each level of chemotherapy drug (paclitaxel or vehicle). Paclitaxel-treated mice demonstrated a significant interaction of drug pre-treatment (nicotine or saline) by day [$F(9, 252) = 6.703$, $P < 0.001$], where a Sidak post hoc test revealed higher threshold responding in nicotine-treated mice compared to saline-treated mice on days 0 - 35 ($P < 0.001$). Vehicle-treated mice also demonstrated a significant interaction of drug pre-treatment (nicotine or saline) by day [$F(9, 252) = 37.064$, $P < 0.001$], where a Sidak post hoc test revealed higher threshold responding in nicotine-treated mice compared to saline-treated mice, but only on days 0, 1, and 3 ($P < 0.001$).



Supplemental Figure 5. Acute administration of nicotine at doses of 0.3, 0.6, and 0.9 mg/kg i.p. does not affect mechanical threshold in vehicle-treated mice. BL, baseline. n = 8 per group; data expressed as mean \pm SEM.



Supplemental Figure 6. Nicotine at doses of 6 and 12 mg/kg/day do not prevent paclitaxel-induced mechanical allodynia. Arrows indicate vehicle/paclitaxel injections on days 0, 2, 4, and 6. Minipumps with nicotine, 6 mg/kg/day (A) or 12 mg/kg/day (B), were implanted s.c. in the mouse, starting 2 days before the vehicle/paclitaxel treatment cycle and ending on day 5. Baseline measurements were taken at BL before saline/nicotine minipump implantation and on day 0 before paclitaxel/vehicle administration. *** $P < 0.001$ Pac-treated mice compared to Veh-treated mice. BL, baseline; Veh, vehicle; Sal, saline; Nic, nicotine; Pac, paclitaxel. n = 6 per group; data expressed as mean \pm SEM. *Statistical analysis:* Comparisons were made between chemotherapy treatments (paclitaxel or vehicle) in nicotine- or saline-treated mice by day for both 6 and 12 mg/kg/day doses of nicotine in a 2 x 2 x 8 Mixed Factor ANOVA. The 6 mg/kg [$F(7, 140) = 0.139$, $P = 0.995$] and 12 mg/kg [$F(7, 140) = 0.054$, $P = 1.000$] nicotine 3-way interactions were not significant. However, both 6 mg/kg [$F(7, 140) = 58.597$, $P < 0.001$] and 12 mg/kg [$F(7, 140) = 42.647$, $P < 0.001$] nicotine produced a significant day by chemotherapy drug interaction, where paclitaxel-treated mice demonstrated lower threshold compared to vehicle-treated mice on days 1, 3, 5, 7, 14, and 21 when compared to both baseline and day 0 responding ($P < 0.001$) as evaluated by Sidak post hoc tests.

To examine the possibility that nicotinic acetylcholine receptors (nAChRs) mediate the antinociceptive effect of nicotine, mecamylamine, a non-selective nAChR antagonist, was administered prior to nicotine. Mecamylamine effectively blocked the antinociceptive effect of nicotine in paclitaxel-treated mice [$F_{\text{time} \times \text{dose}} (6, 42) = 10.38, P < 0.0001$; **Fig. 13A**]. To begin determining which nAChR subtypes are involved in the reversal of paclitaxel-induced mechanical allodynia, we administered MLA, an $\alpha 7$ nAChR antagonist, before nicotine treatment, which effectively blocked the antinociceptive effect of nicotine in paclitaxel-treated mice [$F_{\text{time} \times \text{dose}} (6, 42) = 15.58, P < 0.0001$; **Fig. 13B**].

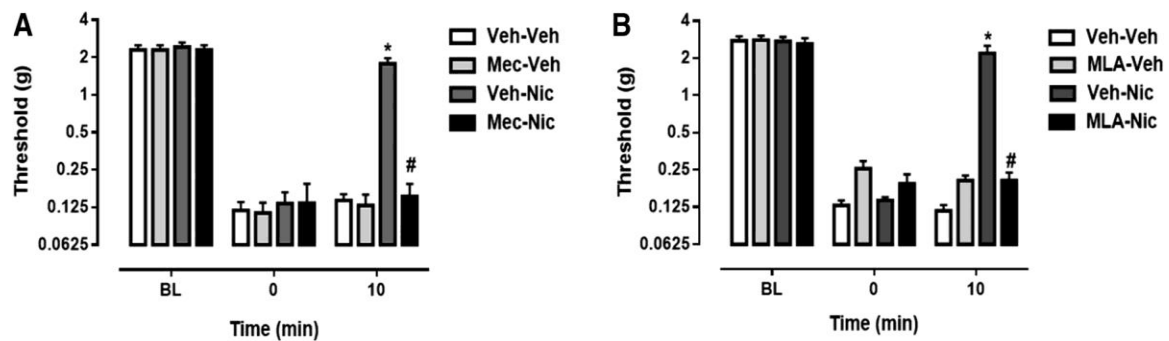


Figure 13. The antinociceptive effect of nicotine is mediated by nicotinic acetylcholine receptors. Mecamylamine, a non-selective nAChR antagonist, was injected at a dose of 2 mg/kg s.c. 15 minutes prior to nicotine to block the nicotine-mediated (0.9 mg/kg, i.p.) reversal of mechanical allodynia in paclitaxel-treated mice (A). MLA, an $\alpha 7$ nAChR antagonist, was administered at a dose of 10 mg/kg s.c. 10 minutes before nicotine treatment (0.9 mg/kg, i.p.) in paclitaxel-treated mice. * $P < 0.0001$ Veh-Nic at 10 min vs 0 min; # $P < 0.0001$ Mec-Nic or MLA-Nic vs Veh-Nic at 10 min. Veh, vehicle; Nic, nicotine; Mec, mecamylamine. MLA, methyllycaconitine. $n = 8$ per group; data expressed as mean \pm SEM.

Nicotine prevents paclitaxel-induced reduction of intra-epidermal nerve fibers. A decrease in the intra-epidermal nerve fiber (IENF) density in the paw epidermis is a common marker for evaluating CIPN in rodent models (Bennett et al., 2011). To determine if nicotine also protects the IENFs from the toxic effect of paclitaxel, mice were treated with vehicle or paclitaxel (8 mg/kg, i.p.) and implanted with minipumps releasing saline or nicotine (24 mg/kg/day), and sacrificed 35 days following the first paclitaxel injection, when their hind paw epidermis was collected for immunohistochemical analysis. Quantification of IENFs revealed a significant overall interaction between paclitaxel and nicotine treatment [$F_{\text{paclitaxel} \times \text{nicotine}}(1, 28) = 11.58, P < 0.01$; **Fig. 14A**]. As illustrated in **Fig. 14B**, mice treated with paclitaxel-saline demonstrated a significant decrease in IENF density when compared to vehicle-saline-treated mice ($P < 0.0001$). In contrast, paclitaxel-nicotine-treated mice showed a significant increase in IENF density when compared to paclitaxel-saline-treated mice ($P < 0.01$). Paclitaxel-nicotine-treated mice did not show a change in the IENF density when compared to vehicle-nicotine-treated mice ($P = 0.54$) and vehicle-nicotine-treated mice did not exhibit an alteration in IENF density when compared to the vehicle-saline group ($P = 0.53$).

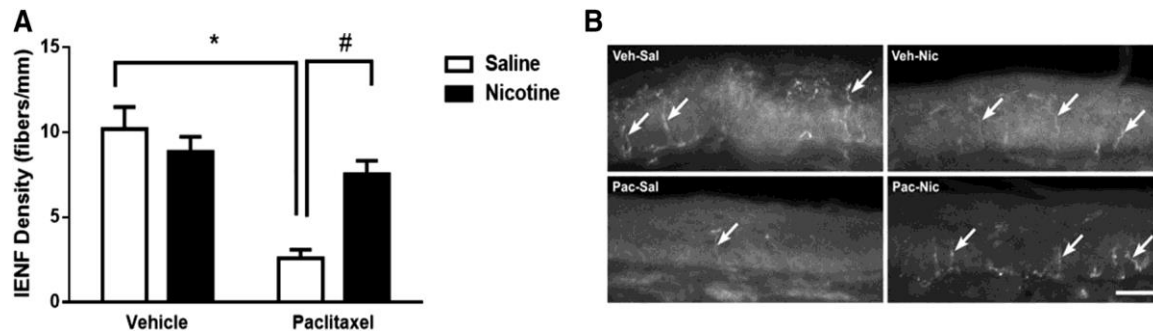


Figure 14. Paclitaxel induces a decrease in IENF density at 35 days post-paclitaxel injection, which is prevented by nicotine administration at a dose of 24 mg/kg/day s.c. Paclitaxel at a dose of 8 mg/kg i.p. significantly decreased IENF density compared to vehicle-saline and paclitaxel-nicotine groups (A). * $P < 0.05$ paclitaxel-saline vs vehicle-saline; # $P < 0.05$ paclitaxel-nicotine vs paclitaxel-saline. Immunostained sections of hind paw epidermis represent the reduction of IENF density by paclitaxel and protection by nicotine (B). Bar represents 20 microns in all images, which were captured under 40x magnification. IENF, intra-epidermal nerve fiber; Veh, vehicle; Sal, saline; Nic, nicotine; Pac, paclitaxel. $n = 8$ per group; data expressed as mean \pm SEM.

Collectively, the behavioral and immunohistochemical studies presented in Figures 1-3 indicate that nicotine reverses paclitaxel-induced mechanical allodynia, via the $\alpha 7$ nAChR, but also protects against paclitaxel-induced mechanical allodynia and IENF loss. However, multiple reports have argued that nicotine can stimulate tumor growth or interfere with cancer chemotherapeutic drug-induced apoptosis, which would severely limit the potential utility of nicotine in the clinic (Zhang et al., 2009; Pillai et al., 2011; Wu et al., 2013; Liu et al., 2015; Dasgupta et al., 2006). As a review of the relevant literature revealed a number of inconsistencies (see Discussion), we re-evaluated the effect of nicotine on tumor cell proliferation and paclitaxel-induced apoptosis.

Nicotine fails to stimulate lung cancer cell proliferation or interfere with paclitaxel-induced cytotoxicity. Initial experiments were performed by utilizing the MTT/MTS colorimetric assay with both A549 and H460 cells, two commonly used experimental models of non-small cell lung cancer (NSCLC) that express multiple nAChRs (Tsurutani et al., 2005; Dasgupta et al., 2006; Yoo et al., 2014). Figure 4 indicates that 48 and 96-hour exposure to nicotine (1 μ M) did not induce a significant increase in viable cell number when compared to untreated cells under both normal (10% FBS) and serum deprivation (0-5% FBS) conditions in A549 (**Fig. 15A**) and H460 (**Fig. 15B**) cells. The only observed effect was a significant increase in viable cell number under serum starvation (0% FBS) conditions in one cell line at a single time point (**Fig. 15B**).

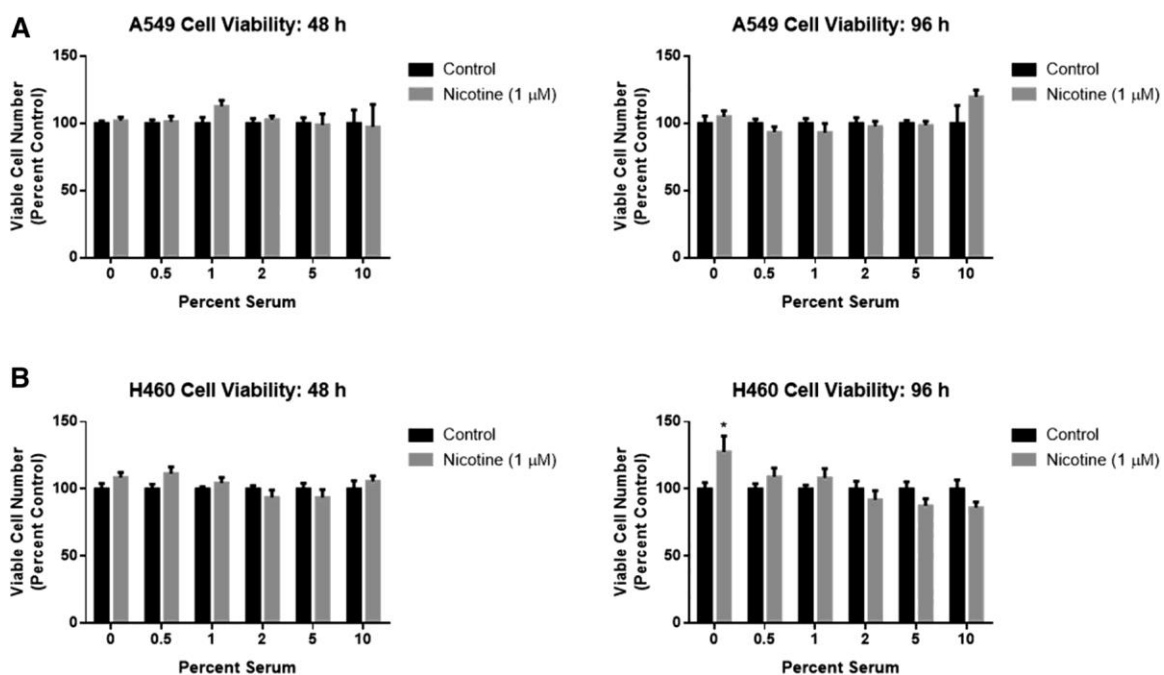
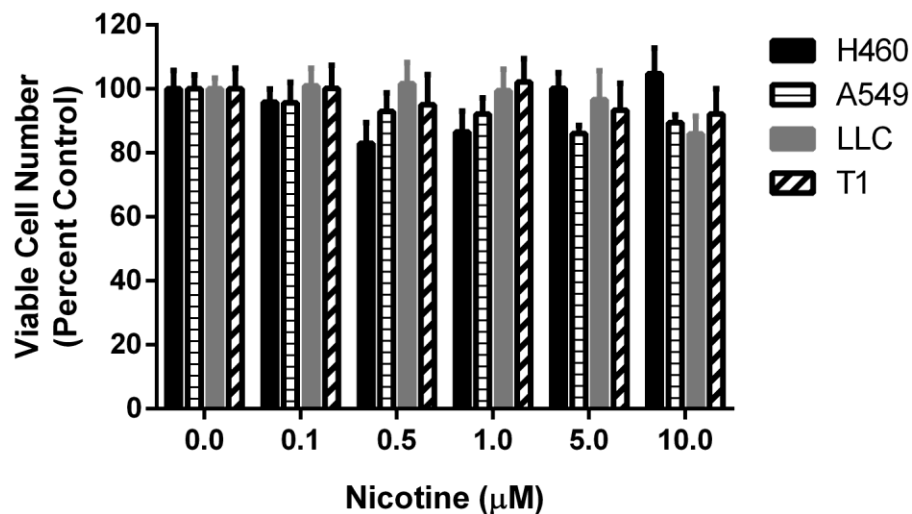


Figure 15. Nicotine fails to enhance NSCLC viable cell number under normal and serum-deprivation conditions. A549 and H460 cells were treated with nicotine (1 μ M) for 48 or 96 hours in DMEM supplemented with various concentrations of FBS. Viability was determined with an MTT or MTS colorimetric assay. * $P < 0.05$ vs control with 0% serum. Data are expressed as the mean + SEM of three independent experiments.

The influence of various concentrations of nicotine on tumor cell proliferation was further investigated under full serum (10% FBS) conditions that are the standard for cancer cell studies. Again, exposure to a range of nicotine concentrations (0.1-10 μ M) for 24 hours under full serum conditions did not significantly increase numbers of viable A549, H460, Lewis lung carcinoma (LLC), or T1 (primary lung cancer) cells (**Supplemental Fig. 7**).



Supplemental Figure 7. Nicotine fails to enhance viable lung cancer cell number. NSCLC cells (A549, H460), Lewis lung carcinoma (LLC) cells, and human primary lung tumor cells (T1) were treated with nicotine for 24 h. Viability was determined with an MTT/MTS colorimetric assay. A one-way ANOVA followed by the Bonferroni post hoc test revealed no significant differences ($P > 0.05$) between control (0.0 μ M) and any nicotine-treated cells within each cell line. Data are expressed as mean + SEM of two independent experiments.

Additional studies were designed to more closely mimic the potential use of nicotine following chemotherapy treatment in the clinic. NSCLC cells were first exposed to paclitaxel (50 nM) for 24 hours, followed by a 24-hour drug-free period, and subsequent treatment with nicotine (1 μ M) for 24 hours. Paclitaxel significantly decreased the number of A549 and H460 colonies, and the impact of paclitaxel was not altered by nicotine; nicotine alone did not stimulate colony formation (**Fig. 16**).

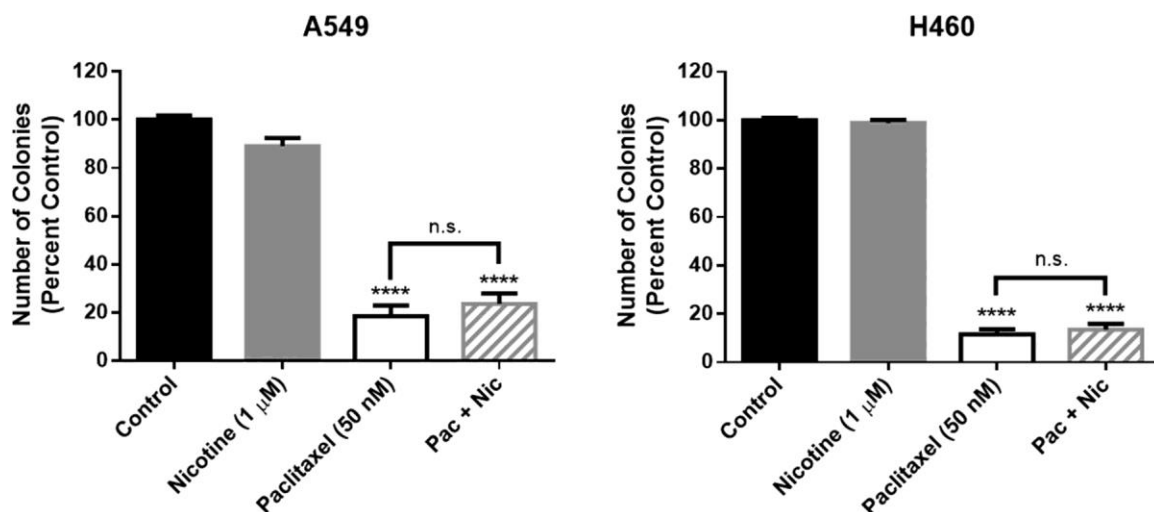


Figure 16. Nicotine fails to stimulate NSCLC colony formation alone or following paclitaxel treatment. For the single drug treatment conditions, A549 and H460 cells were exposed to nicotine (1 μ M) or paclitaxel (50 nM) for 24 h. For the combination treatment, cells were first exposed to paclitaxel for 24 h, followed by a 24 h drug-free period, then treatment with nicotine for 24 h. Colony number was determined by crystal violet staining. **** $P < 0.0001$ vs control; n.s., not significant. Data are expressed as the mean + SEM of three independent experiments.

In previous work (Alotaibi et al., 2016; Emery et al., 2014; Jones et al., 2005; Roberson et al., 2005; Efimova et al., 2010; Webster et al., 2015), we and others have reported that growth arrest induced by cancer therapy is transient and that tumor cells recover proliferative capacity within 7-10 days post-treatment. In order to determine if prior exposure to nicotine stimulates proliferation and/or promotes early tumor cell recovery from paclitaxel-induced growth arrest, NSCLC cell proliferation was monitored for a period of 7 days after treatment with nicotine (1 μ M, 48 hours), paclitaxel (50 nM, 24 hours), or a combination of the two drugs, which consisted of a 24-hour nicotine pretreatment period preceding 24-hour co-treatment. Nicotine did not stimulate the proliferation of either the A549 or H460 cells throughout the duration of the assay, and even induced a slight but significant decrease in H460 cell number on Day 5 (Fig. 17). Most importantly, nicotine did not interfere with the paclitaxel-induced decrease in viable cell number at any time point (Fig. 17). Furthermore, nicotine did not promote an early proliferative recovery in either cell line (Insets of Fig. 17).

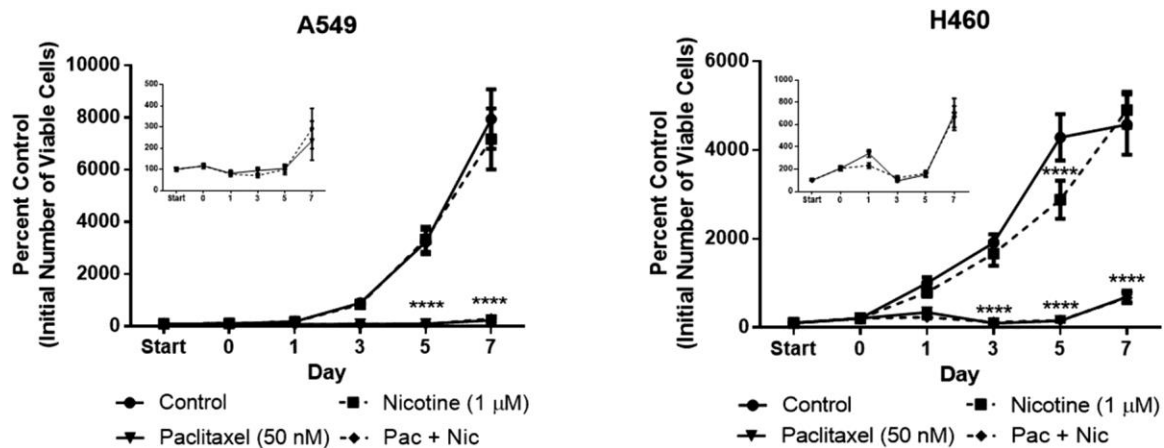


Figure 17. Nicotine fails to stimulate NSCLC cell proliferation alone or interfere with paclitaxel-induced growth inhibition of NSCLC cells. The “start” time point represents the initial number of cells after seeding. A 24-hour nicotine pretreatment period occurred from Start to Day 0 for the Nicotine and Pac + Nic conditions, then all subsequent treatments lasted 24 hours; no drugs were present after Day 1. The number of cells was determined via trypan blue exclusion. **** P < 0.0001 vs control. Data are expressed as the mean \pm SEM of three independent experiments.

Although we failed to detect any interference with the anti-tumor activity of paclitaxel in two different assays, other studies have argued that nicotine suppresses paclitaxel-induced apoptosis (Tsurutani et al., 2005; Dasgupta et al., 2006). Consequently, additional experiments were performed to evaluate the effects of nicotine on paclitaxel-induced apoptosis. Paclitaxel (100 nM) induced significant apoptosis in both the A549 and H460 cells after 48 hours of treatment (**Fig. 18A**). Most importantly, nicotine (1 μ M) did not interfere with the promotion of paclitaxel-induced apoptosis in either NSCLC cell line following co-treatment (**Fig. 18A**); staurosporine (2 μ M), a non-selective protein kinase inhibitor, induced significant apoptosis and was used as a positive control. Similarly, cell cycle analysis revealed that paclitaxel (100 nM) induces significant sub-G1 fragmented DNA content, an indicator of late-stage cell death, in both A549 and H460 cells, and that nicotine does not attenuate this effect (**Fig. 18B**).

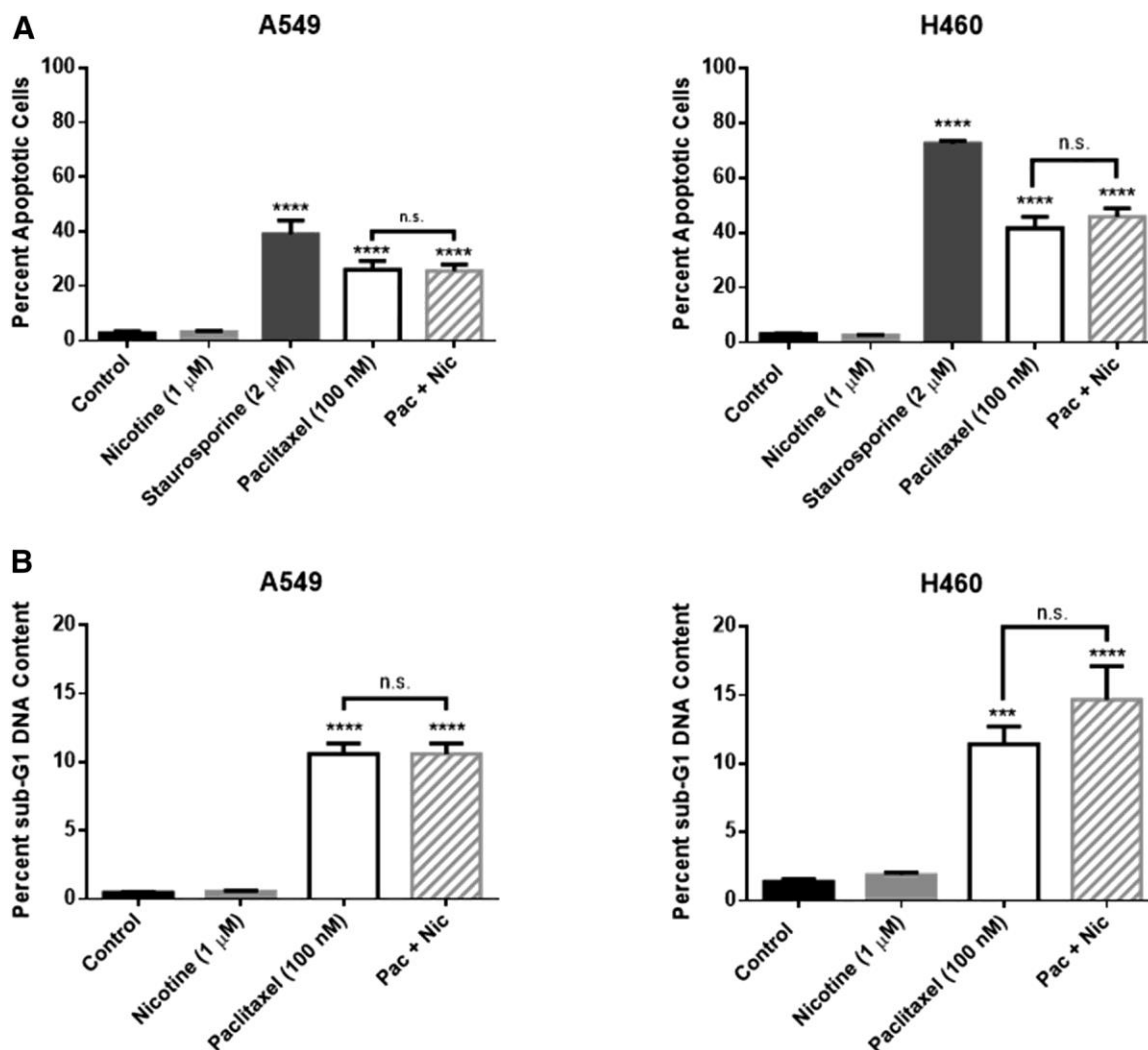
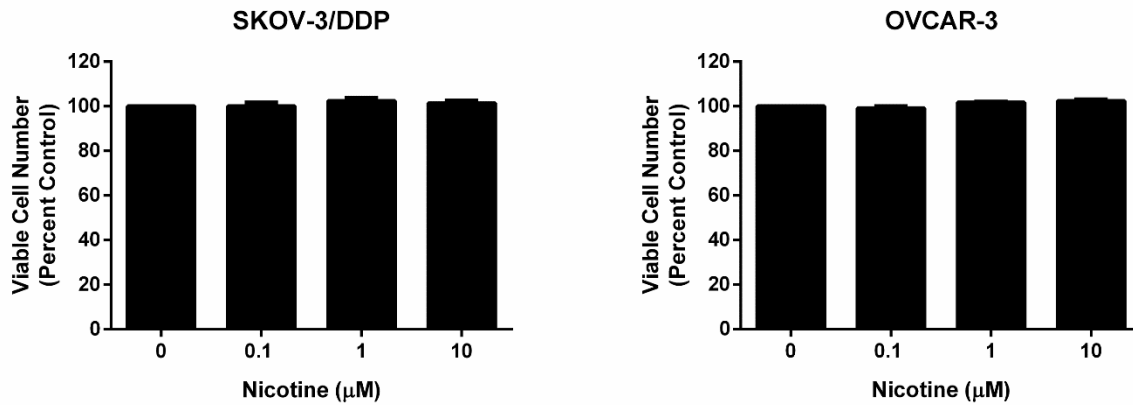


Figure 18. Nicotine fails to interfere with paclitaxel-induced apoptosis (A) and sub-G1 DNA content (B) of NSCLC cells. A549 and H460 cells were treated with nicotine (1 μ M), staurosporine (2 μ M), paclitaxel (100 nM), or the combination of paclitaxel and nicotine for 48 h. Quantification of apoptotic cells and sub-G1 DNA content was determined by the Annexin V/PI assay and propidium iodide staining, respectively, followed by flow cytometry analysis. *** P < 0.001, **** P < 0.0001 vs control; n.s., not significant. Data are expressed as mean + SEM of three (A) or two (B) independent experiments.

To ensure that our observations applied to other cancer types commonly treated with paclitaxel, we also evaluated the effects of nicotine on cancer cell proliferation in two human ovarian cancer cell lines. As was the case with the lung cancer cells, nicotine did not stimulate ovarian cancer cell proliferation in SKOV-3/DDP and OVCAR-3 cells (**Supplemental Fig. 8**).



Supplemental Figure 8. Nicotine fails to stimulate ovarian cancer cell proliferation. SKOV-3/DDP and OVCAR-3 cells were treated with nicotine for 48 h, then counted via trypan blue exclusion. A one-way ANOVA followed by the Bonferroni post-hoc test revealed no significant differences ($p > 0.05$) between any concentration of nicotine vs. control (0 μM) in each cell line. Data are expressed as mean + SEM of one representative study of two independent experiments

To investigate whether the *in vitro* findings are indicative of tumor cell responses *in vivo*, immunocompetent C57BL/6J mice were subcutaneously injected with LLC cells in the flank, a commonly used syngeneic model of lung cancer (Kellar et al., 2015). Once the tumors formed, the mice were treated with nicotine at a dose of 24 mg/kg/day for 7 days via a subcutaneous osmotic minipump in order to mimic the nicotine treatment regimen administered in the peripheral neuropathy studies. In accordance with the *in vitro* findings, chronic administration of nicotine failed to enhance LLC tumor growth (**Fig. 19**).

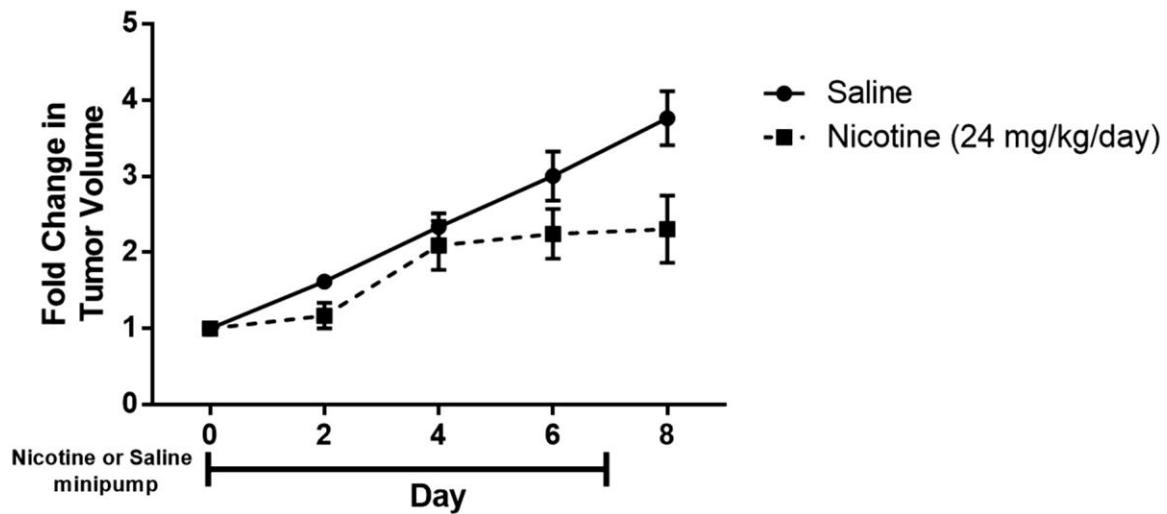


Figure 19. Nicotine fails to enhance Lewis lung carcinoma tumor growth *in vivo*. C57BL/6J mice were subcutaneously injected with 1.5×10^6 LLC cells in both flanks. Once tumors formed, subcutaneous osmotic minipumps were implanted on day 0 to release 24 mg/kg nicotine daily for a total of 7 days. The left and right flank tumor volumes ($l \times w \times h$) were compared to the respective baseline tumor volumes to calculate fold change (A); the fold change values were averaged for each mouse. A linear mixed model analysis revealed a significant effect of time [$F(4, 39) = 25.747$, $P < 0.001$] and treatment [$F(1, 39) = 15.683$, $P < 0.001$], but no interaction between time and treatment [$F(4, 39) = 2.560$, $P = 0.054$]. $n = 5-6$ per group; data are expressed as mean + SEM.

D. Discussion

Effects of nicotine on chemotherapy-induced peripheral neuropathy. To the best of our knowledge, this is the first study to report that nicotine reverses paclitaxel-induced mechanical allodynia, as well as prevents paclitaxel-induced peripheral neuropathy when administered prior to and during paclitaxel treatment in the mouse. Our work also indicates that nAChRs mediate the antinociceptive effects of nicotine, based on interference by mecamylamine, a non-selective nAChR antagonist, and MLA, an $\alpha 7$ nAChR antagonist. Our studies further demonstrate that chronic nicotine infusion prevents the loss of IENFs in the epidermis of the hind paw following paclitaxel treatment. Taken together, these findings suggest that nicotine could have potential utility for the prevention and/or treatment of chemotherapy-induced peripheral neuropathy.

Mice treated with 8 mg/kg of paclitaxel developed significant mechanical allodynia, which is consistent with our recent report (Toma et al., 2017) and previous studies (Deng et al., 2015; Slivicki et al., 2016; Neelakantan et al., 2016). Acute administration of nicotine reverses the mechanical allodynia induced by paclitaxel, which is consistent with studies by Di Cesare Mannelli et al., (2013) in a rat model of oxaliplatin-induced peripheral neuropathy. As nicotine has a very short half-life of approximately 15 minutes in mice (Damaj et al., 2007), it was also administered chronically via 7-day osmotic minipumps in order to achieve and maintain steady-state levels. We have previously reported that subcutaneous minipump administration of 12 and 25 mg/kg/day nicotine leads to plasma nicotine concentrations of approximately 56 and 97 ng/ml, or 0.121 and 0.210 μ M, respectively (Alsharari et al., 2015; Alsharari et al., 2013a). Chronic administration of nicotine (24 mg/kg/day) prior to and during paclitaxel injections significantly prevents both the development of mechanical allodynia and the reduction of intra-epidermal nerve

fibers induced by paclitaxel, as previously described by our group (Toma et al., 2017); others have also shown protection from paclitaxel-induced IENF loss with pifithrin- μ (Krukowski et al., 2015).

The antinociceptive and antiallodynic properties of nicotine have been demonstrated in numerous animal and human studies (Flood and Damaj, 2014), including neuropathic pain in humans (Richarson et al., 2012; Rowbothan et al., 2009). Randomized, double-blind, placebo-controlled trials have reported that intranasal or transdermal administration of nicotine pre- or post-operatively results in significantly decreased pain scores and lower morphine consumption, respectively (Yagoubian et al., 2011; Flood and Daniel, 2004; Habib et al., 2008). Similarly, laboratory animal studies have revealed that nicotine acts as an antinociceptive drug in a variety of acute and chronic pain models in rodents (Alsharari et al., 2015; Alsharari et al., 2012). More specifically, the $\alpha 7$ nAChR subtype has been reported to mediate the antinociceptive effects of nicotine in a mouse model of postoperative pain (Rowley et al., 2008).

Others have also investigated targeting nAChRs for the treatment of CIPN. For example, a recent study indicated that pharmacological and genetic blockade of the $\alpha 9\alpha 10$ nAChR subtype prevents the development of neuropathic pain induced by oxaliplatin in mice (Romero et al., 2017), suggesting that nicotinic acetylcholine receptors play a significant role in the development and potentially the treatment of CIPN. Furthermore, nicotine reduces the ratio of pro-inflammatory monocytes compared to anti-inflammatory monocytes in murine bone marrow via the $\alpha 7$ nAChR subtype, thus significantly decreasing the level of pro-inflammatory cytokines, including TNF α and IL-1 β , and enhancing the release of anti-inflammatory cytokines, such as IL-12 (St-Pierre et al., 2016). Moreover, nicotine exhibits a neuroprotective effect in animal models of

neurodegenerative diseases, such as Alzheimer's disease, an action that is predominantly mediated through the $\alpha 7$ nAChR subtype (Ferrea and Winterer, 2009). Overall, it appears that the $\alpha 7$ nAChR may be one of the predominant nAChR subtypes involved in the neuroprotective actions of nicotine.

Although the current work clearly demonstrates the potential for nicotine to both prevent and reverse paclitaxel-induced peripheral neuropathy, there is an extensive body of literature suggesting that nicotine may stimulate tumor growth and/or interfere with the effectiveness of chemotherapy. This untoward effect is thought to occur via the binding of nicotine to an nAChR on the plasma membrane of the tumor cell, thereby promoting proliferative and anti-apoptotic signaling via the ERK and PI3K/Akt pathways, respectively (Grando, 2014). However, the only experimental condition under which we identified an effect of nicotine was on tumor cell proliferation in serum-free media, in which cells are deprived of nutrients, cytokines, and other growth factors, which is a non-physiological environment. Under standard cell growth conditions, nicotine did not enhance viability, colony formation, or proliferation of a number of experimental tumor cell lines or interfere with apoptosis induced by paclitaxel.

It is somewhat difficult to make direct comparisons between our studies and those in the literature focusing on human NSCLC cell lines as the concentrations of paclitaxel and nicotine vary widely in these experiments, with paclitaxel concentrations ranging between 0.1 μM and 20 μM , and nicotine ranging from 0.1 μM to 10 μM . The human steady-state plasma concentration of paclitaxel falls between 5 nM and 200 nM, while nicotine in cigarette smokers ranges from 20 to 60 ng/ml, or 0.1 to 0.4 μM (Blagosklonny and Fojo, 1999; Benowitz et al., 2009). In addition to

the lack of consistency in the concentrations of paclitaxel and nicotine, the duration of drug exposure (18 hours – 7 days) and serum concentration (0-10%) also cover a wide range. In our work, we used 1 μ M nicotine for 24 to 96 hours, a treatment regimen that involves both acute and chronic exposure to a nicotine concentration that is slightly higher than peak human plasma levels in order to utilize a clinically relevant dose of nicotine. Similarly, we used paclitaxel concentrations of 50 nM and 100 nM because the former is appropriate for experiments involving low cell numbers, such as the clonogenic assay, and the latter induces substantial apoptosis; yet, most importantly, both concentrations are within the range of human plasma levels.

Given the various experimental conditions, it is perhaps not surprising that the reported effects of nicotine vary widely as well. For example, some studies have shown increases of 23-200% in NSCLC cell proliferation (Zhang et al., 2009; Pillai et al., 2011; Wu et al., 2013; Liu et al., 2015), whereas others demonstrate modest increases of 7-18% (Chen et al., 2002; Jarzynka et al., 2006; Puliappadamba et al., 2010) and in one case decreases of 40-72% (Gao et al., 2016). Nicotine has been reported to reduce paclitaxel-induced apoptosis by a significant 50% (Dasgupta et al., 2006) or only by a modest 8% (Tsurutani et al., 2005). These studies utilized sub-G1 DNA content, the TUNEL assay, and PARP cleavage to assess the impact of nicotine on paclitaxel-induced apoptosis, whereas we included quantification of early and late apoptotic populations with the Annexin V/Propidium Iodide assay. In part, this may provide a rationale for the inconsistencies in outcomes since sub-G1 DNA content alone does not distinguish between apoptotic and necrotic cell death (Mattes, 2007). The observation of substantially more apoptosis than sub-G1 DNA content following 48 hours of paclitaxel treatment likely reflects the possibility that early apoptotic cells had not yet become fragmented.

With regard to *in vivo* studies, while nicotine exposure has been reported to significantly increase lung tumor incidence, volume, weight, and Ki-67+ populations (Jarzynka et al., 2006; Heeschen et al., 2001; Improgo et al., 2013; Liu et al., 2015; Iskandar et al., 2012), other reports have shown that chronic nicotine treatment does not significantly stimulate lung tumor growth in mice (Warren et al., 2012; Maier et al., 2011; Murphy et al., 2011). Similarly, we found that chronic nicotine administration did not enhance LLC tumor growth in immunocompetent mice, suggesting that nicotine may be a potential therapy for CIPN prior to or following chemotherapy with the aim of preventing and reversing peripheral neuropathy, respectively.

In summary, our results provide a proof of concept that nicotine is efficacious in preventing and reversing CIPN, actions that may enhance the quality of life of cancer patients and survivors. In addition, our findings suggest that nicotine does not significantly promote tumor cell proliferation or interfere with chemotherapy in lung cancer cell lines. In this context, we are encouraged by the report that nicotine replacement therapy is not a significant predictor of cancer in humans (Murray et al., 2009).

Conflicts of interest

The authors declare no conflicts of interest.

Acknowledgements:

The research was supported by the National Institutes of Health (NIH) [Grant 1R01-CA-206028-01] (to M.I.D. and D.A.G.), [Grant T32-DA-007027-41] (to S.L.K.), [Grant 1F31-NS-095628-01A1] (to L.D.S.) and, in part, by a Massey Cancer Center Pilot Project Grant (to D.A.G. and M.I.D.). Microscopy was performed at the VCU Microscopy Facility, and flow cytometry analysis was conducted at the VCU Massey Cancer Center Flow Cytometry Shared Resource, which were supported, in part, with funding by NIH-National Cancer Institute Cancer Center Support Grant P30-CA-016059. The content is solely the responsibility of the authors and does not necessarily represent the official views of the NIH.

Authorship Contributions:

Participated in research design: S.L.K., W.T., D.B., X.F., M.I.D., D.A.G.

Conducted experiments: S.L.K., W.T., D.B., J.A.M., X.F.

Contributed new reagents or analytic tools: J.W.B.

Performed data analysis: S.L.K., W.T., D.B., L.D.S.

Wrote or contributed to the writing of the manuscript: S.L.K., W.T., L.D.S., A.H.L., Z.C., E.D., M.I.D., D.A.G.

CHAPTER FOUR

The Regulatory Role of the $\alpha 7$ Nicotinic Acetylcholine Receptor (nAChR) Subtype in the Initiation and Maintenance of Paclitaxel-Induced Peripheral Neuropathy in Mice

A. Introduction

Cancer chemotherapeutics have a beneficial effect in destroying cancer cells and increasing the survival rates of cancer patients. However, chemotherapeutics cause several side effects on the body. One of the serious side effects is Chemotherapy-Induced Peripheral Neuropathy (CIPN). Paclitaxel belongs to the taxane family of chemotherapeutics. Paclitaxel used for the treatment of different types of solid tumors such as breast, ovarian, and non-small cell lung cancers (Hagiwara and Sunada, 2004). However, paclitaxel causes multiple sensory symptoms in human patients suffering from neuropathy. These symptoms distribute in feet and hands of patients as so-called “stocking and glove.” Patients describe these symptoms as burning pain, numbness, tingling, mechanical and cold allodynia. The sensory symptoms can persist in about 30% of patients and for several years after cessation of chemotherapy (Ewertz et al., 2015). Unfortunately, there is no effective treatment to alleviate the peripheral neuropathy. Therefore, there is a dire need to develop novel therapies to mitigate or prevent CIPN.

Our previous work showed that targeting nAChR by nicotine; a prototypical agonist reverses and prevents the CIPN induced by paclitaxel, at least in part via an $\alpha 7$ nAChR dependent mechanism (Kyte et al., 2018). A growing body of evidence suggests that neuronal nicotinic acetylcholine receptors, specifically, the homomeric $\alpha 7$ nAChR subtype, present as a viable target for the treatment of inflammatory, acute and chronic pain, and neurodegenerative diseases. (Bencherif et al., 2011). These anti-inflammatory-neuroprotective effects mediated via the cholinergic anti-inflammatory pathway which is a neural mechanism that contributes to downregulation of pro-inflammatory cytokines in an $\alpha 7$ nAChR dependent manner (Pavlov and Tracey, 2005). The $\alpha 7$ nAChR has a high permeability to both Na^+ and Ca^{2+} ions, low probability of channel opening, and rapid desensitization (Williams et al., 2012). The $\alpha 7$ nAChR express

throughout the pain transmission pathway; either on neuronal cells located in the brain, spinal cord, or peripheral DRG (Cordero-Erausquin et al., 2004) , and on non-neuronal cells, specifically, immune cells such as macrophages (Tracey, 2002).

Our previous reports show that endogenous $\alpha 7$ nAChR tone play an important role in chronic inflammatory pain (Alsharari et al., 2016; Alsharari et al., 2013a). There are several $\alpha 7$ nAChR agonists, allosteric modulators (such as type I PAMs, type II PAMs, and Ago-PAMs) that depend on their activation of the channel through opening the channel (Bagdas et al., 2017). However, a new series of ligands that bind selectively to the $\alpha 7$ nAChR and induce conformational changes in the receptor that does not require channel opening, was recently described. These ligands are named silent agonists. Silent agonists have low efficacy ($< 2\%$) but bind to the $\alpha 7$ nAChR, do not induce a current, and stabilize the sensitive desensitized (D_s) state of the receptor to produce pharmacological effect (Papke et al., 2017). For example, the administration of the selective silent agonist NS6740 into mice underwent CCI, a neuropathic pain model, results in a dose-dependent reversal of mechanical hypersensitivity (Papke et al., 2015). Additionally, our drug of interest is another silent agonist called R-47. R-47 has high affinity and selectivity to the $\alpha 7$ nAChR ($K_i = 6.9$ nM). Administration of R-47 at a dose of 10 mg/kg orally reduces synovitis significantly and shows 48% attenuation of arthritis score in murine collagen-induced arthritis (CIA) model (van Maanen et al., 2015).

Our main hypothesis was that the $\alpha 7$ nAChR subtype plays a regulatory role in pathogenesis of paclitaxel-induced CIPN. Thus, we aimed to characterize the role of $\alpha 7$ nAChR in the development and maintenance of CIPN in mice treated with paclitaxel via genetic, behavioral and molecular approaches. Additionally, we investigated the potential of targeting the $\alpha 7$ nAChR with the silent agonist R-47 in the paclitaxel CIPN mouse model. Furthermore, we studied the

impact of R-47 on the induction of inflammatory responses in microglia induced by paclitaxel. Moreover, we probed the ability of R-47 to induce a relief of a state of spontaneous pain relief in paclitaxel-treated mice using the Conditioned place preference (CPP) test.

B. Materials and Methods

Animals

Adult male C57BL/6J mice (8 weeks at beginning of experiments, 20-30 g) were purchased from The Jackson Laboratory (Bar Harbor, ME). Mice were housed in an AAALAC-accredited facility in groups of four. Food and water were available ad libitum. The mice in each cage were randomly allocated to different treatment groups. All behavioral testing on animals was performed in a blinded manner; behavioral assays were conducted by an experimenter blinded to the treatment groups. Experiments were performed during the light cycle (7:00 am to 7:00 pm) and were approved by the Institutional Animal Care and Use Committee of Virginia Commonwealth University and followed the National Institutes of Health Guidelines for the Care and Use of Laboratory Animals. Animals were euthanized via CO₂ asphyxiation, followed by cervical dislocation. Any subjects that showed behavioral disturbances unrelated to chemotherapy-induced pain were excluded from further behavioral testing. Male and female C57BL/6J and $\alpha 7$ KO mice were purchased from Jackson Laboratories (Bar Harbor, ME). The null mice and their wild-type littermates were bred in an animal care facility at Virginia Commonwealth University and were maintained on a C57BL/6J background and have been backcrossed to at least ten generations. For all experiments, mutant- and wild- type controls were obtained from crossing heterozygote mice. This breeding scheme allowed us to rigorously control for any anomalies that may occur with crossing solely mutant mice.

Drugs

Paclitaxel was purchased from Tocris (1097, Bristol, United Kingdom) and dissolved in a mixture of 1:1:18 [1 volume ethanol/1 volume Emulphor-620 (Rhone-Poulenc, Inc., Princeton,

NJ)/18 volumes distilled water]. Paclitaxel was administered at a dose of 8 mg/kg i.p for one cycle to induce CIPN intraperitoneally (i.p.) every other day for a total of four injections to induce neuropathy, as previously described by Toma et al., (2017). Additionally, paclitaxel was administered at a lower dose of 1 mg/kg i.p. for one cycle to the $\alpha 7$ nAChR WT or KO mice to evaluate the differences in the mechanical hypersensitivity. All the reversal and mechanistic studies were conducted at day 7-14 after initial paclitaxel injection unless otherwise noticed. The silent agonist PMP-072 or R-47 (structure shown in Figure 20), (R)-N-(4-methoxyphenyl)-2-((pyridin-3-yloxy)methyl)piperazine-1-carboxamide was synthesized and supplied by our collaborator (Dr. Ganesh Thakur; Department of Pharmaceutical Sciences, Northeastern University). R-47 was dissolved in distilled water (D.W).

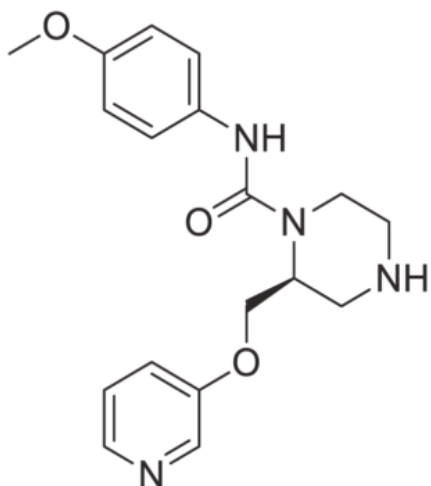


Figure 20. The chemical structure of R-47. Adapted from van Maanen et al., 2015.

For acute administration, R-47 was injected per os (p.o.) at doses of 1, 5, 10 mg/kg. The range of doses used in this study were chosen based on the previous studies that showed R-47 was effective

to reduce the inflammatory response in different inflammatory pain assays (van Maanen et al., 2015; Clark et al., 2014). For chronic administration (prevention study), R-47 was injected p.o. at a dose of 10 mg/kg twice daily (8 hours apart) 3 days prior and during paclitaxel injection cycle. For the tolerance study, we chose the dose that fully reversed and prevented CIPN. For that, R-47 was administered p.o. at a dose of 10 mg/kg twice daily (8 hours apart) for 4 days to paclitaxel-treated group of mice. Methyllaconitine (MLA) was purchased from RBI (Natick, MA, USA), dissolved in saline and was administered at a dose of 10 mg/kg subcutaneously (s.c.) 10 minutes before administration of R-47 (Freitas et al., 2013). All i.p., s.c., and p.o. injections were given in a volume of 1 ml/100 g body weight.

Immunohistochemistry and quantification of intra-epidermal nerve fibers (IENFs)

The hind paw plantar skin was collected from the following groups of mice (prevention study): vehicle-vehicle, vehicle-R-47 (10 mg/kg), paclitaxel (8 mg/kg)-vehicle, and paclitaxel (8 mg/kg)-R-47 (10 mg/kg). The staining procedure was performed as previously described (Toma et al., 2017) with slight modifications. The glabrous skin of the hind paw was excised, placed in freshly prepared 4% paraformaldehyde in 0.1 M PBS (pH 7.4), and stored overnight at 4°C in the same fixative. Tissues were transferred to 30% sucrose and stored overnight in the refrigerator. Samples were embedded in optimum cutting temperature (O.C.T) compound (cat# 23-730-571, fisher scientific, USA) and the frozen sections were sectioned at 25 µm. Sections were immersed in ice-cold acetone for 20 minutes, washed with PBS, and incubated at room temperature for 30 min in blocking solution (5% normal goat serum and 0.3% Triton X-100 in PBS). Sections were incubated with a 1:1000 dilution of the primary antibody, PGP9.5 (Fitzgerald - cat# 70R-30722, MA, USA) overnight at 4°C in a humidity chamber. Following PBS washes, sections were incubated for 90 min at room temperature with a 1:250 dilution of goat anti-rabbit IgG (H+L)

secondary antibody conjugated with Alexa Fluor® 594 (Life Technologies - cat# A11037, OR, USA). Sections were mounted in Vectashield (Vector Laboratories, Burlingame, CA, USA) and examined using a Zeiss Axio Imager A1 – Fluorescence microscope (Carl Zeiss, AG, Germany). Sections were examined in a blinded fashion under 63x magnification. The IENFs in each section were counted in a blinded fashion, and the density of fibers is expressed as fibers/mm.

Immunohistochemistry and Characterization of Morphological Changes of Microglial Cells

Spinal cords from the same groups of mice were collected by Hydraulic extrusion (Richner et al., 2017). The L4-L6 lumbar region of the spinal cord was collected and transferred to a freshly prepared 4% paraformaldehyde in 0.1 M PBS (pH 7.4) and stored overnight at 4°C in the same fixative. Twenty-micron cryostat sections were collected on glass slides and immunostained for microglia according to the same protocol used for the IENF's using the rabbit polyclonal anti-Ionized calcium binding adaptor molecule 1 (Iba1) antibody at a dilution of 1:1000 (Wako chemicals, cat# 019-19741, Richmond, VA, USA). Characterization of microglial cell morphology was based on a previous study (Zheng et al., 2011) with modifications. Microglial cells were binned into three main stages. Stage I: Cells with long, thin, and highly ramified processes. Stage II: Cells with shorter, thickened processes with less branching. Stage III: Cells displaying more hypertrophic changes such as short, thickened processes and enlargement of the cell body.

Regions of the dorsal horn including laminae 1-5 were examined using a Zeiss AxioImager Z2 equipped with a motorized XY stage, microcator Microbrightfield Neurolucida and Stereo Investigator image analysis software (MBF Bioscience, VT, USA). Microglia were identified and scored as indicated above using a 63x oil immersion objective in an experimenter-blinded fashion. Images were acquired as z-stacks and results are reported as number of microglial cells per section.

Mechanical Sensitivity Evaluation (von Frey test)

Mechanical hypersensitivity thresholds were determined using von Frey filaments according to the method suggested by Chaplan et al. (1994) and as described in our previous report (Bagdas et al., 2015). The mechanical threshold is expressed as \log_{10} (10 \times force in [mg]).

Real-Time PCR (qRT-PCR) Analysis

Alive, unanesthetized mice treated either with vehicle or paclitaxel at a dose of 8 mg /kg i.p. for one cycle were rapidly sacrificed at Day 7 or Day 28 by decapitation post vehicle or paclitaxel treatment. Dorsal root ganglia and spinal cord at the level of L4-6 were collected and snap frozen in liquid nitrogen. Total RNA was extracted with TRIzol RNA Isolation Reagents (Ambion RNA by Life Technologies, ThermoFisher Scientific, Waltham, MA; Cat. #15596-026), followed by reverse transcription with iScript™ cDNA Synthesis Kit (Bio-Rad Laboratories, Hercules, CA; Cat. #1708890). Amplification of the cDNA products was performed with TaqMan® Universal PCR Master Mix (Applied Biosystems by ThermoFisher Scientific, Cat. #4304437) and predesigned primers (18 μ M) and FAM/Minor Groove Binder-NFQ probes (5 μ M) (ThermoFisher Scientific) according to the manufacturer's directions. The housekeeping gene β -actin (Actb, Cat. #4331182: Mm02619580_g1) was selected as an internal control. Data are expressed as nAChR $\alpha 7$ (*Chrna7*, Cat. #4331182: Mm01312230_m1) mRNA levels (Mean \pm SEM) relative to Actb levels using the $\Delta\Delta C_t$ method. RNase/DNase free reagents were used at all steps of the procedure.

Locomotor Activity Test

The test was performed as described previously in Bagdas et al. (2015). Briefly, mice were placed into individual Omnitech (Columbus, OH) photocell activity cages (28 x 16.5 cm)

containing two banks of eight cells each. Interruptions of the photocell beams, which assess walking and rearing, were then recorded for the next 30 min. Data are expressed as the number of photocell interruptions. R-47 10 mg/kg p.o. or distilled water were administered to paclitaxel or vehicle groups of mice 180 min before testing in locomotor boxes.

Conditioned Place Preference Test

To determine the possibility of R-47 to alleviate spontaneous, ongoing pain in paclitaxel-treated mice but not vehicle-treated mice, an unbiased CPP paradigm was conducted as previously described (Grabus et al., 2006) with modifications. Briefly the CPP test boxes (20x20x20 cm each; ENV3013; Med Associates, St Albans, VT, USA) consist of two main chambers and equipped with two different colors and textures (white mesh or black rod), and a neutral gray middle chamber with a smooth PVC floor. Mice were handled for three weeks totally prior to start conditioning. Mice were put into the gray chamber to acclimate for five min and later allowed freely to move between all CPP boxes for 15 min. This is considered the preconditioning baseline measurement. After that, mice were assigned randomly into four groups; one paclitaxel group received vehicle of R-47 which is distilled water and the other paclitaxel group received R-47 at a dose of 10 mg/kg p.o.; similar approach was applied to vehicle-treated group. Mice that received R-47 or its vehicle were administered on alternative days. i.e. the group that receive R-47 in one day (one injection per day) should receive the vehicle of R-47 on the next. A total 8 conditioning days paradigm was applied (see **Figure 27** which depicts the timeline of the CPP experiment). R-47 or vehicle were administered two hours before putting mice into CPP boxes and kept inside boxes for 30 min. On the test day, mice were placed into CPP boxes and allowed freely to move between the boxes for 15 min in a drug-free state. The preference score was calculated by

determining the difference between time spent in the drug paired side on the test day minus the time in drug paired side on the baseline day.

Statistical Analyses

Data were analyzed using the GraphPad Prism software version 7.04 (GraphPad Software, Inc., La Jolla, CA) and expressed as the mean \pm S.E.M. Three-way ANOVA repeated measure was used to determine the overall interaction of the three factors in the $\alpha 7$ nAChR WT, KO mice treated with either vehicle or paclitaxel, and in the R-47 prevention study. A subsequent Two-way ANOVA repeated measure followed by Sidak post hoc analyses were used to determine the difference between treatment groups over multiple time points in the reversal, prevention studies with R-47, and in the $\alpha 7$ nAChR WT, KO genotype study when comparing treatment and time too. Unpaired *t* test was used to evaluate the difference in the *Chrna7* expression in the selected tissues from vehicle or paclitaxel-treated mice. Ordinary Two-way ANOVA followed by Sidak post hoc analyses were conducted in the R-47 tolerance, immunohistochemistry, and CPP studies. Differences were set to be significant at $P < 0.05$.

C. Results

The $\alpha 7$ nAChR Subtype Regulates Development and Maintenance of CIPN

The first set of experiments was conducted to elucidate the role of $\alpha 7$ nAChR subtype in the pathophysiology of CIPN. Administration of paclitaxel at a dose of 1 mg/kg i.p. for one cycle to $\alpha 7$ WT or KO mice show that $\alpha 7$ KO mice develop significant mechanical hypersensitivity compared to $\alpha 7$ WT mice starting the first day after paclitaxel injection with prolonged maintenance of mechanical hypersensitivity. Although a three-way ANOVA analysis did not show significant interaction between genotype x treatment x days [$F(8,324) = 1.680$, $P = 0.102$]. However, a subsequent two-way ANOVA repeated measure followed by Sidak post hoc analysis reveal significant interaction between genotype x treatment [$F(1,324) = 89.096$, $P < 0.0001$], genotype x days [$F(8,324) = 2.089$, $P < 0.036$], and treatment x days [$F(8,324) = 6.470$, $P < 0.0001$] (**Figure 21**). Suggesting that $\alpha 7$ nAChR plays a pivotal role in the protection of developing CIPN in mice.

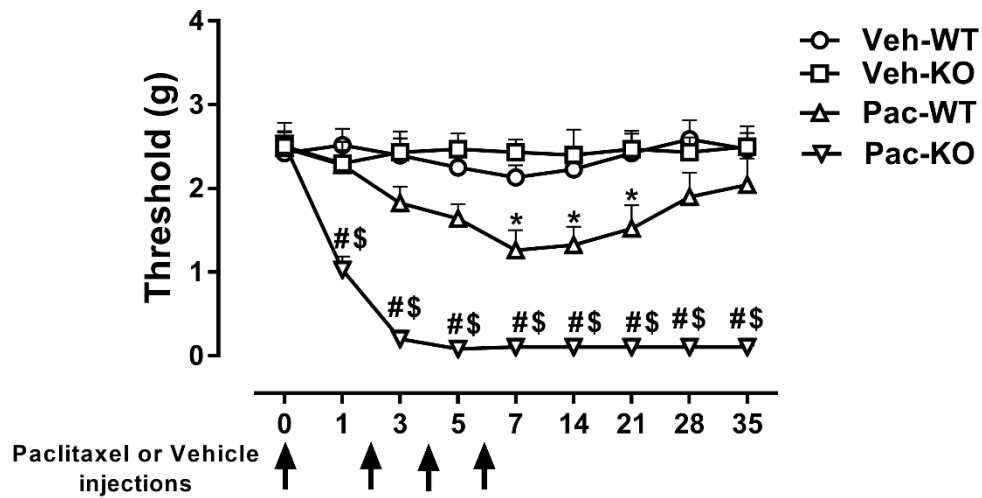


Figure 21. The $\alpha 7$ nAChR subtype regulates the development and maintenance of mechanical hypersensitivity. Administration of paclitaxel at a dose of 1 mg/kg i.p. for one cycle reveals that KO mice show worsening and significantly lower threshold of mechanical hypersensitivity compared to WT mice. Arrows indicate vehicle/paclitaxel injections on days 0, 2, 4, and 6. Baseline measurements were taken before vehicle/paclitaxel administration on day 0. * $P < 0.05$ Pac-WT vs Veh-WT; # $P < 0.05$ Pac-KO vs Veh-KO; \$ $P < 0.05$ Pac-KO vs Pac-WT; $n = 11$ for Veh-WT (5 males, 6 females), $n = 8$ for Veh-KO (4 males, 4 females), $n = 13$ for Pac-WT (6 males, 7 females), $n = 8$ for Pac-KO (4 males, 4 females). Data expressed as mean \pm SEM. Veh, vehicle; Pac, paclitaxel; WT, wildtype; KO, knockout.

Paclitaxel Induces Alterations in *Chrna7* Expression Peripherally and Centrally

The next experiment determined the possible alteration of $\alpha 7$ nAChR (*Chrna7*) mRNA expression in the peripheral nervous tissue (specifically, DRG), and centrally (specifically, spinal cord) following paclitaxel injection. Administration of paclitaxel at a dose of 8 mg/kg i.p. for one cycle results in significant upregulation of *Chrna7* mRNA expression in DRG collected at day 7 post-first paclitaxel injection compared to control [$t = 2.51$, $df = 13$; $P < 0.05$] (**Figure 22A**). In contrast, similar treatment reveals downregulation of *Chrna7* mRNA expression in DRG collected at day 28 post-first paclitaxel injection compared to control [$t = 2.545$, $df = 10$; $P < 0.05$] (**Figure**

22B). However, paclitaxel treatment leads to upregulation of *Chrna7* mRNA expression in spinal cord collected at day 28 post-first paclitaxel injection compared to control [$t = 2.214$, $df = 15$; $P < 0.05$], (**Figure 22C**).

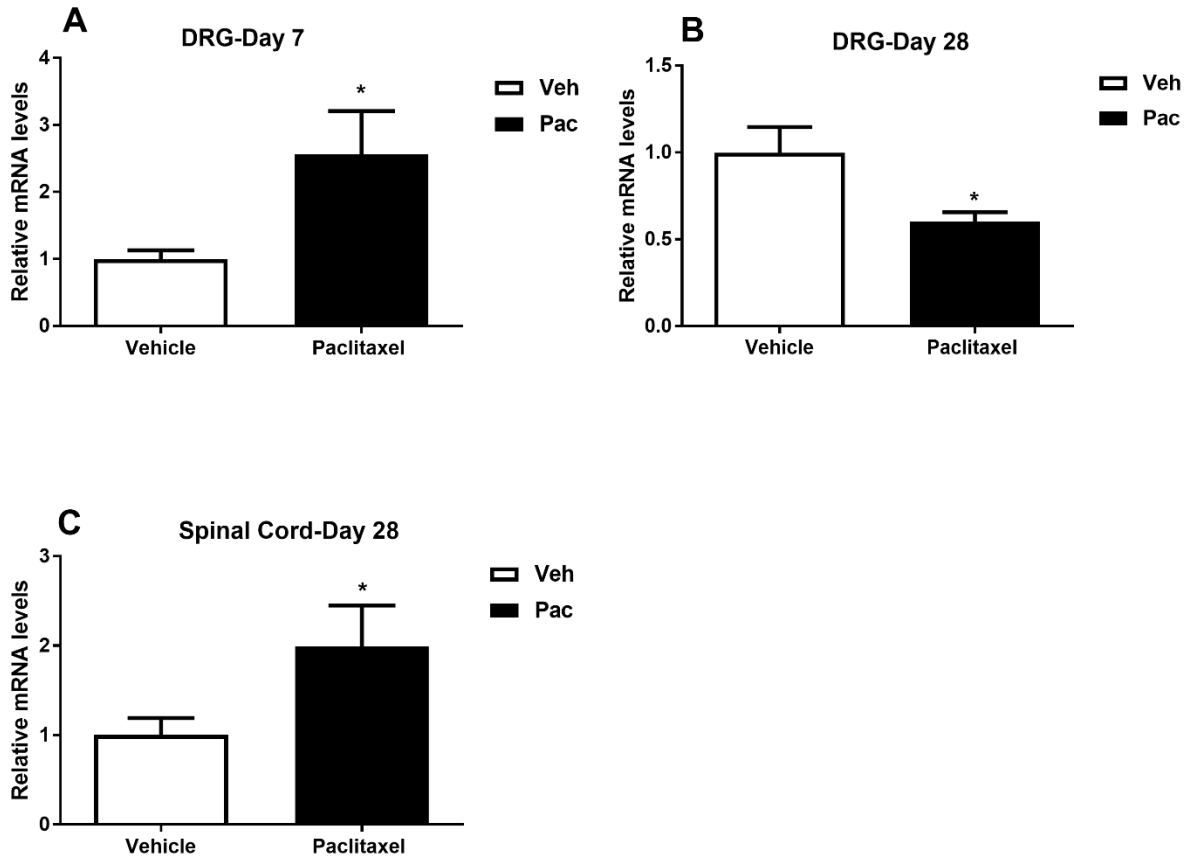


Figure 22. Paclitaxel alters the expression of *Chrna7* mRNA in peripheral and spinal nervous tissues. Administration of paclitaxel at a dose of 8 mg/kg for one cycle i.p. produces significant upregulation in DRG at day 7; $n = 8$ for vehicle group, $n = 7$ for paclitaxel group (A), and downregulation in DRG at day 28; $n = 6$ for vehicle group, $n = 6$ for paclitaxel group (B). Additionally, paclitaxel significantly upregulates the expression of *Chrna7* mRNA in the spinal cord at day 28; $n = 10$ for vehicle group, $n = 8$ for paclitaxel group (C). * $P < 0.05$ vs vehicle. Data expressed as mean \pm SEM.

R-47 Reverses and Prevents Paclitaxel-Induced Mechanical Hypersensitivity

Here we show that injection of selective $\alpha 7$ nAChR silent agonist, R-47 both reverses and prevents mechanical hypersensitivity. Acute administration of R-47 at doses of 1, 5, and 10 mg/kg p.o. reverses mechanical hypersensitivity in paclitaxel-treated mice in a time- and dose-dependent manners, respectively, [$F_{\text{dose} \times \text{time}} (24, 168) = 14.92, P < 0.0001$], (**Figure 23A**). The highest dose of R-47 (10 mg/kg) reverses the mechanical hypersensitivity fully, and the middle dose of R-47 (5 mg/kg) reverses the mechanical hypersensitivity partially. However, Administration of R-47 to vehicle-treated mice does not alter the mechanical threshold [$F_{\text{dose} \times \text{time}} (24, 168) = 0.3442, P = 0.9984$], (**Supplementary figure 9**). We further extended the finding that R-47 reverses the mechanical hypersensitivity induced by paclitaxel to use R-47 to prevent the development of CIPN induced by paclitaxel. Interestingly, chronic administration of R-47 10 mg/kg p.o., twice a day, three days before, and during the paclitaxel injection cycle significantly prevents the development of mechanical hypersensitivity induced by paclitaxel through the entire period of experiment [$F_{\text{paclitaxel or vehicle} \times \text{R-47 or vehicle} \times \text{days}} (9, 280) = 8.567; P < 0.0001$], (**Figure 23B**). Importantly, comparing the paclitaxel group of mice received vehicle versus paclitaxel group of mice received R-47 over time, a two-way ANOVA followed by Sidak post hoc test reveals a significant interaction between the two treatment groups [$F_{\text{dose} \times \text{time}} (9, 63) = 25.1, P < 0.0001$], (**Figure 23B**). Furthermore, comparing the paclitaxel group of mice received vehicle versus vehicle group of mice received also vehicle over time, reveals that vehicle-paclitaxel group of mice exhibit significant mechanical hypersensitivity when compared to the vehicle-vehicle group [$F_{\text{dose} \times \text{time}} (9, 63) = 19.4, P < 0.0001$], (**Figure 23B**).

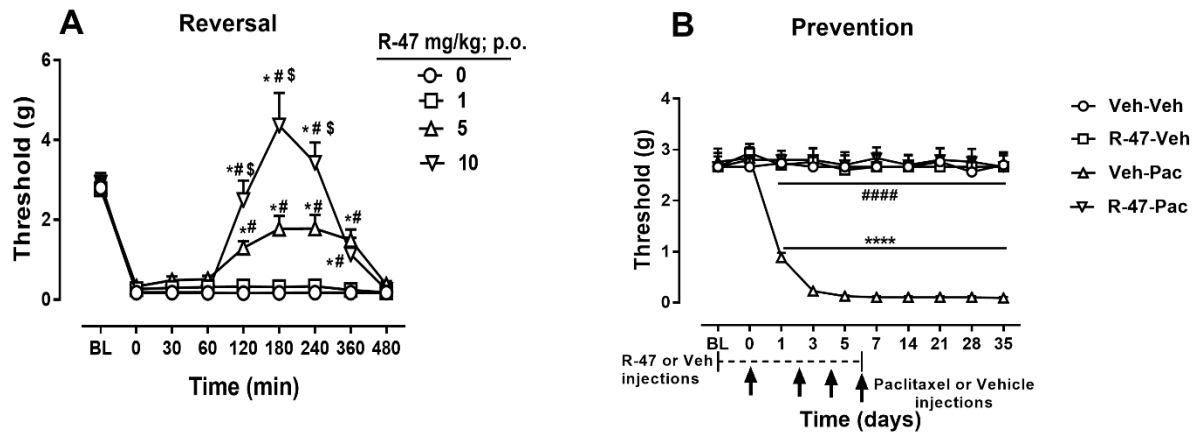
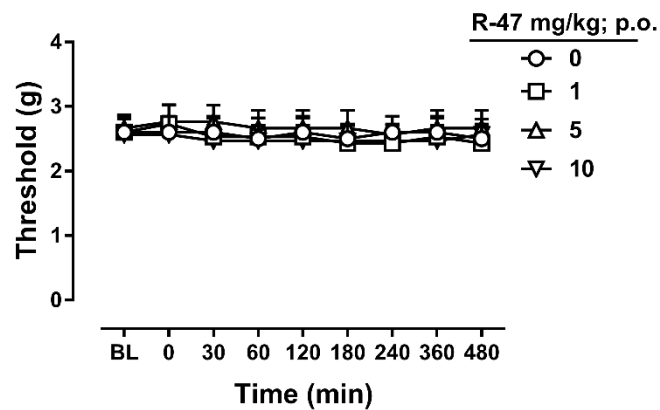


Figure 23. Reversal and prevention of CIPN in mice. A) Acute administration of R-47 at doses of 1, 5, and 10 mg/kg p.o. reverses mechanical hypersensitivity in paclitaxel-treated mice. * $P < 0.0001$ vs distilled water (0 mg/kg); # $P < 0.0001$ vs R-47(1 mg/kg); \$ $P < 0.0001$ vs R-47 (5 mg/kg). B) Chronic administration of R-47 at a dose of 10 mg/kg completely prevents the development of mechanical hypersensitivity. **** $P < 0.0001$ Veh-Veh vs Veh-Pac; ##### $P < 0.0001$ R-47-Pac vs Veh-Pac. BL, baseline; Veh, Vehicle; Pac, Paclitaxel. $n=8$ per group; Data expressed as mean \pm SEM.



Supplemental Figure 9. Acute administration of R-47 at doses of 1, 5, and 10 mg/kg p.o. does not alter mechanical threshold in vehicle-treated mice. BL, baseline. $n = 8$ per group; data expressed as mean \pm SEM.

To further validate that the antinociceptive effect of selective silent agonist, R-47 is mediated through $\alpha 7$ nAChR, we administered MLA, an $\alpha 7$ nAChR antagonist before R-47 administration. MLA significantly blocks the antinociceptive effect of R-47 in paclitaxel-treated mice [$F_{\text{dose} \times \text{time}}$ (6, 42) = 16.81, $P < 0.0001$], (**Figure 24**).

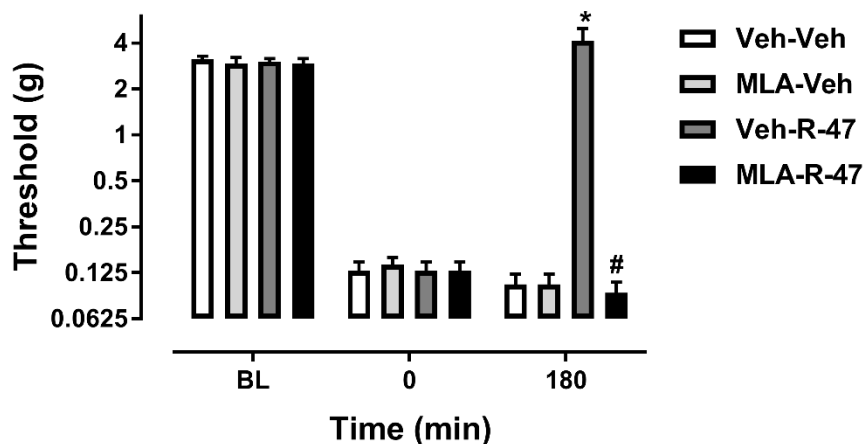


Figure 24. The $\alpha 7$ nAChR subtype mediates the antinociceptive effect of R-47. Administration of MLA, an $\alpha 7$ nAChR antagonist at a dose of 10 mg/kg s.c. 10 minutes before R-47 (10 mg/kg, p.o.) blocked the antinociceptive effect of R-47 in paclitaxel-treated mice. * $P < 0.0001$ Veh-R-47 at 180 min vs 0 min; # $P < 0.0001$ MLA-R-47 vs Veh-R-47 at 180 min. BL, Baseline; Veh, vehicle; MLA, methyllycaconitine. $n = 8$ per group; data expressed as mean \pm SEM.

Lack of Tolerance Development to R-47 After Repeated Administration

The next experiment designed to investigate if sub chronic administration of R-47 would produce tolerance in paclitaxel-treated mice. Interestingly, administration of R-47 at a dose of 10 mg/kg p.o. twice daily for four days, and on day five as a challenging day shows that R-47 maintains its antinociceptive effect in paclitaxel-treated mice [$F_{\text{dose} \times \text{time}}$ (6, 42) = 33.41, $P < 0.0001$], (**Figure 25**).

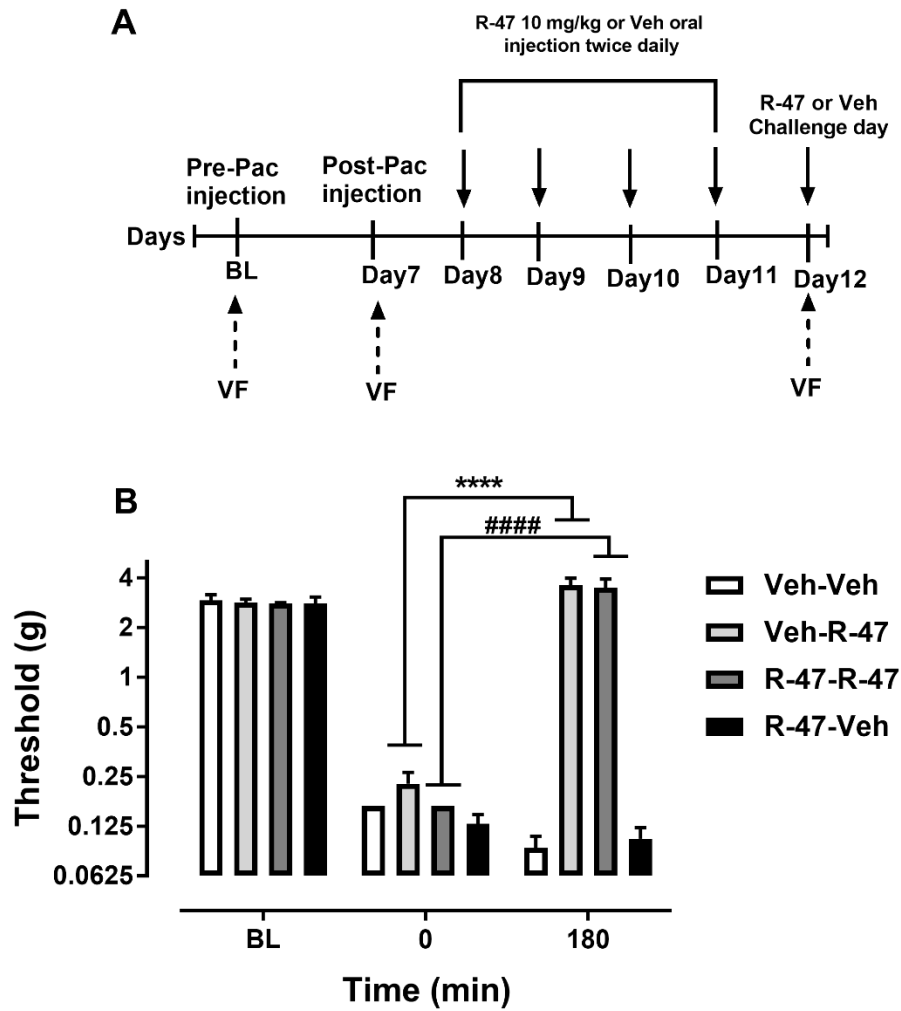
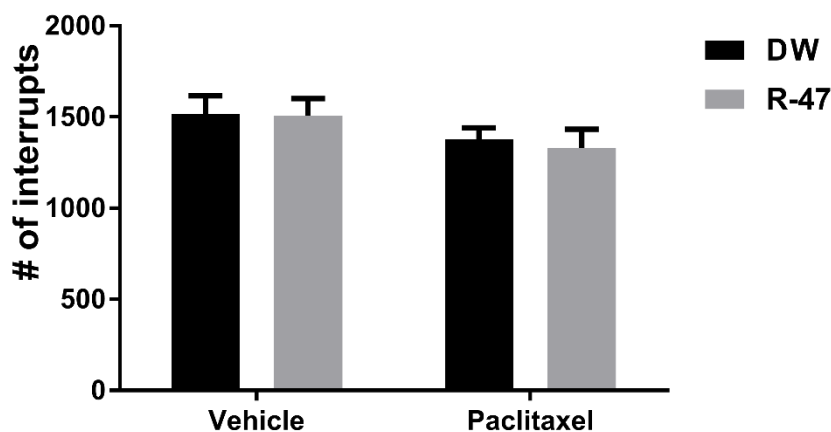


Figure 25. No tolerance develops following sub chronic R-47 injection. A) Timeline depiction of R-47 treatment in paclitaxel-treated mice. B) The administration of R-47 a dose of 10 mg/kg p.o. four days and on challenging day five shows the antinociceptive effect in paclitaxel-treated mice. * $P < 0.0001$ Veh-R-47 at 180 min vs 0 min; # $P < 0.0001$ R-47-R-47 at 180 vs R-47-R-47 at 0 min. BL, Baseline; Veh, vehicle; Pac, paclitaxel; VF, von Frey; $n = 8$ per group; data expressed as mean \pm SEM.

R-47 Does Not Induce Motor Deficits

To investigate whether R-47 would induce motor deficits in paclitaxel-treated mice, we administered R-47 at a dose of 10 mg/kg p.o to the mice and tested them in locomotor activity boxes. Importantly, R-47 does not show motor impairment in any treatment group [$F_{\text{paclitaxel} \times \text{R-47}}$ (1, 28) = 0.04181; $P=0.8395$], (**Supplementary Figure 10**).



Supplementary figure 10. No motor deficits are seen following R-47 injection. Administration of R-47 at a dose of 10 mg/kg p.o. to paclitaxel- or vehicle-treated mice does not induce motor impairment. $n = 8$ per group; data expressed as mean \pm SEM.

R-47 Prevents Reduction of Intraepidermal Nerve Fibers Induced by Paclitaxel

To study whether R-47 has protective effect on the reduction of IENFs induced by paclitaxel, administration of R-47 at a dose of 10 mg/kg p.o. or distilled water to paclitaxel- or vehicle-treated mice reveals a significant interaction between paclitaxel and R-47 treatment [$F_{\text{paclitaxel} \times \text{R-47}}$ (1, 20) = 27.85; $P < 0.0001$], (**Figure 26A**). As seen in the representative **Figure 26B**, the vehicle-paclitaxel group of mice reveals a significant reduction of IENFs density compared to

the vehicle-vehicle treated group of mice ($P < 0.0001$). Importantly, the group of mice treated with R-47-paclitaxel demonstrates a significant increase of IENFs compared to the group of mice treated with vehicle-paclitaxel ($P < 0.0001$). Additionally, R-47-paclitaxel - treated mice do not show alteration in IENFs counts compared to R-47-vehicle -treated mice ($P = 0.0753$). Furthermore, R-47-vehicle-treated mice do not indicate a change in the IENFs density compared to vehicle-vehicle-treated mice ($P = 0.3563$).

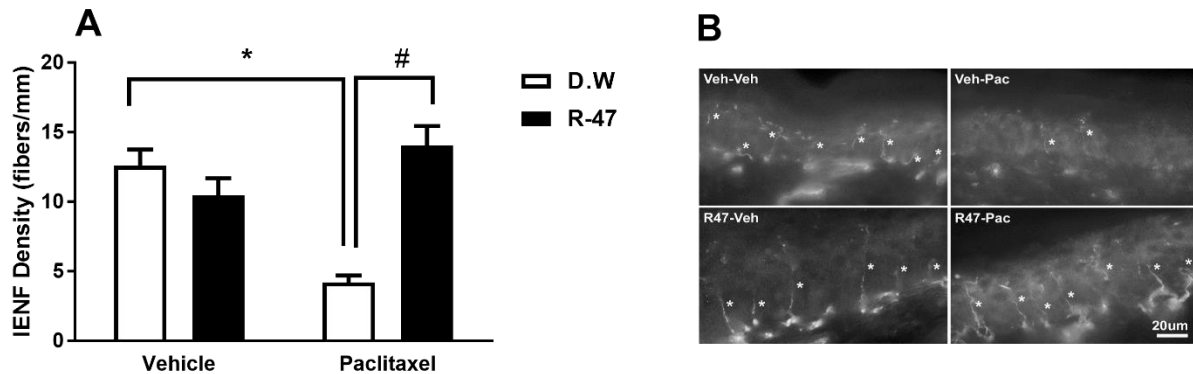


Figure 26. Prevention of IENFs reduction with R-47. Mice injected with paclitaxel at a dose of 8 mg/kg i.p. for one cycle demonstrate a significant reduction of IENFs 35 days post-paclitaxel injection. However, pre- and co-administration of R-47 at a dose of 10 mg/kg p.o. to paclitaxel- treated mice completely prevents the reduction of IENFs (A). * $P < 0.0001$ D.W-paclitaxel vs D.W-vehicle; # $P < 0.0001$ R-47-paclitaxel vs D.W-paclitaxel. Immunostained sections of hind paw epidermis represent the reduction of IENF density by paclitaxel and protection by R-47 (B). Bar represents 20 microns in all images. Images captured under 63x magnification. IENFs, intra-epidermal nerve fibers; D.W, distilled water. Asterisks denote IENFs. $n = 6$ per group; data expressed as mean \pm SEM.

R-47 Attenuates the Altered Morphology of Microglia induced by Paclitaxel

A growing body of evidence suggests the involvement of glial cells, specifically, microglia in the pathology of neuropathic pain(Mcmahon et al., 2015). To investigate a potential role for microglia in our CIPN mouse model, we first assessed the extent to which paclitaxel treatment alters the morphology of microglial cell morphology in the lumbar spinal cord. As seen in Figure 26, paclitaxel treatment results in a reduction in the number of stage I cells with a parallel increase in stage III cells, consistent with a modest immune response. Next, we asked the question whether R-47 treatment would attenuate or prevent the alteration of microglial cell morphology induced by paclitaxel. Results from these studies demonstrate that R-47 prevents the shift from stage I to stage III microglial cells. Results from both sets of experiments are discussed in detail below.

Administration of R-47 at a dose of 10 mg/kg p.o. or distilled water to paclitaxel-or vehicle-treated mice reveals a significant interaction between paclitaxel and R-47 treatment in the stage I [$F_{\text{paclitaxel} \times \text{R-47}} (1, 20) = 101.7; P < 0.0001$], (**Figure 27A**). The vehicle-paclitaxel group of mice reveals a significant decrease of stage I microglial cells compared to the vehicle-vehicle treated group of mice ($P < 0.0001$). Interestingly, mice treated with R-47 – paclitaxel show a significant increase in stage I of microglial cells compared to vehicle-paclitaxel-treated mice ($P < 0.0001$). Additionally, mice treated with R-47-paclitaxel do not indicate a change in stage I of microglial cells compared to mice treated with the R-47-vehicle group ($P = 0.6576$). Furthermore, the group of mice treated with R-47-vehicle does not show an alteration in stage I of microglial cells compared to the group of mice treated with vehicle-vehicle ($P = 0.2503$), (**Figure 27D**).

In a similar fashion of treatment mentioned in the above section. Administration of R-47 at a dose of 10 mg/kg p.o. or distilled water to paclitaxel-or vehicle-treated mice reveals a significant interaction between paclitaxel and R-47 treatment in stage III [$F_{\text{paclitaxel} \times \text{R-47}} (1, 20) =$

20.65; $P < 0.0001$], (**Figure 27C**). Interestingly, mice treated with vehicle-paclitaxel show a significant increase in stage III of microglial cells compared to mice treated with vehicle-vehicle ($P < 0.0001$). Importantly, the group of mice treated with R-47-paclitaxel demonstrates a significant decrease in stage III of microglial cells compared to the group of mice treated with vehicle-paclitaxel ($P < 0.0001$). Additionally, R-47-paclitaxel group of mice do not reveal an alteration in stage III of microglial cells compared to the R-47-vehicle group of mice ($P = 0.8637$). Furthermore, the group of mice treated with R-47-vehicle does not illustrate a change in stage III of microglial cells compared to the group of mice treated with vehicle-vehicle ($P = 0.7218$), (**Figure 27F**).

Lastly, the stage II of microglial cells does not show a significant change between paclitaxel and R-47 treatment in the stage II treatment groups [$F_{\text{paclitaxel} \times \text{R-47}} (1, 20) = 0.4718$; $P = 0.5000$], (**Figure 27B, E**).

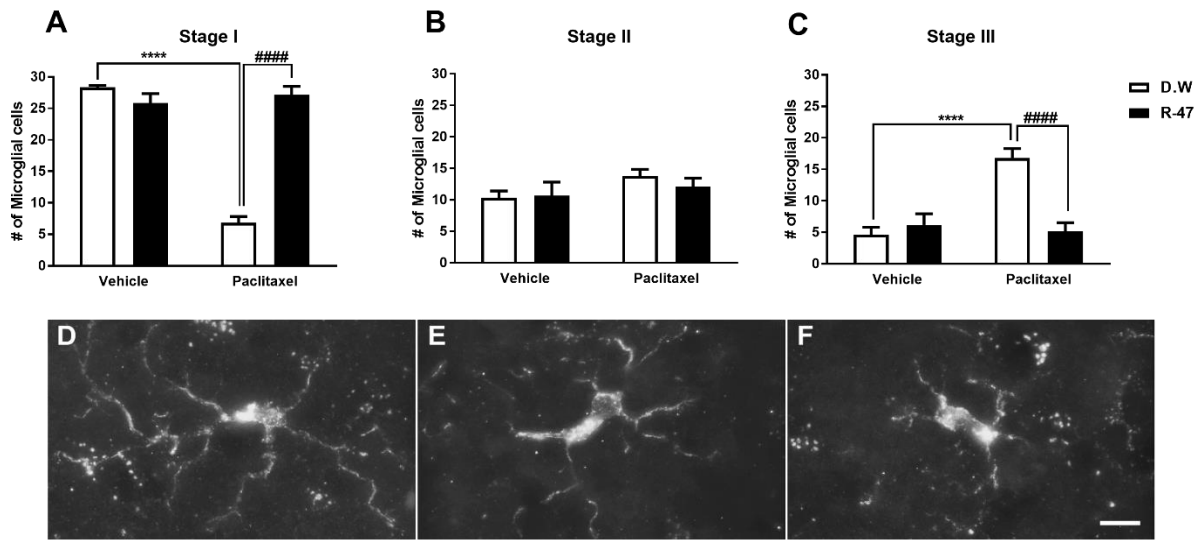


Figure 27. Paclitaxel alters the morphology of microglia in the dorsal horn, however, R-47 prevents the changes in microglia morphology. (A) Mice injected with paclitaxel (8 mg/kg i.p. for one cycle) plus distilled water (DW, the vehicle for R-47) reveal a significant decrease in the number of stage I microglial cells at 35 days post-paclitaxel injection, which was prevented by pre-and co-administration of R-47 at a dose of 10 mg/kg p.o. (C) Mice injected with paclitaxel plus DW show a significant elevation in the number of stage III microglial cells which was prevented by pre-and co-administration of R-47. (B) There were no significant changes in the number of stage II microglial cells between the treatment groups. (D-F) Representative images of microglial stages: (D) Stage I, cells with long, thin, and highly ramified processes; (E) Stage II, cells with shorter, thickened processes with less branching; and (F) Stage III, cells with increased hypertrophic changes such as shorter, thickened processes and cell body enlargement. **** $P < 0.0001$ D.W-paclitaxel vs D.W-vehicle; ##### $P < 0.0001$ R-47-paclitaxel vs D.W-paclitaxel. Bar represents 10 microns in all images. Images captured under 63x magnification. D.W, distilled water. $n = 6$ per group; data expressed as mean \pm SEM.

R-47 Induces Conditioned Place Preference in Paclitaxel-Treated Mice

In the current experiment, we used the CPP test in a model of peripheral neuropathy to evaluate the ability of R-47 to induce preference in paclitaxel-treated mice, which would be interpreted as pain relief in mice experiencing ongoing, spontaneous pain (Navratilova et al., 2016). Administration of R-47 at a dose of 10 mg/kg p.o. shows a significant CPP in paclitaxel-treated mice [$F_{\text{paclitaxel} \times \text{R-47}} (1, 56) = 5.4; P = 0.0238$], but not in vehicle-treated mice (**Figure 28**). However, paclitaxel-treated mice continue showing mechanical hypersensitivity before or after CPP test compared to vehicle-treated mice [$F_{\text{dose} \times \text{time}} (24, 168) = 0.3442, P = 0.9984$], (**Supplementary Figure 11**).

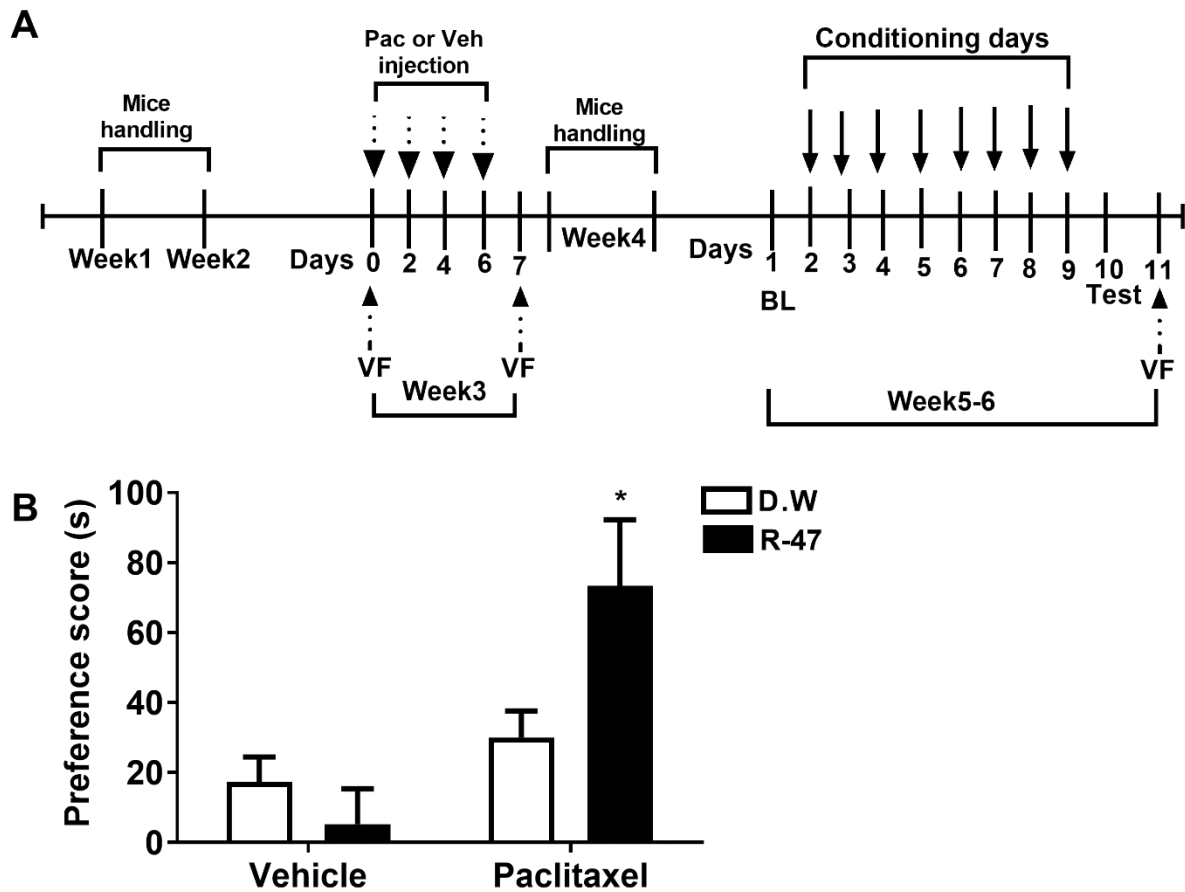
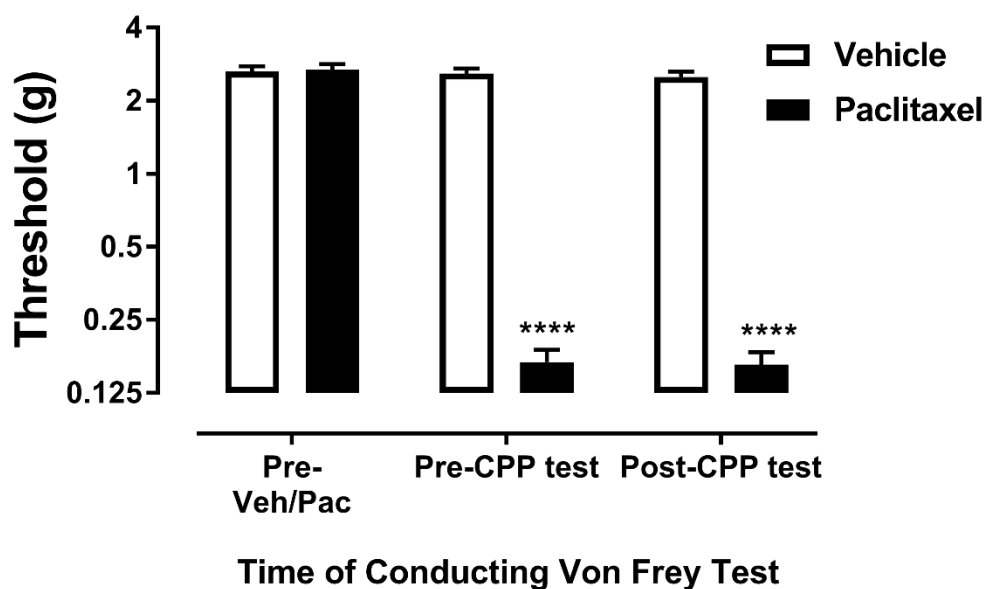


Figure 28. R-47 shows a CPP in mice developed neuropathy induced by paclitaxel. A) Timeline depiction of CPP test. B) The administration of R-47 at dose of 10 mg/kg p.o. induces CPP in paclitaxel-treated mice but not in vehicle-treated mice. * $P < 0.05$ vs D.W-Paclitaxel. BL, Baseline which represents pre-conditioning day; Test represents post-conditioning drug-free preference; D.W, Distilled Water; Veh, vehicle; Pac, paclitaxel; VF, von Frey. $n = 15$ per group; data expressed as mean \pm SEM.



Supplementary Figure 11. Paclitaxel induces mechanical hypersensitivity. Administration of paclitaxel at a dose of 8 mg/kg i.p. for one cycle produces significant mechanical hypersensitivity compared to vehicle-treated mice. These paclitaxel-treated mice are from the CPP experiment which continued showing mechanical hypersensitivity before and after conducting the CPP test . ****P < 0.0001 vs vehicle. Veh, vehicle; Pac, paclitaxel. n = 30 per group; data expressed as mean ± SEM.

R-47 Neither Promotes Tumor Cell Growth Both *in vitro* or *in vivo* Nor Interferes with Paclitaxel-Induced Antitumor Activity

Disclosure: The studies investigating the potential actions of R-47 in cancer were performed and described by Dr. David Gewirtz laboratory-primarily by S. Lauren Kyte as follows:

Prior to considering the potential of $\alpha 7$ silent agonists such as R-47 for the treatment of CIPN in cancer patients, it will be critical to evaluate R-47 in preclinical cancer models, both alone and in combination with cancer chemotherapeutic drugs in both *in vitro* and *in vivo* models. Our

goals were to confirm that R-47 that was shown to be effective in our animal CIPN Paclitaxel model, will not promote tumor cell growth or attenuate the growth inhibitory/cell killing actions of cancer chemotherapy. A similar experimental design described in Chapter 3 was followed. R-47 fails to significantly increase A549 and H460 non-small cell lung cancer (NSCLC) viable cell number at both 48 and 72 hours following 24-hour exposure to 0.1-10 μ M R-47. Likewise, treatment with R-47 (1 μ M) for 48 hours does not cause an increase in A549 or H460 viable cell number for up to 7 days post-treatment when compared to untreated cells. In a clonogenic assay, 24-hour treatment with 1 μ M R-47 does not increase the number of A549 or H460 colonies when compared to control. In addition, R-47 (1 μ M) pretreatment and subsequent co-treatment with paclitaxel (50 nM) does not interfere with the significant reduction in viable A549 or H460 cell number induced by paclitaxel alone. Collectively, these data suggest that R-47 alone does not have a significant effect on NSCLC viability, proliferation, or colony formation. In addition, the antitumor activity of paclitaxel is not affected by R-47.

To test whether these *in vitro* findings translate to an animal cancer model, A549 NSCLC cells were subcutaneously injected into the flanks of male, immunodeficient NSG mice. Once the tumors were established, mice were given R-47 (10 mg/kg, p.o.) twice daily for 3 days, then once daily in combination with paclitaxel (10 mg/kg, i.p.) for 4 days. Tumor volume was determined over time with calipers and tumors were weighed following extraction 17 days after treatment began. The paclitaxel regimen significantly decreases the tumor volume when compared to vehicle-treated mice. R-47 does not increase tumor volume either alone or in combination with paclitaxel when compared to vehicle- and paclitaxel-treated mice, respectively. The tumor weights followed the same trend, with R-47 having no significant effect alone or when administered with paclitaxel. The *in vivo* data suggest that R-47 will most likely not affect lung tumor growth when

administered prior to and during cancer chemotherapy for the purposes of preventing chemotherapy-induced peripheral neuropathy.

D. Discussion

The present work shows for the first time that the $\alpha 7$ nAChR subtype plays an important role in the development and maintenance of peripheral neuropathy induced by paclitaxel. Furthermore, targeting the $\alpha 7$ nAChR with a selective silent agonist R-47, reverses and prevents the development of mechanical hypersensitivity and protects the degeneration of IENFs as well. In addition, R-47 does not induce tolerance following repeated administration. Importantly, R-47 prevents the morphological alteration of microglia induced by paclitaxel in the dorsal horn of the spinal cord. Finally, administration of R-47 produce CPP in paclitaxel-treated mice but not in vehicle-treated mice, suggesting pain relief in neuropathic mice.

A substantial body of literatures suggest that the $\alpha 7$ nAChR plays major roles in various physiological processes in the body such as cognition, attention, and neuroprotection in addition to their role in neurodegeneration and neuroinflammation disease states (Bencherif et al., 2014). Here we show that $\alpha 7$ KO mice treated with a low dose of paclitaxel (1 mg/kg i.p. for one cycle) exhibit a significant mechanical hypersensitivity, which develop earlier with a delayed recovery compared to their $\alpha 7$ WT littermates. This is in accordance to our previous work, which demonstrated that $\alpha 7$ KO mice develop a significant increase in edema, hyperalgesia, and mechanical hypersensitivity in the complete Freund's adjuvant (CFA) test when compared with the $\alpha 7$ WT littermates. Thses results suggest that presence of $\alpha 7$ nAChR endogenous tone particularly on the immune cells protects against inflammation (AlSharari et al., 2013b). The existence of $\alpha 7$ nAChR on the immune cells both in the periphery and in the CNS stands for their important role in dampening the inflammatory cascade initiated following nerve injury which is induced by several toxins and noxious stimuli. This $\alpha 7$ nAChR anti-inflammatory dependent

mechanism is a part of an endogenous cholinergic anti-inflammatory pathway (Pavlov and Tracey, 2006).

Acute administration of R-47 dose- and time-dependently shows antinociceptive effect in paclitaxel-treated mice but not vehicle-treated mice, thus, the antinociceptive effect continued up to 8 hours. The time course of reversal of the drug is consistent with its half-life (104 min) in the mouse (van Maanen et al., 2015). Furthermore, the antinociceptive effect is consistent with our recent report showing that administration of NS6740 reverses the mechanical hypersensitivity in CCI mice (with shorter time of reversal compared to R-47) but not in sham mice (Papke et al., 2015). The administration of MLA, an $\alpha 7$ nAChR antagonist, blocked the antinociceptive effect of R-47, indicating that the effect is mediated through the $\alpha 7$ nAChR dependent mechanism. Moreover, the sub chronic administration of R-47 does not show tolerance to antinociceptive effect in paclitaxel-treated mice which is in contrast to other known antinociceptive/analgesics such as morphine that shows tolerance after repeated administration in mice (Lin et al., 2018) or rats (Legakis and Negus, 2018) treated with paclitaxel.

The properties of R-47 make it as an attractive candidate for drug development to treat CIPN. For that, we extended the finding that R-47 reverses the mechanical hypersensitivity into the aim of using R-47 to prevent the development of CIPN in mice. Chronic administration of R-47 at a dose of 10 mg/kg p.o. prior and during paclitaxel injection cycle completely prevents the development the mechanical hypersensitivity in mice received the combination of R-47 and Paclitaxel compared to the group of mice received paclitaxel alone. The preventive effect of R-47 extends to the fully protection of IENFs degeneration induced by paclitaxel which last up to 35 days in mice. This is consistent with our recent reports where we reveal that paclitaxel treated mice show reduction of IENFs density (Toma et al., 2017) and nicotine treatment prevents the reduction

of IENFs (Kyte et al., 2018). (Pacini et al., 2010) show that the $\alpha 7$ nAChR has a protective role in rats underwent CCI. Acute and chronic administration of PNU 282987 p.o. demonstrate a significant antinociceptive effect in paw pressure test, reduction of edema, and infiltration of macrophages into the sciatic nerve. Also, neither paclitaxel at a dose of 8 mg/kg nor R-47 at a dose of 10 mg/kg produces any locomotor impairment in mice, which is consistent with our previous report and another report that indicates paclitaxel does not produce motor impairment (Toma et al., 2017; Deng et al., 2015).

An extensive body of evidence suggests that microglial cells play a pivotal role in the normal physiological processes in the CNS such as surveillance, neuronal plasticity, and synaptic pruning (Salter and Stevens, 2017). These cells possess a normal ramified shape during normal conditions. However, once the injury occurs, pathological, chronic pain extend along with central sensitization into the affected are of spinal dorsal horn and brain. Here, microglial cells react to the glial modulators released from the central terminals of the nociceptors. Thus, microglia in turns become activated and release further the pro-inflammatory cytokines and chemokines which stimulate the secondary nociceptive neurons and enhance the pain chronification (Salter and Stevens, 2017). Here we show that paclitaxel-treated mice demonstrate an alteration in the morphology of microglial cells from stage I to stage III, suggesting the shifting of microglial cells from resting into more reactive state. Furthermore, R-47 in paclitaxel-treated mice prevents the alteration of the morphology of the microglia. Our results are in accordance with several studies showing the role of microglia in chronic neuropathic pain. (Gu et al., 2016) demonstrate that rats underwent spinal nerve transection (SNT) show mechanical hypersensitivity along with significant microgliosis in the spinal cord due to proliferating microglia but not due to peripheral monocytes which do not infiltrate into the spinal cord. Also, pharmacologic inhibition of microgliosis in the

spinal cord alleviate the mechanical hypersensitivity. Furthermore, rats underwent PSNL demonstrate microglial activation in the spinal cord for more than 3 months post-PSNL surgery. Additionally, intrathecal administration of selective inhibitor of microglia Mac-1 saponin reverses the microgliosis and attenuates the mechanical hypersensitivity (Echeverry et al., 2017). Also, (Makker et al., 2017) report that repeated paclitaxel injection to C57 BL/6J mice results in significant mechanical hypersensitivity. In the peripheral nervous tissue, paclitaxel treatment leads to elevations in the expression level of the neuronal injury marker ATF-3 in IB4+ and NF200+ sensory neurons and increases the level of the chemokines CCL2 and CCL3 in the lumbar DRG. Furthermore, in the CNS, paclitaxel treatment results in a significant astrocyte activation in the dorsal horn of the spinal cord and enhances the release of pro-inflammatory cytokines and chemokines. In addition, a rat model of single prolonged stress (SPS) induces mechanical hypersensitivity, glial activation, and elevation of pro-inflammatory cytokines level. Thus, intrathecal injection of PHA-543613, an $\alpha 7$ nAChR agonist leads to reversal of mechanical hypersensitivity, suppression of spinal glial activation, and downregulation of spinal pro-inflammatory cytokines level via $\alpha 7$ nAChR dependent manner (Sun et al., 2016). Furthermore, systemic and ventrolateral periaqueductal gray (vlPAG) injection of PHA-543613 results in anti-nociceptive effect in the rat formalin test via $\alpha 7$ nAChR dependent manner (Umana et al., 2017).

Our study shows that paclitaxel treatment downregulates the $\alpha 7$ nAChR expression level at day 28 post-paclitaxel injection. Although we did not measure the receptor expression level of the $\alpha 7$ nAChR following chronic administration of R-47, we expect that R-47 will prevent the downregulation of the receptor. In addition, at day 7 post-paclitaxel injection, we see that paclitaxel upregulates the expression level of the $\alpha 7$ nAChR, suggesting that early inflammatory process where paclitaxel accumulates and initiate the inflammatory cascade and that the body would need

to upregulate the $\alpha 7$ nAChR expression in DRG to counteract the inflammation. In contrast, at day 28 post-paclitaxel injection, we demonstrate that paclitaxel upregulates the $\alpha 7$ nAChR expression at the L4-L6 level of the spinal cord, suggesting that there is a transitioning state from the peripheral sensitization into central sensitization which involve the activation of glial cells, release of pro-inflammatory cytokines and chemokines. Our results are consistent with one study that shows that oxaliplatin in treated rats downregulates the $\alpha 7$ nAChR expression level in the DRG, sciatic nerve, and spinal cord 21 days post-oxaliplatin injection and that repeated administration of PNU 282987 p.o. protects the downregulation of the $\alpha 7$ nAChR (Di Cesare Mannelli et al., 2014).

Our present study reveals that R-47 show preference in the CPP test in paclitaxel-treated mice, suggesting that R-47 produces a relief of pain and aversive state in the mice induced by paclitaxel. Our results are consistent with another study using non-nicotinic ligands to alleviate the aversive, painful state. For example, administration of MJN110, an endocannabinoid monoacylglycerol lipase (MAGL) inhibitor, at a dose of 5 mg/kg i.p. produces preference in the CPP test in paclitaxel-treated mice but not in vehicle-treated mice (Curry et al., 2018). Importantly and in contrast to several drugs of abuse such as nicotine (Jackson et al., 2017), and morphine (Neelakantan et al., 2016), R-47 does not show preference in the CPP test in vehicle-treated mice, suggesting that R-47 lacks the intrinsic rewarding properties of drugs that have abuse liability.

Several reports indicate that nicotine and nicotinic analogues may enhance the proliferation of tumor growth and increases the expression of the $\alpha 7$ nAChR on the cell surface (Grando, 2014; Davis et al., 2009). In collaboration with David Gewirtz lab, we tested the possibility of R-47 would enhance tumor proliferation in A549 and H460 non-small cell lung cancer cell lines *in vitro* and A549 NSCLC into immunodeficient NSG mouse model *in vivo*. R-47 does not produce a

significant effect on NSCLC viability, proliferation, or colony formation. Additionally, R-47 does not affect on the paclitaxel anti-tumor effect both *in vitro* and *in vivo*. These results are in accordance with our previous report where we show nicotine does not promote the proliferation of tumor cells *in vitro* or in animal bearing tumors *in vivo* (Kyte et al., 2018).

Collectively, our results show that $\alpha 7$ nAChR subtype plays an important role in the CIPN pathogenesis. Additionally, targeting the $\alpha 7$ nAChR with the use of the selective ligands such as silent agonist R-47 as a potential treatment of CIPN without potential tumor proliferation or interfering with the chemotherapy.

CHAPTER FIVE

GENERAL DISCUSSION

A. Paclitaxel Induces CIPN – Overview

Paclitaxel (chemical structure is shown in Figure 29) is an efficacious anti-tumor drug used in the treatment of different types of solid tumors such as lung, breast, ovarian, head, and neck cancers. Paclitaxel induces its anticancer effect through polymerization of tubulin, thus, disturbing the microtubules by preventing their depolymerization and arresting cell cycle division which leads to apoptosis and cell death (Mekhail and Markman, 2002). However, it induces several side effects, such as hypersensitivity, neurotoxicity, and hematological toxicities. One of the most reported side effect in the clinic is chemotherapy-induced peripheral neuropathy (CIPN) (Rowinsky et al., 1993). Patients report multiple neuropathic pain symptoms such as paresthesia, numbness, burning pain, and allodynia. These symptoms present mostly in their hands and feet (Dougherty et al., 2004). The distribution of clinical symptoms in hands and feet is attributed to the effect of paclitaxel on the longer nerves first which disturb the axonal transport process leading to the inhibition of microtubule function and eventually cell death (Ferrier et al., 2013). Unfortunately, about 40% of patients experiencing CIPN symptoms. These symptoms could last for months or years after chemotherapy cessation which leads to a decrease in the quality of life (Poupon et al., 2015; Boyette-Davis et al., 2013). Additionally, CIPN in patients treated with chemotherapy can be accompanied by distress, anxiety, depression, sleep disturbance, and cognitive deficits (Colloca et al., 2017; Hong et al., 2014). The incidence of CIPN may range from

10 to 100 % depending on the chemotherapeutic agent and the dose used in the treatment of cancer (Balayssac et al., 2011). While several adjuvant therapies are used in the clinic, such as gabapentin, duloxetine, and tricyclic antidepressants, these compounds show modest or no effect in the relief of the CIPN symptoms (Majithia et al., 2016). Therefore, it is critical to identify newer targets and develop novel therapies to mitigate or prevent CIPN.

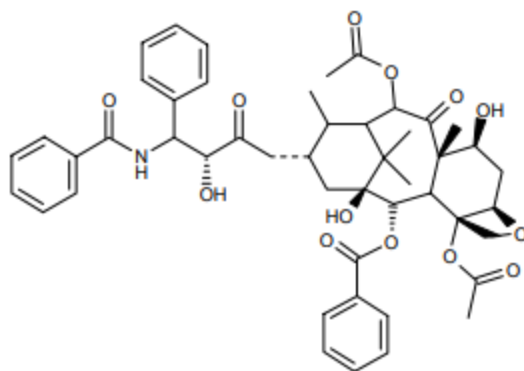


Figure 29. The chemical structure of paclitaxel. Adapted from Rowinsky et al., 1993.

B. Establishment of a CIPN Model in Mice

Establishing animal (rodents) models of CIPN enable us to better investigate and identify pathophysiological mechanisms that lead to the development of CIPN and to find novel therapies for CIPN treatment. In chapter two of this dissertation, we characterize a CIPN mouse model in C57 BL/6J male mice. Administration of paclitaxel to mice at doses of 2,4, and 8 mg/kg i.p. for one cycle induces dose and time-dependent mechanical and cold hypersensitivity by using von Frey and acetone tests, respectively. This is consistent with other reports that show paclitaxel induces similar mechanical and cold hypersensitivity in mice (Donvito et al., 2016; Deng et al., 2015). These outcome measures are considered reflexive - sensory measures commonly used in the animal model of CIPN. We see development of mechanical hypersensitivity following the first paclitaxel injection at a dose of 8 mg/kg. Interestingly, patients receiving paclitaxel develop what

so-called acute pain syndrome (APS) which characterize by the appearance of the peripheral neuropathy symptoms, such as numbness and tingling following the first round of paclitaxel administration (Reeves et al., 2012). We further show that mice treated with paclitaxel at a dose of 2 mg/kg i.p. after the second cycle develop a robust mechanical hypersensitivity which lasts longer and delays in recovery. Interestingly, our mouse model of CIPN show that carboplatin-treated mice do not demonstrate mechanical hypersensitivity. However, administration of carboplatin at a dose of 5 mg/kg i.p for one cycle followed by a lower dose of paclitaxel (1 mg/kg i.p. for one cycle), lead to sensitization of mice to paclitaxel, this is similar what is observed in the clinic. These results add a translational value to our mouse model of CIPN. Moreover, we demonstrate that paclitaxel-treated mice show robust reduction of IENFs compared to vehicle-treated mice, consistently with other reports showing similar effect of paclitaxel in rodent model of CIPN (Krukowski et al., 2015; Bennett et al., 2011). The activation of nociceptive fibers (which are mostly polymodal C unmyelinated and thinly myelinated A δ) lead to the transmission of pain signal from the peripheral to the central nervous system. These nociceptive fibers express multiple ligand-gated and voltage-gated ion channels. Peripheral sensitization involves upregulation of ion channels and increased firing of the action potential of the nociceptors. In addition, nociceptive fibers here are hyperactive and release several chemical mediators of inflammation such as substance P and CGRP. These mediators act as a chemoattractant to immune cells such as neutrophils, macrophages, and mast cells which in turn lead to the release of serotonin, histamine, TNF- α , IL-1 β , PGE₂ that further sensitize nerve fibers and augment the inflammatory process (Pinho-Ribeiro et al., 2017). The nociceptor neurons in the spinal cord will further release the inflammatory mediators such as ATP, CCL2, and CSF-1 which in turn activate microglia and astrocytes and infiltration of T-cells as well. Glial cells will further release cytokines, chemokines,

nerve growth factors to stimulate further the second order nociceptive neuron that lead to central sensitization and chronification of pain (Pinho-Ribeiro et al., 2017).

C. Paclitaxel Induces Affective-Like Changes in Mice

Patients experience chronic pain (in particularly, neuropathic pain) are frequently exhibit mood disorders such as anxiety, stress, depression, and sleep disturbance (Gruener et al., 2018; Yalcin and Barrot, 2014). In addition, pre-clinical models of a non-chemotherapy induced neuropathic pain show negative affective symptoms, i.e., anxiety-depression like behaviors (La Porta et al., 2016; Yalcin et al., 2011) in a time-dependent manner. This is consistent with our report where we observed that paclitaxel-treated mice develop anxiety-depression like behaviors and anhedonia-like state in multiple behavioral assays (Toma et al., 2017). In addition, different regions of the brain might be involved in the development of affective-like changes such as anterior cingulate cortex (ACC), prefrontal cortex (PFC), amygdala, nucleus accumbens, hippocampus, and locus coeruleus in which multiple functional changes occur to induce the affective symptoms. (for further details: see (Yalcin et al., 2014)).

D. Nicotinic Acetylcholine Receptors as a Putative Target in CIPN

Several lines of evidence suggest that targeting nicotinic acetylcholine receptors result in analgesic and/or antinociceptive effects in both experimental human and animal pain studies (Umana et al., 2013). For example, nicotine, a prototypical nAChRs agonist, shows a reduction in pain scores in a cold pressor test in both smokers and ex-smokers (Fertig et al., 1986). Likewise, nicotine demonstrates an antinociceptive properties in multiple acute and chronic pain models in mice (AlSharari et al., 2012; AlSharari et al., 2015). Indeed, our recent work show that acute administration of nicotine reverses in a dose-and time-dependent manner the mechanical

hypersensitivity in a mouse model of CIPN. Consistently, administration of nicotine at a dose of 1.5 mg/kg i.p reverses mechanical hypersensitivity in rats treated with oxaliplatin. Furthermore, chronic infusion of nicotine via minipumps at a dose of 24 mg/kg s.c for seven days completely prevents the development of mechanical hypersensitivity and rescues the reduction of IENFs as well (Kyte et al., 2018). Moreover, we found the protective effects of nicotine are mediated at least in part via $\alpha 7$ nAChR subtype.

A substantial body of evidence demonstrate the important role of $\alpha 7$ nAChR subtype in facilitation of memory, cognition, and attention in the brain. In addition, their neuroprotective role in neuroinflammatory diseases is well documented in animal models (Corradi and Bouzat, 2016). These properties correlated well with the expression of the $\alpha 7$ nAChR subtype in several neuronal regions including the hippocampus, spinal cord, DRG, and non-neuronal cells including cells of immune system (see Figure 30 that depicts the proposed role of $\alpha 7$ nAChR on immune cells in dampening the inflammation induced by paclitaxel), (Corradi and Bouzat., 2016). The pharmacology of the $\alpha 7$ nAChR can be modulated by several ligands such as agonists, PAMs, Ago-PAMs, and the recent discovery of silent agonists, makes these receptors an attracting target for the treatment of pain and inflammatory diseases. Several reports indicate that $\alpha 7$ nicotinic agonists can induce antinociception, anti-inflammatory, neuroprotection, and an anti-allodynic effect in rodent models of pain (Flood and Damaj., 2014; Freitas et al., 2013a; Freitas et al., 2013b). interestingly, our recent reports demonstrate that the $\alpha 7$ nAChR subtype may play a protective role in chronic inflammatory pain mouse models (AlSharari et al., 2016; AlSharari et al., 2013b), suggesting the presence of a endogenous cholinergic anti-inflammatory tone mediated by $\alpha 7$ nAChRs (Pavlov et al., 2009). For that, our main hypothesis was that $\alpha 7$ nAChRs play a modulatory role in the initiation and/or maintenance of CIPN induced by paclitaxel. In addition,

targeting the $\alpha 7$ nAChR with R-47, a selective silent agonist for $\alpha 7$ nAChR would reverse and prevent the CIPN in mice. Consistent with our hypothesis, we see that mice lacking the $\alpha 7$ nAChR show robust mechanical hypersensitivity (with early onset and delayed recovery) compared to their WT littermates, suggesting a protective role in the pathology of CIPN. Furthermore, the altered expression of $\alpha 7$ nAChR induced by paclitaxel in DRG (where paclitaxel mostly accumulates) and spinal cord suggest their anti-inflammatory role and that time gap between the DRG and spinal cord may suggest the transitioning state from peripheral to central sensitization of pain (for further details on the inflammation induced by paclitaxel peripherally or centrally: see the introduction chapter section A.3) and A.4).

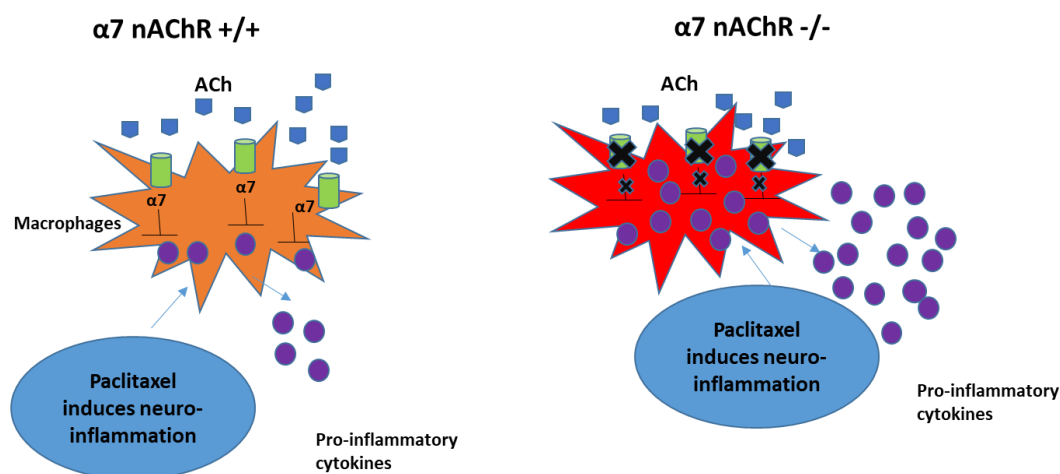


Figure 30. The $\alpha 7$ nAChR plays A Regulatory Role Through Endogenous Cholinergic Anti-Inflammatory Pathway. A simplified schematic showing that the presence of $\alpha 7$ nAChR subtype on the immune cells leads to downregulations of the pro-inflammatory cytokines whereas the inflammatory response induced by paclitaxel is augmented when the $\alpha 7$ nAChR are absent.

Importantly, unlike other $\alpha 7$ nAChR agonists or nicotine which show an inverted U shape dose-effect curve and tolerance after repeated administration (AlSharari et al., 2016; Grabus et al., 2012; Damaj et al., 1996), R-47 effects in our CIPN model are dose-dependent and

no tolerance developed after chronic exposure to the drug. In addition, the pharmacological profile of R-47 makes it a potential candidate for drug development with a translational value to treat CIPN due to suitable pharmacokinetic profile, activity after oral administration, lack of tolerance after repeated administration, and anti-inflammatory properties. Indeed, we demonstrate that R-47 reverses and prevents the development of CIPN induced by paclitaxel such as the development of mechanical hypersensitivity and reduction of IENFs. Additionally, repeated administration of R-47 prevents the transitioning of microglial cells from stage I to stage III in the spinal cord which suggest that microglial cells play an important role in the CIPN pathogenesis and that the existence of $\alpha 7$ nAChR on the microglia makes them a viable target to reduce the inflammatory process. Finally, R-47 at a dose of 10 mg/kg p.o. produces preference in paclitaxel-treated mice but not vehicle-treated mice in CPP test, suggesting the lack of intrinsic rewarding effect of R-47 and low probability of abuse liability. This is consistent with other reports using non-nicotinic ligands to explore the analgesic potential of candidate drugs to produce a pain relief in animals undergoing spontaneous, ongoing pain. For example, administration of clonidine and/or conotoxin to SNL rats produce preference to the paired chamber where they received the drugs but not in the sham rats (King et al., 2009). Similarly, administration of a histone deacetylase (HDAC6) inhibitor ACY-1083, produces CPP in cisplatin-treated mice, suggesting a relief from spontaneous pain (Krukowski et al., 2017). In contrast, (Neelakantan et al., 2016) show that both paclitaxel or vehicle-treated mice demonstrate preference to morphine in a dose-dependent manner, suggesting that morphine's rewarding effect is a potential of drug abuse liability, while R-47 does not show that profile in mice.

E. Future Directions

Studies conducted in this dissertation project support an important role for $\alpha 7$ nAChR in paclitaxel-induced CIPN. However, the mechanisms and circuitry/sites of this effect is currently unknown. Our results with microglia suggest the possibility that $\alpha 7$ nAChR expressed on these immune cells represent an important target for paclitaxel-induced CIPN. This could be investigated by creating and breeding a line of $\alpha 7$ nAChR Flox P mouse x Cre recombinase from the lysozyme M-encoding locus (Lyz2) mouse. This will enable us to better understand the important role of the $\alpha 7$ nAChR in development of CIPN, since the inflammatory component is one of the crucial factors that induce CIPN. Further, the role of $\alpha 7$ nAChR in other forms of cancer chemotherapy is unknown. Future studies could examine how $\alpha 7$ nAChR is modulated in response to chemotherapies with other mechanisms of action, such as cisplatin.

So far, the downstream signaling pathway associated with the $\alpha 7$ nAChR after R-47 binding and changing the conformational state of the receptor is unknown. One of the possible pathways to explore is the cross-talk of $\alpha 7$ nAChR with GPCRs (Kabbani and Nichols, 2018) which could explain the prolonged action of R-47. Furthermore, our lab recently showed that there is another pathway and cross-talk between the $\alpha 7$ nAChR and PPAR- α (Donvito et al., 2017).

It is important to note that our results with R-47 that show its usefulness in the reversal and prevention of CIPN in preclinical studies add an important translational value to advance and to advocate the use of R-47 or possible analogues to treat CIPN in cancer patients undergoing chemotherapy. Thus, the pharmacological profile of R-47 such as its convenient pharmacokinetic parameters, its good bioavailability after oral administration, the lack of tolerance following repeated administration and its anti-inflammatory effect, makes R-47 a potential candidate for drug development. However,, further short term and long term toxicological studies in various animal

species are required to elucidate if there are any adverse effect that could result following R-47 administration before initiating phase I human clinical trials. Lastly, an interesting study to conduct in animal models of CIPN, is the opioid-sparing effect of R-47 which could lead to a decrease in the prescription of opioids in the clinical practice (opioid crisis), i.e., this could reduce the dose of the opioid required to show analgesia and pain relief, without an increase in the abuse liability and side effects of opioids.

REFERENCES

- Alotaibi M, Sharma K, Saleh T, Povirk LF, Hendrickson EA, and Gewirtz DA (2016) Radiosensitization by PARP inhibition in DNA repair proficient and deficient tumor cells: Proliferative recovery in senescent cells. *Radiat Res* **185**: 229-245.
- Abdin, M.J., Morioka, N., Morita, K., Kitayama, T., Kitayama, S., Nakashima, T., Dohi, T., 2006. Analgesic action of nicotine on tibial nerve transection (TNT)-induced mechanical allodynia through enhancement of the glycinergic inhibitory system in spinal cord. *Life Sci.* 80, 9–16. doi:10.1016/j.lfs.2006.08.011
- Albuquerque, E.X., Pereira, E.F.R., Alkondon, M., Rogers, S.W., 2009. Mammalian Nicotinic Acetylcholine Receptors: From Structure to Function. *Physiol. Rev.* 89, 73–120. doi:10.1152/physrev.00015.2008.
- AlSharari, S.D., Akbarali, H.I., Abdullah, R.A., Shahab, O., Auttachoat, W., Ferreira, G.A., White, K.L., Lichtman, A.H., Cabral, G.A., Damaj, M.I., 2013a. Novel insights on the effect of nicotine in a murine colitis model. *J. Pharmacol. Exp. Ther.* 344, 207–17. doi:10.1124/jpet.112.198796
- AlSharari, S.D., Bagdas, D., Akbarali, H.I., Lichtman, P.A., Raborn, E.S., Cabral, G.A., Carroll, F.I., McGee, E.A., Damaj, M.I., 2016. Sex Differences and Drug Dose Influence the Role of the $\alpha 7$ Nicotinic Acetylcholine Receptor in the Mouse Dextran Sodium Sulfate-Induced Colitis Model. *Nicotine Tob. Res.* ntw245. doi:10.1093/ntr/ntw245
- AlSharari, S.D., Carroll, F.I., McIntosh, J.M., Damaj, M.I., 2012. The antinociceptive effects of nicotinic partial agonists varenicline and sazetidine-A in murine acute and tonic pain

- models. *J. Pharmacol. Exp. Ther.* 342, 742–9. doi:10.1124/jpet.112.194506
- AlSharari, S.D., Freitas, K., Damaj, M.I., 2013b. Functional role of alpha7 nicotinic receptor in chronic neuropathic and inflammatory pain: Studies in transgenic mice. *Biochem. Pharmacol.* 86, 1201–1207. doi:10.1016/j.bcp.2013.06.018
- Alsharari SD, King JR, Nordman JC, Muldoon PP, Jackson A, Zhu AZX, Tyndale RF, Kabbani N, and Damaj MI (2015) Effects of menthol on nicotine pharmacokinetic, pharmacology and dependence in mice. *PLoS One* **10**:1–16.
- Areti, A., Yerra, V.G., Naidu, V., Kumar, A., 2014. Oxidative stress and nerve damage: Role in chemotherapy induced peripheral neuropathy. *Redox Biol.* 2, 289–95. doi:10.1016/j.redox.2014.01.006
- Arrieta, O., Michel Ortega, R.M., Villanueva-Rodríguez, G., Serna-Thomé, M.G., Flores-Estrada, D., Diaz-Romero, C., Rodríguez, C.M., Martínez, L., Sánchez-Lara, K., 2010. Association of nutritional status and serum albumin levels with development of toxicity in patients with advanced non-small cell lung cancer treated with paclitaxel-cisplatin chemotherapy: a prospective study. *BMC Cancer* 10, 50. doi:10.1186/1471-2407-10-50
- Asaoka, Y., Kato, T., Ide, S., Amano, T., Minami, M., 2018. Pregabalin induces conditioned place preference in the rat during the early, but not late, stage of neuropathic pain. *Neurosci. Lett.* 668, 133–137. doi:10.1016/j.neulet.2018.01.029
- Authier, N., Balayssac, D., Marchand, F., Ling, B., Zangarelli, A., Descoeur, J., Coudore, F., Bourinet, E., Eschalier, A., 2009. Animal Models of Chemotherapy-Evoked Painful Peripheral Neuropathies. *Neurotherapeutics* 6, 620–629. doi:10.1016/j.nurt.2009.07.003

- Bagdas D, Alsharari SD, Freitas K, Tracy M, and Damaj MI (2015) The role of $\alpha 5$ nicotinic acetylcholine receptors in mouse models of chronic inflammatory and neuropathic pain. *Biochem Pharmacol* **97**:590–600.
- Bagdas D, Ergun D, Jackson A, Toma W, Schulte MK, and Damaj MI (2017) Allosteric modulation of $\alpha 4\beta 2^*$ nicotinic acetylcholine receptors: Desformylflustrabromine potentiates antiallodynic response of nicotine in a mouse model of neuropathic pain. *Eur J Pain* 1–10.
- Bagdas, D., Gurun, M.S., Flood, P., Papke, R.L., Damaj, M.I., 2017. New Insights on Neuronal Nicotinic Acetylcholine Receptors as Targets for Pain and Inflammation: A Focus on $\alpha 7$ nAChRs. *Curr. Neuropharmacol.* doi:10.2174/1570159X15666170818102108
- Bagdas D, Muldoon PP, Zhu AZX, Tyndale RF, and Damaj MI (2014) Effects of methoxsalen, a CYP2A5/6 inhibitor, on nicotine dependence behaviors in mice. *Neuropharmacology* **85**:67–72.
- Bagdas, D., AlSharari, S.D., Freitas, K., Tracy, M., Damaj, M.I., 2015. The role of $\alpha 5$ nicotinic acetylcholine receptors in mouse models of chronic inflammatory and neuropathic pain. *Biochem. Pharmacol.* 97, 590–600. doi:10.1016/j.bcp.2015.04.013
- Balayssac D, Ferrier J, Descoeur J, Ling B, Pezet D, Eschalier A, and Authier N (2011) Chemotherapy-induced peripheral neuropathies: from clinical relevance to preclinical evidence. *Expert Opin Drug Saf* **10**:407–417.
- Basbaum, A.I., Bautista, D.M., Scherrer, G., Julius, D., 2009. Review Cellular and Molecular Mechanisms of Pain 267–284. doi:10.1016/j.cell.2009.09.028
- Beijers AJM, Jongen JLM, and Vreugdenhil G (2012) Chemotherapy-induced neurotoxicity: The value of neuroprotective strategies. *Neth J Med* **70**:18–25.

- Beijers, A.J.M., Jongen, J.L.M., Vreugdenhil, G., 2012. Chemotherapy-induced neurotoxicity: The value of neuroprotective strategies. *Neth. J. Med.* 70, 18–25.
- Bencherif, M., Lippiello, P.M., Lucas, R., Marrero, M.B., 2011. Alpha7 nicotinic receptors as novel therapeutic targets for inflammation-based diseases. *Cell. Mol. Life Sci.* 68, 931–949. doi:10.1007/s00018-010-0525-1
- Bencherif, M., Narla, S.T., Stachowiak, M.S., 2014. Alpha7 neuronal nicotinic receptor: a pluripotent target for diseases of the central nervous system. *CNS Neurol Disord Drug Targets* 13, 836–845. doi:10.2174/1871527313666140711094525
- Bennett GJ, Liu GK, Xiao WH, Jin HW, and Siau C (2011) Terminal arbor degeneration (TAD): a novel lesion produced by the antineoplastic agent, paclitaxel. *Eur J Neurosci* **33**:1667–1676.
- Bennett, G.J., Liu, G.K., Xiao, W.H., Jin, H.W., Siau, C., 2011. Terminal arbor degeneration - a novel lesion produced by the antineoplastic agent paclitaxel. *Eur. J. Neurosci.* 33, 1667–1676. doi:10.1111/j.1460-9568.2011.07652.x
- Benowitz NL, Hukkanen J, and Jacob P (2009) Nicotine chemistry, metabolism, kinetics and biomarkers. *Handb Exp Pharmacol* **192**: 29–60.
- Blagosklonny MV and Fojo T (1999) Molecular effects of paclitaxel: Myths and reality (a critical review). *Int J Cancer* **83**:151–156.
- Bodnoff, S.R., Suranyi-Cadotte, B., Aitken, D.H., Quirion, R., Meaney, M.J., 1988. The effects of chronic antidepressant treatment in an animal model of anxiety. *Psychopharmacology (Berl)*. 95, 298–302.
- Boehmerle, W., Huehnchen, P., Peruzzaro, S., Balkaya, M., Endres, M., 2014. Electrophysiological, behavioral and histological characterization of paclitaxel, cisplatin, vincristine and bortezomib-induced neuropathy in C57Bl/6 mice. *Sci. Rep.* 4, 6370.

doi:10.1038/srep06370

- Bogdanova, O. V, Kanekar, S., Anci, K.E.D., Renshaw, P.F., 2013. Factors influencing behavior in the forced swim test. *Physiol. Behav.* 118, 227–239. doi:10.1016/j.physbeh.2013.05.012
- Boyette-Davis, J.A., Cata, J.P., Driver, L.C., Novy, D.M., Bruel, B.M., Mooring, D.L., Wendelschafer-Crabb, G., Kennedy, W.R., Dougherty, P.M., 2013. Persistent chemoneuropathy in patients receiving the plant alkaloids paclitaxel and vincristine. *Cancer Chemother. Pharmacol.* 71, 619–626. doi:10.1007/s00280-012-2047-z
- Carozzi, V.A., Canta, A., Chiorazzi, A., 2015. Chemotherapy-induced peripheral neuropathy: What do we know about mechanisms? *Neurosci. Lett.* 596, 90–107. doi:10.1016/j.neulet.2014.10.014
- Chaplan SR, Bach FW, Pogrel JW, Chung JM, and Yaksh TL (1994) Quantitative assessment of tactile allodynia in the rat paw. *J Neurosci Methods* **53**:55–63.
- Chaplan, S.R., Bach, F.W., Pogrel, J.W., Chung, J.M., Yaksh, T.L., 1994. Quantitative assessment of tactile allodynia in the rat paw. *J. Neurosci. Methods* 53, 55–63.
- Charan J, and Kantharia ND (2013) How to calculate sample size in animal studies? *J. Pharmacolo. Pharmacothera.* **4**: 303-306.
- Charan, J., Kantharia, N.D., 2013. How to calculate sample size in animal studies? *J. Pharmacol. and Pharmacother.* 4, 303-306. doi:10.4103/0976-500X.119726
- Chen GQ, Lin B, Dawson MI, and Zhang X (2002) Nicotine modulates the effects of retinoids on growth inhibition and RAR β expression in lung cancer cells. *Int J Cancer* **99**: 171-178.
- Colloca, L., Ludman, T., Bouhassira, D., Baron, R., Dickenson, A.H., Yarnitsky, D., Freeman, R., Truini, A., Attal, N., Finnerup, N.B., 2017. Neuropathic pain. *Nat Rev Dis Prim.* 3, 17002. doi:10.1038/nrdp.2017.2.Neuropathic

- Cordero-Erausquin, M., Pons, S., Faure, P., Changeux, J.P., 2004. Nicotine differentially activates inhibitory and excitatory neurons in the dorsal spinal cord. *Pain* 109, 308–318. doi:10.1016/j.pain.2004.01.034
- Crawley, J., Goodwin, F.K., 1980. Preliminary report of a simple animal behavior model for the anxiolytic effects of benzodiazepines. *Pharmacol. Biochem. Behav.* 13, 167–170.
- Curry, Z., Wilkerson, J., Bagdas, D., Kyte, S., Patel, N., Donvito, G., Mustafa, M.A., Poklis, J., Niphakis, M., Hsu, K.-L., Cravatt, B.F., Gewirtz, D.A., Damaj, M.I., Lichtman, A.H., 2018. Monoacylglycerol lipase inhibitors reverse paclitaxel-induced nociceptive behavior and proinflammatory markers in a mouse model of chemotherapy-induced neuropathy. *J. Pharmacol. Exp. Ther.* jpet.117.245704. doi:10.1124/jpet.117.245704
- Damaj MI, Siu ECK, Sellers EM, Tyndale RF, and Martin BR (2007) Inhibition of nicotine metabolism by methoxysalen: pharmacokinetic and pharmacological studies in mice. *JPET* **320**: 250-257.
- Damaj, M.I., Carroll, F.I., Eaton, J.B., Navarro, H.A., Blough, B.E., Mirza, S., Lukas, R.J., Martin, B.R., 2004. Enantioselective effects of hydroxy metabolites of bupropion on behavior and on function of monoamine transporters and nicotinic receptors. *Mol Pharmacol* 66, 675–682. doi:10.1124/mol.104.001313
- Damaj, M.I., Welch, S.P., Martin, B.R., 1996. Characterization and modulation of acute tolerance to nicotine in mice. *J Pharmacol Exp Ther* 277, 454–461.
- Dasgupta P, Kinkade R, Joshi B, DeCook C, Haura E, and Chellappan S (2006) Nicotine inhibits apoptosis induced by chemotherapeutic drugs by up-regulating XIAP and survivin. *Proc Natl Acad Sci* **103**:6332–6337.

- Davidson, B.A., Foote, J., Clark, L.H., Broadwater, G., Havrilesky, L.J., 2016. Tumor grade and chemotherapy response in endometrioid endometrial cancer. *Gynecol. Oncol. Reports* 17, 3–6. doi:10.1016/j.gore.2016.04.006
- Davis, R., Rizwani, W., Banerjee, S., Kovacs, M., Haura, E., Coppola, D., Chellappan, S., 2009. Nicotine promotes tumor growth and metastasis in mouse models of lung cancer. *PLoS One* 4, 1–9. doi:10.1371/journal.pone.0007524
- Deng L, Guindon J, Cornett BL, Makriyannis A, Mackie K, and Hohmann AG (2015) Chronic cannabinoid receptor 2 activation reverses paclitaxel neuropathy without tolerance or cannabinoid receptor 1-dependent withdrawal. *Biol Psychiatry* **77**:475–487.
- Deng, L., Guindon, J., Cornett, B.L., Makriyannis, A., Mackie, K., Hohmann, A.G., 2015. Chronic cannabinoid receptor 2 activation reverses paclitaxel neuropathy without tolerance or cannabinoid receptor 1-dependent withdrawal. *Biol Psychiatry* 77, 475–487. doi:10.1016/j.biopsych.2014.04.009
- Di Cesare Mannelli, L., Pacini, A., Matera, C., Zanardelli, M., Mello, T., De Amici, M., Dallanocce, C., Ghelardini, C., 2014. Involvement of $\alpha 7$ nAChR subtype in rat oxaliplatin-induced neuropathy: Effects of selective activation. *Neuropharmacology* 79, 37–48. doi:10.1016/j.neuropharm.2013.10.034
- Di Cesare Mannelli L, Zanardelli M, and Ghelardini C (2013) Nicotine is a pain reliever in trauma- and chemotherapy-induced neuropathy models. *Eur J Pharmacol* **711**:87–94.
- Donvito, G., Wilkerson, J.L., Damaj, M.I., Lichtman, A.H., 2016. Palmitoylethanolamide Reverses Paclitaxel-Induced Allodynia in Mice. *J. Pharmacol. Exp. Ther.* 359, 310–318. doi:10.1124/jpet.116.236182
- Dougherty, P.M., Cata, J.P., Cordella, J. V., Burton, A., Weng, H.R., 2004. Taxol-induced

- sensory disturbance is characterized by preferential impairment of myelinated fiber function in cancer patients. *Pain* 109, 132–142. doi:10.1016/j.pain.2004.01.021
- Dranitsaris G, Yu B, King J, Kaura S, and Zhang A (2015) Nab-paclitaxel, docetaxel, or solvent-based paclitaxel in metastatic breast cancer: A cost-utility analysis from a Chinese health care perspective. *Clin Outcomes Res* 7:249–256.
- Dranitsaris, G., Yu, B., King, J., Kaura, S., Zhang, A., 2015. Nab-paclitaxel, docetaxel, or solvent-based paclitaxel in metastatic breast cancer: A cost-utility analysis from a Chinese health care perspective. *Clin. Outcomes Res.* 7, 249–256. doi:10.2147/CEOR.S82194
- Echeverry, S., Shi, X.Q., Yang, M., Huang, H., Wu, Y., Lorenzo, L.E., Perez-Sanchez, J., Bonin, R.P., De Koninck, Y., Zhang, J., 2017. Spinal microglia are required for long-term maintenance of neuropathic pain. *Pain* 158, 1792–1801. doi:10.1097/j.pain.0000000000000982
- Efimova EV, Mauceri HJ, Golden DW, Labay E, Bindokas VP, Darga TE, Chakraborty C, Barreto-Andrade JC, Crawley C, Sutton HG, Kron SJ, and Weichselbaum RR (2010) Poly(ADP-Ribose) polymerase inhibitor induces accelerated senescence in irradiated breast cancer cells and tumors. *Cancer Res* 70: 6277-6282.
- Emery SM, Alotaibi MR, Tao Q, Selley DE, Lichtman AH, and Gewirtz DA (2014) Combined antiproliferative effects of the aminoalkylindole WIN55,212-2 and radiation in breast cancer cells. *J Pharm Exp Ther* 348: 293-302.
- Ewertz, M., Qvortrup, C., Eckhoff, L., 2015. Chemotherapy-induced peripheral neuropathy in patients treated with taxanes and platinum derivatives. *Acta Oncol. (Madr).* 54, 587–591. doi:10.3109/0284186X.2014.995775
- Ferrea S and Winterer C (2009) Neuroprotective and neurotoxic effects of nicotine.

Pharmacopsychiatry **42**:255–265.

Ferrier, J., Pereira, V., Busserolles, J., Authier, N., Balayssac, D., 2013. Emerging Trends in Understanding Chemotherapy-Induced Peripheral Neuropathy. *Curr. Pain Headache Rep.* 17, 364. doi:10.1007/s11916-013-0364-5

Fertig, J.B., Pomerleau, O.F., Sanders, B., 1986. Nicotine-produced antinociception in minimally deprived smokers and ex-smokers. *Addict. Behav.* 11, 239–248. doi:10.1016/0306-4603(86)90052-3

Fillington, R.B., King, C.D., Ribeiro-Dasilva, M.C., Rahim-Williams, B., Riley, J.L., 2009. Sex, Gender, and Pain: A Review of Recent Clinical and Experimental Findings. *J. Pain* 10, 447–485. doi:10.1016/j.jpain.2008.12.001

Flood P and Damaj MI (2014) Nicotine is out: Nicotinic agonists may have utility as analgesics. *Anesth Analg* **119**:232–233.

Fornasari, D., 2012. Pain mechanisms in patients with chronic pain. *Clin. Drug Investig.* 32, 45–52. doi:10.2165/11630070-0000000000-00000

Freitas K, Ghosh S, Ivy Carroll F, Lichtman AH, and Imad Damaj M (2013) Effects of alpha 7 positive allosteric modulators in murine inflammatory and chronic neuropathic pain models. *Neuropharmacology* **65**:156–164.

Freitas, K., Carroll, F.I., Damaj, M.I., 2013. The antinociceptive effects of nicotinic receptors α 7-positive allosteric modulators in murine acute and tonic pain models. *J. Pharmacol. Exp. Ther.* 344, 264–75. doi:10.1124/jpet.112.197871

Freitas, K., Negus, S., Carroll, F.I., Damaj, M.I., 2013. In vivo pharmacological interactions between a type II positive allosteric modulator of α 7 nicotinic ACh receptors and nicotinic agonists in a murine tonic pain model. *Br. J. Pharmacol.* 169, 567–579. doi:10.1111/j.1476-

- Gangloff, A., Hsueh, W.-A., Kesner, A.L., Kiesewetter, D.O., Pio, B.S., Pegram, M.D., Beryt, M., Townsend, A., Czernin, J., Phelps, M.E., Silverman, D.H.S., 2005. Estimation of paclitaxel biodistribution and uptake in human-derived xenografts in vivo with (18)F-fluoropaclitaxel. *J. Nucl. Med.* 46, 1866–1871. doi:46/11/1866 [pii]
- Grabus, S.D., Carroll, F.I., Damaj, M.I., 2012. Bupropion and its main metabolite reverse nicotine chronic tolerance in the mouse. *Nicotine Tob. Res.* 14, 1356–1361. doi:10.1093/ntr/nts088
- Grabus, S.D., Martin, B.R., Brown, S.E., Damaj, M.I., 2006. Nicotine place preference in the mouse: Influences of prior handling, dose and strain and attenuation by nicotinic receptor antagonists. *Psychopharmacology (Berl)*. 184, 456–463. doi:10.1007/s00213-006-0305-7
- Grando SA (2014) Connections of nicotine to cancer. *Nat Rev Cancer* **14**:419–429.
- Gu, N., Peng, J., Murugan, M., Wang, X., Eyo, U.B., Sun, D., Ren, Y., DiCicco-Bloom, E., Young, W., Dong, H., Wu, L.J., 2016. Spinal Microgliosis Due to Resident Microglial Proliferation Is Required for Pain Hypersensitivity after Peripheral Nerve Injury. *Cell Rep.* 16, 605–614. doi:10.1016/j.celrep.2016.06.018
- Gruener, H., Zeilig, G., Laufer, Y., Nava Blumen, ●, Defrin, R., 2018. Increased psychological distress among individuals with spinal cord injury is associated with central neuropathic pain rather than the injury characteristics. *Spinal Cord* 56, 176–184. doi:10.1038/s41393-017-0014-6
- Gustorff, B., Dorner, T., Likar, R., Grisold, W., Lawrence, K., Schwarz, F., Rieder, A., 2008. Prevalence of self-reported neuropathic pain and impact on quality of life: A prospective

- representative survey. *Acta Anaesthesiol. Scand.* 52, 132–136. doi:10.1111/j.1399-6576.2007.01486.x
- Habib AS, White WD, El Gasim MA, Saleh G, Polascik TJ, Moul JW, and Gan TJ (2008) Transdermal Nicotine for Analgesia after Radical Retropubic Prostatectomy. *Anesth Analg* **107**:999–1004.
- Hagiwara, H., Sunada, Y., 2004. Mechanism of taxane neurotoxicity. *Breast Cancer* 11, 82–85. doi:10.1007/BF02968008
- Hama A and Takamatsu H (2016) Chemotherapy-Induced Peripheral Neuropathic Pain and Rodent Models. *CNS Neurol Disord Drug Targets* **15**: 7–19.
- Heeschen C, Jang JJ, Weis M, Pathak A, Kaji S, Hu RS, Tsao PS, Johnson FL, and Cooke JP (2001) Nicotine stimulates angiogenesis and promotes tumor growth and atherosclerosis. *Nat Med* **7**:833–839.
- Hershman DL, Lacchetti C, Dworkin RH, Lavoie Smith EM, Bleeker J, Cavaletti G, Chauhan C, Gavin P, Lavino A, Lustberg MB, Paice J, Schneider B, Smith M Lou, Smith T, Terstriep S, Wagner-Johnston N, Bak K, and Loprinzi CL (2014) Prevention and management of chemotherapy-induced peripheral neuropathy in survivors of adult cancers: American Society of Clinical Oncology clinical practice guideline. *J Clin Oncol* **32**:1941–1967.
- Improgo MR, Soll LG, Tapper AR, and Gardner PD (2013) Nicotinic acetylcholine receptors mediate lung cancer growth. *Front Physiol* **4** (doi: 10.3389/fphys.2013.00251).
- Iskandar AR, Liu C, Smith DE, Hu K, Choi S, Ausman LM, and Wang X (2012) β -Cryptoxanthin restores nicotine-reduced lung SIRT1 to normal levels and inhibits nicotine-promoted lung tumorigenesis and emphysema in A/J mice. *Cancer Prev Res* **6**: 309-320.
- Jackson, A., Bagdas, D., Muldoon, P.P., Lichtman, A.H., Carroll, F.I., Greenwald, M., Miles,

- M.F., Damaj, M.I., 2017. In vivo interactions between $\alpha 7$ nicotinic acetylcholine receptor and nuclear peroxisome proliferator-activated receptor- α : Implication for nicotine dependence. *Neuropharmacology* 118, 38–45. doi:10.1016/j.neuropharm.2017.03.005
- Jarzynka MJ, Gou P, Bar-Joseph I, Hu B, and Cheng SY (2006) Estradiol and nicotine exposure enhances A549 bronchioloalveolar carcinoma xenograft growth in mice through the stimulation of angiogenesis. *Int J Oncol* **28**:337–344.
- Jin Z, Gao F, Flagg T, and Deng X (2004) Nicotine induces multi-site phosphorylation of Bad in association with suppression of apoptosis. *J Biol Chem* **279**:23837–23844.
- Jones KR, Elmore LW, Jackson-Cook C, Demasters G, Povirk LF, Holt SE, and Gewirtz DA (2005) p53-Dependent accelerated senescence induced by ionizing radiation in breast tumor cells. *Int J Radiat Biol* **81**: 445-458.
- Jordan, M.A., Wilson, L., 2004. Microtubules as a target for anticancer drugs. *Nat. Rev. Cancer* 4, 253–265. doi:10.1038/nr1317
- Kellar A, Egan C, and Morris D (2014) Preclinical murine models for lung cancer: clinical trial applications. *Biomed Res Int* **2015**: 621324.
- Kemper, E.M., Van Zandbergen, A.E., Cleypool, C., Mos, H.A., Boogerd, W., Beijnen, J.H., Van Tellingen, O., 2003. Increased penetration of paclitaxel into the brain by inhibition of P-glycoprotein. *Clin. Cancer Res.* 9, 2849–2855.
- Kilkenny, C., Browne, W., Cuthill, I.C., Emerson, M., Altman, D.G., 2010. Animal research: reporting in vivo experiments: the ARRIVE guidelines. *Br. J. Pharmacol.* 160, 1577–1579.
- Kim JH, Dougherty PM, and Abdi S (2015) Basic science and clinical management of painful and non-painful chemotherapy-related neuropathy. *Gynecol Oncol* **136**:453–459.

- Ko, M., Hu, M., Hsieh, Y., Lan, C., Tseng, T., 2014. Neuropeptides Peptidergic intraepidermal nerve fibers in the skin contribute to the neuropathic pain in paclitaxel-induced peripheral neuropathy. *Neuropeptides* 48, 109–117. doi:10.1016/j.npep.2014.02.001
- Krukowski K, Nijboer CH, Huo X, Kavelaars A, and Heijnen CJ (2015) Prevention of chemotherapy-induced peripheral neuropathy by the small-molecule inhibitor pifithrin-[mu]. *Pain* **156**:2184–2192.
- Krukowski, K., Ma, J., Golonzhka, O., Laumet, G.O., Gutti, T., van Duzer, J.H., Mazitschek, R., Jarpe, M.B., Heijnen, C.J., Kavelaars, A., 2017. HDAC6 inhibition effectively reverses chemotherapy-induced peripheral neuropathy. *Pain* 158, 1126–1137. doi:10.1097/j.pain.0000000000000893
- La Porta, C., Lara-Mayorga, I.M., Negrete, R., Maldonado, R., 2016. Effects of pregabalin on the nociceptive, emotional and cognitive manifestations of neuropathic pain in mice. *Eur. J. Pain* (United Kingdom) 1–13. doi:10.1002/ejp.868
- Legakis, L.P., Negus, S.S., 2018. Repeated Morphine Produces Sensitization to Reward and Tolerance to Antiallodynia in Male and Female Rats with Chemotherapy-Induced Neuropathy. *J. Pharmacol. Exp. Ther.* 365, 9–19. doi:10.1124/jpet.117.246215
- Lin, X., Dhopeswarkar, A.S., Huibregtse, M., Mackie, K., Hohmann, A.G., 2018. Slowly Signaling G Protein – Biased CB 2 Cannabinoid Receptor Agonist LY2828360 Suppresses Neuropathic Pain with Sustained Efficacy and Attenuates Morphine Tolerance and Dependence s. *Mol Pharmacol* 93, 49–62. doi:10.1124/mol.117.109355
- Little RJA, and Rubin DB (1987) Statistical analysis with missing data. New York: Wiley.

- Liu W, Yi D, Guo J, Xiang Z, Deng L, and He L (2015) Nuciferine, extracted from *Nelumbo nucifera Gaertn*, inhibits tumor-promoting effect of nicotine involving Wnt/ β -catenin signaling in non-small cell lung cancer. *J Ethnopharmacol* **165**: 83-93.
- Maier CR, Hollander MC, Hobbs EA, Dogan I, Dennis PA (2011) Nicotine does not enhance tumorigenesis in mutant K-Ras-driven mouse models of lung cancer. *Cancer Prev Res (Phila)* **4**:1743-1751.
- Majithia N, Temkin SM, Ruddy KJ, Beutler AS, Hershman DL, and Loprinzi CL (2016) National Cancer Institute-supported chemotherapy-induced peripheral neuropathy trials: outcomes and lessons. *Support Care Cancer* **24**:1439–1447.
- Makker, P.G.S., Duffy, S.S., Lees, J.G., Perera, C.J., Tonkin, R.S., Butovsky, O., Park, S.B., Goldstein, D., Moalem-Taylor, G., 2017. Characterisation of immune and neuroinflammatory changes associated with chemotherapy-induced peripheral neuropathy. *PLoS One* 12, e0170814. doi:10.1371/journal.pone.0170814
- Markman, M., Elson, P., Kulp, B., Peterson, G., Zanotti, K., Webster, K., Belinson, J., 2003. Carboplatin plus paclitaxel combination chemotherapy: Impact of sequence of drug administration on treatment-induced neutropenia. *Gynecol. Oncol.* 91, 118–122. doi:10.1016/S0090-8258(03)00517-1
- Massie, M.J., 2004. Prevalence of depression in patients with cancer. *J. Natl. Cancer Inst. Monogr.* 10021, 57–71. doi:10.1093/jncimonographs/lgh014
- Mattes MJ (2007) Apoptosis assays with lymphoma cell lines: problems and pitfalls. *Br J Cancer* **96**: 928-936.
- Mcmahon, S.B., La Russa, F., Bennett, D.L.H., 2015. Crosstalk between the nociceptive and immune systems in host defence and disease. *Nat. Rev. Neurosci.* 16, 389–402.

doi:10.1038/nrn3946

McWhinney, S.R., Goldberg, R.M., McLeod, H.L., 2009. Platinum neurotoxicity pharmacogenetics. *Mol. Cancer Ther.*, 8, 10–16.

Mehnert, A., Brähler, E., Faller, H., Härter, M., Keller, M., Schulz, H., Wegscheider, K., Weis, J., Boehncke, A., Hund, B., Reuter, K., Richard, M., Sehner, S., Sommerfeldt, S., Szalai, C., Wittchen, H.U., Koch, U., 2014. Four-week prevalence of mental disorders in patients with cancer across major tumor entities. *J. Clin. Oncol.* 32, 3540–3546. doi:10.1200/JCO.2014.56.0086

Murphy SE, von Weymarn LB, Schutten MM, Kassie F, Modiano JF (2011) Chronic nicotine consumption does not influence 4-(methylnitrosamino)-1-(3-pyridyl)-1-butanone induced lung tumorigenesis. *Cancer Prev Res (Phila)*. **4**:1752-1760.

Murray RP, Connett JE, and Zapawa LM (2009) Does nicotine replacement therapy cause cancer? Evidence from the Lung Health Study. *Nicotine Tob Res* **11**:1076–1082.

Naji-Esfahani, H., Vaseghi, G., Safaeian, L., Pilehvarian, A.A., Abed, A., Rafieian-Kopaei, M., 2015. Gender differences in a mouse model of chemotherapy-induced neuropathic pain. *Lab Anim*. doi:10.1177/0023677215575863

Neelakantan H, Ward SJ, and Walker EA (2016) Effects of paclitaxel on mechanical sensitivity and morphine reward in male and female C57Bl6 mice. *Exp Clin Psychopharmacol* **24**:485–495.

Negus, S.S., Neddenriep, B., Altarifi, A.A., Carroll, F.I., Leidl, M.D., Miller, L.L., 2015. Effects of ketoprofen, morphine, and kappa opioids on pain-related depression of nesting in mice. *Pain* 156, 1153–1160. doi:10.1097/j.pain.000000000000171

- Neijt, J.P., Engelholm, S.A., Tuxen, M.K., Sørensen, P.G., Hansen, M., Sessa, C., De Swart, C.A.M., Hirsch, F.R., Lund, B., Van Houwelingen, H.C., 2000. Exploratory phase III study of paclitaxel and cisplatin versus paclitaxel and carboplatin in advanced ovarian cancer. *J. Clin. Oncol.* 18, 3084–3092.
- Navratilova, E., Morimura, K., Xie, J.Y., Atcherley, C.W., Ossipov, M.H., Porreca, F., 2016. Positive emotions and brain reward circuits in chronic pain. *J. Comp. Neurol.* 524, 1646–1652. doi:10.1002/cne.23968
- Nieto, F.R., Entrena, J.M., Cendan, C.M., Pozo, E. Del, Vela, J.M., Baeyens, J.M., 2008. Tetrodotoxin inhibits the development and expression of neuropathic pain induced by paclitaxel in mice. *Pain* 137, 520–531. doi:10.1016/j.pain.2007.10.012
- Otrubova, K., Brown, M., McCormick, M.S., Han, G.W., O’Neal, S.T., Cravatt, B.F., Stevens, R.C., Lichtman, A.H., Boger, D.L., 2013. Rational design of fatty acid amide hydrolase inhibitors that act by covalently bonding to two active site residues. *J. Am. Chem. Soc.* 135, 6289–6299. doi:10.1021/ja4014997
- Pacini, A., Di Cesare Mannelli, L., Bonaccini, L., Ronzoni, S., Bartolini, A., Ghelardini, C., 2010. Protective effect of alpha7 nAChR: Behavioural and morphological features on neuropathy. *Pain* 150, 542–549. doi:10.1016/j.pain.2010.06.014
- Pavlov, V.A., Tracey, K.J., 2005. The cholinergic anti-inflammatory pathway. *Brain. Behav. Immun.* 19, 493–499. doi:S0889-1591(05)00066-8 [pii]10.1016/j.bbi.2005.03.015
- Pavlov, V. a, Tracey, K.J., 2006. Controlling inflammation: the cholinergic anti-inflammatory pathway. *Biochem. Soc. Trans.* 34, 1037–1040. doi:10.1042/BST0341037
- Pillai S, Rizwani W, Li X, Rawal B, Nair S, Schell MJ, Bepler G, Haura E, Coppolar D, and Chellappan S (2011) ID1 facilitates the growth and metastasis of non-small cell lung cancer

- in response to nicotinic acetylcholine receptor and epidermal growth factor receptor signaling. *Mol Cell Biol* **31**: 3052-3067.
- Puliyappadamba VT, Cheriyan VT, Thulasidasan AKT, Bava S V, Vinod BS, Prabhu PR, Varghese R, Bevin A, Venugopal S, and Anto RJ (2010) Nicotine-induced survival signaling in lung cancer cells is dependent on their p53 status while its down-regulation by curcumin is independent. *Mol Cancer* **9**:220.
- Pyter, L.M., Pineros, V., Galang, J.A., McClintock, M.K., Prendergast, B.J., 2009. Peripheral tumors induce depressive-like behaviors and cytokine production and alter hypothalamic-pituitary-adrenal axis regulation. *Proc. Natl. Acad. Sci. U. S. A.* 106, 9069–74. doi:10.1073/pnas.0811949106
- Reagan-Shaw, S., Nihal, M., Ahmad, N., 2008. Dose translation from animal to human studies revisited. *FASEB J.* 22, 659–661. doi:10.1096/fj.07-9574LSF
- Richardson EJ, Ness TJ, Redden DT, Stewart CC, and Richards JS (2012) Effects of nicotine on spinal cord injury pain vary among subtypes of pain and smoking status: Results from a randomized, controlled experiment. *J Pain* **13**:1206–1214.
- Richner, M., Jager, S.B., Siupka, P., Vaegter, C.B., 2017. Hydraulic Extrusion of the Spinal Cord and Isolation of Dorsal Root Ganglia in Rodents. *J. Vis. Exp.* 1–6. doi:10.3791/55226
- Roberson RS, Kussick SJ, Vallieres E, Chen SY, and Wu DY (2005) Escape from therapy-induced accelerated cellular senescence in p53-null lung cancer cells and in human lung cancers. *Cancer Res* **65**: 2795-2803.
- Rock, M.L., Karas, A.Z., Rodriguez, K.B.G., Gallo, M.S., Pritchett-Corning, K., Karas, R.H., Aronovitz, M., Gaskill, B.N., 2014. The time-to-integrate-to-nest test as an indicator of wellbeing in laboratory mice. *J. Am. Assoc. Lab. Anim. Sci.* 53, 24–8.

- Romero HK, Christensen SB, Di Cesare Mannelli L, Gajewiak J, Ramachandra R, Elmslie KS, Vetter DE, Ghelardini C, Iadonato SP, Mercado JL, Olivera BM, and McIntosh JM (2017) Inhibition of $\alpha 9\alpha 10$ nicotinic acetylcholine receptors prevents chemotherapy-induced neuropathic pain. *Proc Natl Acad Sci USA* **114**: E1825-E1832.
- Rowbotham MC, Rachel Duan W, Thomas J, Nothaft W, and Backonja MM (2009) A randomized, double-blind, placebo-controlled trial evaluating the efficacy and safety of ABT-594 in patients with diabetic peripheral neuropathic pain. *Pain* **146**:245–252.
- Rowley TJ, Payappilly J, Lu J, and Flood P (2008) The Antinociceptive Response to Nicotinic Agonists in a Mouse Model of Postoperative Pain. *Anesth Analg* **107**:3–8.
- Salter, M.W., Stevens, B., 2017. Microglia emerge as central players in brain disease. *Nat. Med.* **23**, 1018–1027. doi:10.1038/nm.4397
- Schaal C and Chellappan SP (2014) Nicotine-mediated cell proliferation and tumor progression in smoking related cancers. *Mol Cancer Res* **12**:14–23.
- Scholz, J., Woolf, C.J., 2007. The neuropathic pain triad: neurons, immune cells and glia. *Nat. Neurosci.* **10**, 1361–1368. doi:10.1038/nn1992
- Seidman, A.D., Berry, D., Cirrincione, C., Harris, L., Muss, H., Marcom, P.K., Gipson, G., Burstein, H., Lake, D., Shapiro, C.L., Ungaro, P., Norton, L., Winer, E., Hudis, C., 2008. Randomized phase III trial of weekly compared with every-3-weeks paclitaxel for metastatic breast cancer, with trastuzumab for all HER-2 overexpressors and random assignment to trastuzumab or not in HER-2 nonoverexpressors: final results of Cancer and Leukemia Group B protocol 9840. *J. Clin. Oncol.* **26**, 1642–1649. doi:10.1200/JCO.2007.11.6699
- Seretny M, Currie GL, Sena ES, Ramnarine S, Grant R, Macleod MR, Colvin LA, and Fallon M (2014) Incidence, prevalence, and predictors of chemotherapy-induced peripheral

- neuropathy: A systematic review and meta-analysis. *Pain* **155**:2461–2470.
- Seretny, M., Currie, G.L., Sena, E.S., Ramnarine, S., Grant, R., Macleod, M.R., Colvin, L.A., Fallon, M., 2014. Incidence, prevalence, and predictors of chemotherapy-induced peripheral neuropathy: A systematic review and meta-analysis. *Pain* **155**, 2461–2470. doi:10.1016/j.pain.2014.09.020
- Slivicki RA, Ali YO, Lu H, and Hohmann AG (2016) Impact of Genetic Reduction of NMNAT2 on Chemotherapy-Induced Losses in Cell Viability In Vitro and Peripheral Neuropathy In Vivo. *PLoS One* **11**: 1–15. doi: 10.1371/journal.pone.0147620.
- Slivicki, R.A., Ali, Y.O., Lu, H.-C., Hohmann, A.G., 2016. Impact of genetic reduction of NMNAT2 on chemotherapy-induced losses in cell viability in vitro and peripheral neuropathy in vivo. *PLoS One* **11**, e0147620. doi:10.1371/journal.pone.0147620
- So, W.K.W., Marsh, G., Ling, W.M., Leung, F.Y., Lo, J.C.K., Yeung, M., Li, G.K.H., 2009. The symptom cluster of fatigue, pain, anxiety, and depression and the effect on the quality of life of women receiving treatment for breast cancer: a multicenter study. *Oncol. Nurs. Forum* **36**, E205–14. doi:10.1188/09.ONF.E205-E214
- St-Pierre S, Jiang W, Roy P, Champigny C, LeBlanc É, Morley BJ, Hao J, and Simard AR (2016) Nicotinic acetylcholine receptors modulate bone marrow-derived pro-inflammatory monocyte production and survival. *PLoS One* **11**:1–18.
- Sun, R., Zhang, W., Bo, J., Zhang, Z., Lei, Y., Huo, W., Liu, Y., Ma, Z., Gu, X., 2016. Spinal activation of alpha7-nicotinic acetylcholine receptor attenuates posttraumatic stress disorder-related chronic pain via suppression of glial activation. *Neuroscience* **344**, 243–254. doi:10.1016/j.neuroscience.2016.12.029
- Tate EH, Wilder ME, Cram WL, Wharton W (1983) A method for staining 3T3 cell nuclei with

- propidium iodide in hypotonic solution. *Cytometry* **4**: 211-215.
- Thompson, R.D., Grant, C. V, 1971. Automated preference testing apparatus for rating palatability of foods. *J. Exp. Anal. Behav.* 15, 215–220. doi:10.1901/jeab.1971.15-215
- Toma W, Kyte SL, Bagdas D, Alkhlaif Y, Alsharari SD, Lichtman AH, Chen Z, Del Fabbro E, Bigbee JW, Gewirtz DA, Damaj MI (2017) Effects of paclitaxel on the development of neuropathy and affective behaviors in the mouse. *Neuropharmacol* **117**: 305-315.
- Tracey, K.J., 2002. The inflammatory reflex -. *Nature* 420, 835–859. doi:10.1111/j.1365-2796.2004.01440.x
- Tsurutani J, Castillo SS, Brognard J, Granville CA, Zhang C, Gills JJ, Sayyah J, and Dennis PA (2005) Tobacco components stimulate Akt-dependent proliferation and NF- κ B-dependent survival in lung cancer cells. *Carcinogenesis* **26**:1182–1195.
- Turcott, J.G., Juarez-Hernandez, E., De la Torre-Vallejo, M., Sanchez-Lara, K., Luvian-Morales, J., Arrieta, O., 2016. Value: Changes in the detection and recognition thresholds of three basic tastes in lung cancer patients receiving cisplatin and paclitaxel and its association with nutritional and quality of life parameters. *Nutr. Cancer* 68, 241–249. doi:10.1080/01635581.2016.1144075
- Umana, I.C., Daniele, C.A., Miller, B.A., Gallagher, K., Brown, M.A., 2017. Nicotinic Modulation of Descending Pain Control Circuitry. *Pain* 158, 1938–1950.
- Vichaya, E.G., Chiu, G.S., Krukowski, K., Lacourt, T.E., Kavelaars, A., Dantzer, R., Heijnen, C.J., Walker, A.K., 2015. Mechanisms of chemotherapy-induced behavioral toxicities. 9, 1–17. doi:10.3389/fnins.2015.00131
- Ward, S.J., Ramirez, M.D., Neelakantan, H., Walker, E.A., 2011. Cannabidiol prevents the development of cold and mechanical allodynia in paclitaxel-treated female c57bl6 mice.

Anesth. Analg. 113, 947–950. doi:10.1213/ANE.0b013e3182283486

Warren GW, Romano MA, Kudrimoti MR, Randall ME, McGarry RC, Singh AK, and Rangnekar VM (2012) Nicotinic modulation of therapeutic response *in vitro* and *in vivo*. *Int J Cancer* **131**:2519–2527.

Webster MR, Xu M, Kinzler KA, Kaur A, Appleton J, O’Connell MP, Marchbank K, Valiga A, Dang VM, Perego M, Zhang G, Slipicevic A, Keeney F, Lehrmann E, Wood W 3rd, Becker KG, Kossenkova AV, Frederick DT, Flaherty KT, Xu X, Herlyn M, Murphy ME, and Weeraratna AT (2015) Wnt5A promotes an adaptive, senescent-like stress response, while continuing to drive invasion in melanoma cells. *Pigment Cell Melanoma Res* **28**: 184-195.

Wilkerson, J.L., Ghosh, S., Bagdas, D., Mason, B.L., Crowe, M.S., Hsu, K.L., Wise, L.E., Kinsey, S.G., Damaj, M.I., Cravatt, B.F., Lichtman, A.H., 2016. Diacylglycerol lipase β inhibition reverses nociceptive behaviour in mouse models of inflammatory and neuropathic pain. *Br. J. Pharmacol.* 173, 1678–1692. doi:10.1111/bph.13469

Wozniak, K.M., Vornov, J.J., Wu, Y., Nomoto, K., Littlefield, B.A., DesJardins, C., Yu, Y., Lai, G., Reyderman, L., Wong, N., Slusher, B.S., 2016. Sustained accumulation of microtubule-binding chemotherapy drugs in the peripheral nervous system: correlations with time course and neurotoxic severity. *Cancer Res.* 76, 3332–3339. doi:10.1158/0008-5472.CAN-15-2525

Wu S, Lv Y, Lin B, Luo L, Lv S, Bi A, and Jia Y (2013) Silencing of periostin inhibits nicotine-mediated tumor cell growth and epithelial-mesenchymal transition in lung cancer cells. *Mol Med Rep* **7**: 875-880.

Yagoubian B, Akkara J, Afzali P, Alfi DM, Olson L, Conell-Price J, Yeh J, Eisig SB, and Flood P (2011) Nicotine Nasal Spray as an Adjuvant Analgesic for Third Molar Surgery. *J Oral Maxillofac Surg* **69**:1316–1319.

- Yalcin, I., Bohren, Y., Waltisperger, E., Sage-Ciocca, D., Yin, J.C., Freund-Mercier, M.J., Barrot, M., 2011. A time-dependent history of mood disorders in a murine model of neuropathic pain. *Biol. Psychiatry* 70, 946–953. doi:10.1016/j.biopsych.2011.07.017
- Yoo SS, Lee SM, Do SK, Lee WK, Kim DS, and Park JY (2014) Unmethylation of the *CHRNA4* gene is an unfavorable prognostic factor in non-small cell lung cancer. *Lung Cancer* **86**:85–90.
- Zhang J, Kamdar O, Le W, Rosen GD, and Upadhyay D (2009) Nicotine induces resistance to chemotherapy by modulating mitochondrial signaling in lung cancer. *Am J Respir Cell Mol Biol* **40**:135–146.
- Zheng, F.Y., Xiao, W.H., Bennett, G.J., 2011. The response of spinal microglia to chemotherapy-evoked painful peripheral neuropathies is distinct from that evoked by traumatic nerve injuries. *Neuroscience* 176, 447–454. doi:10.1016/j.neuroscience.2010.12.052

Vita

Wisam Botros Toma was born on November 8th, 1982, in Bartella, Mosul, Iraq, and is an Iraqi citizen. He graduated from the University of Mosul, Mosul, Iraq, in 2005 with a Doctor of Veterinary Medicine, from the College of Veterinary Medicine. He went on to receive a Master of Science degree in Veterinary Pharmacology and Toxicology from the same university in 2011. He worked as an instructor in the laboratory for pharmacology and toxicology classes at the University of Mosul from 2005-2013. He joined Dr. Damaj's lab in the Department of Pharmacology & Toxicology, in the School of Medicine, at Virginia Commonwealth University in spring 2014. Wisam's research in The Damaj Lab focuses on pain.

Curriculum Vitae

Wisam Botros Toma

1007 N Hamilton Street Apt A, Richmond, VA. 23321. USA

804-625-1169. tomawb@vcu.edu

Education

Virginia Commonwealth University (VCU), Richmond, VA, USA
Doctor of Philosophy Candidate, Pharmacology and Toxicology
2014 – Present
current GPA 3.5

University of Mosul, Mosul, Iraq
2009-2011
Master of Science in Veterinary Pharmacology and Toxicology

University of Mosul, Mosul, Iraq
2000-2005
Doctor of Veterinary Medicine

Relevant Coursework

Basic Concepts in Pharmacology, Principles of Pharmacology, Special Topics: Pain pharmacology, Biochemistry, Cell and Molecular Biology, Systems Neuroscience, and Scientific Writing and Grantsmanship.

Research Experience

Virginia Commonwealth University
Ph.D. Candidate in Dr. M. Imad Damaj's laboratory
2014 – Present

- Characterizing the chemotherapy Induced Peripheral Neuropathy (CIPN) in various nociceptive and affective pain – related behaviors in a mouse model.
- Testing candidate nicotinic analogues in several nociceptive related behaviors in mice
- Targeting the alpha7 Nicotinic Acetyl Choline Receptor as a potential strategy to mitigate CIPN in mouse model by using multiple approaches including behavioral, immunohistochemical, and ultrastructural changes.
- Training undergraduate students on different behavioral and immunohistochemical techniques.

Publications

Kyte, S.L., **Toma, W.**, Bagdas, D., Meade, J.A., Schurman, L.D., Lichtman, A.H., Chen, Z.-J., Del Fabbro, E., Fang, X., Bigbee, J.W., Damaj, M.I., Gewirtz, D.A., 2018. Nicotine prevents and reverses paclitaxel-induced mechanical allodynia in a mouse model of CIPN. *J. Pharmacol. Exp.*

Ther. 364. <https://doi.org/10.1124/jpet.117.243972>.

El Nebrisi EG, Bagdas D, **Toma W**, Al Samri H, Brodzik A, Alkhlaif Y, Yang KS, Howarth FC, Damaj IM, Oz M. 2018. Curcumin acts as a positive allosteric modulator of $\alpha 7$ -nicotinic acetylcholine receptors and reverses nociception in mouse models of inflammatory pain. *J. Pharmacol. Exp. Ther.* pii: jpet.117.245068. doi: 10.1124/jpet.117.245068.

Toma, W., Kyte, S.L., Bagdas, D., Alkhlaif, Y., Alsharari, S.D., Lichtman, A.H., Chen, Z.J., Del Fabbro, E., Bigbee, J.W., Gewirtz, D.A., Damaj, M.I., 2017. Effects of paclitaxel on the development of neuropathy and affective behaviors in the mouse. *Neuropharmacology* 117, 305–315. <https://doi.org/10.1016/j.neuropharm.2017.02.02>

Bagdas, D., Ergun, D., Jackson, A., **Toma, W.**, Schulte, M.K., Damaj, M.I., 2017. Allosteric modulation of $\alpha 4\beta 2^*$ nicotinic acetylcholine receptors: Desformylflustrabromine potentiates antiallodynic response of nicotine in a mouse model of neuropathic pain. *Eur. J. Pain* 1–10. <https://doi.org/10.1002/ejp.1092>.

Donvito, G., Bagdas, D., **Toma, W.**, Rahimpour, E., Jackson, A., Meade, J.A., AlSharari, S., Kulkarni, A.R., Ivy Carroll, F., Lichtman, A.H., Papke, R.L., Thakur, G.A., Imad Damaj, M., 2017. The interaction between $\alpha 7$ nicotinic acetylcholine receptor and nuclear peroxisome proliferator-activated receptor- γ represents a new antinociceptive signaling pathway in mice. *Exp. Neurol.* 295, 194–201. <https://doi.org/10.1016/j.expneurol.2017.06.014>.

Bagdas, D., Wilkerson, J.L., Kulkarni, A., **Toma, W.**, AlSharari, S., Gul, Z., Lichtman, A.H., Papke, R.L., Thakur, G.A., Damaj, M.I., 2016. The $\alpha 7$ nicotinic receptor dual allosteric agonist and positive allosteric modulator GAT107 reverses nociception in mouse models of inflammatory and neuropathic pain. *Br. J. Pharmacol.* <https://doi.org/10.1111/bph.13528>.

In Press:

Rachel Wodarski, Deniz Bagdas, Jason J. Parisb, Tim Pheby, **Wisam Toma**, Ruqiang Xud, M. Imad Damaj,

Pamela E. Knapp, Andrew S.C. Ric, Kurt F. Hauser. 2018. Reduced intraepidermal nerve fibre density, glial activation, and sensory changes in HIV type-1 Tat expressing female mice: involvement of Tat during early stages of HIV-associated painful sensory neuropathy. In press: *Pain Reports*

Submitted:

Marta Quadri, Deniz Bagdas, **Wisam Toma**, Clare Stokes, Roger. L. Papke, Nicole A. Horenstein, M. Imad Damaj. 2018. The antinociceptive and anti-inflammatory properties of the $\alpha 7$ nAChR silent agonist p-CF3 N,N-diethyl-N'-phenylpiperazine. Submitted to: *J. Pharmacol. Exp. Ther.*

Book Chapter

Deniz Bagdas*, S. Lauren Kyte, **Wisam Toma**, M. Sibel Gurun, M. Imad Damaj. 2018. "Targeting Nicotinic Acetylcholine Receptors for the Treatment of Pain" in: *The Neuroscience of Nicotine: Mechanisms and Treatment*. Academic Press, an imprint of Elsevier.

Presentations

Toma W, Kyte SL, Bagdas D, Julie Meade, Thakur, G, Bigbee, J, Gewirtz D, Damaj MI. The Modulatory Role of the $\alpha 7$ Nicotinic Acetylcholine Receptors (nAChRs) in a Mouse Model of Chemotherapy-Induced Peripheral Neuropathy (CIPN). Poster presented at: 34th Daniel T. Watts Research Poster Symposium; October 26, 2017. Virginia Commonwealth University, Richmond, Va.

Toma W, Kyte SL, Bagdas D, Julie Meade, Thakur, G, Bigbee, J, Gewirtz D, Damaj MI. The Modulatory Role of the $\alpha 7$ Nicotinic Acetylcholine Receptors (nAChRs) in a Mouse Model of Chemotherapy-Induced Peripheral Neuropathy (CIPN). Poster presented at: VCU Massey Cancer 2017 Cancer Research Retreat; June 16, 2017; Richmond, VA.

Toma W, Kyte SL, Bagdas D, Julie Meade, Bigbee, J, Gewirtz D, Damaj MI . Investigating the role of $\alpha 7$ Nicotinic Acetylcholine Receptors (nAChRs) as a potential target for the treatment of chemotherapy-induced peripheral neuropathy (CIPN). Poster presented at: VCU; Virginia Academy of Science 95th Annual Meeting; May 17-19, 2017. Richmond, VA.

Damaj MI, Alkhlaif Y, Bagdas D, **Toma W**, Meade JA, Kyte SL, Gewirtz D, and Selley DE. Role of Kappa Receptors in Chemotherapy-Induced Neuropathy and Emotional-like Deficit Behaviors in Mice. Poster presentation, The Fourth Conference on the "Therapeutic Potential of Kappa Opioids", 2017, Philadelphia, PA

Toma W, Kyte SL, Alkhlaif Y, Bagdas D, Lichtman A, Bigbee J, Gewirtz D, Damaj MI. Sensory and affective pain behaviors of paclitaxel in a mouse model of chemotherapy- induced peripheral neuropathy. Poster presented at: VCU Massey Cancer Center 2016 Cancer Research Retreat; June 17, 2016; Richmond, VA.

Kyte SL, **Toma W**, Damaj MI, Fang X, Gewirtz DA. Nicotine Prevents Chemotherapy-Induced Peripheral Neuropathy in vivo, and Fails to Stimulate the Growth of Lung Cancer Cells or Interfere with the Effectiveness of Chemotherapy in vitro. Poster presented at: Virginia Academy of Science 94th Annual Meeting; May 19, 2016; Fredericksburg, VA.

Kyte SL, **Toma W**, Damaj MI, Fang X, Gewirtz DA. Nicotine Prevents Chemotherapy-Induced Peripheral Neuropathy in vivo, and Fails to Stimulate the Growth of Lung Cancer Cells or Interfere with the Effectiveness of Chemotherapy in vitro. Poster presented at: AACR Annual Meeting 2016; April 19, 2016; New Orleans, LA.

Toma W, Kyte SL, Bagdas D, Gewirtz D, Damaj MI. Nicotinic acetyl choline receptors as a potential target in treatment of chemotherapy- induced peripheral neuropathy in a mouse model. Poster presented at: VCU Massey Cancer Center 2015 Cancer Research Retreat; May 22, 2015; Richmond, VA.

Kyte SL, **Toma W**, Damaj MI, Gewirtz DA. Nicotinic Acetylcholine Receptor Agonists Fail to Stimulate Growth of Non-Small Cell Lung Cancer Cells or Interfere with the Effectiveness of Chemotherapy. Poster presented at: VCU Massey Cancer Center 2015 Cancer Research Retreat; May 22, 2015; Richmond, VA.

Conferences

Toma W, Kyte SL, Bagdas D, Julie Meade, Thakur, G, Bigbee, J, Gewirtz D, Damaj MI. The $\alpha 7$ nicotinic acetylcholine receptors (nAChRs) Regulate the Development and Maintenance of Chemotherapy Induced Peripheral Neuropathy (CIPN) Induced by Paclitaxel in a Mouse Model. The 47th annual Society for Neuroscience (SFN). November 11-17, 2017. Washington, DC.

The 11th annual NIH pain consortium symposium: Advances in pain research innovative models and methods, May 31-June 1, 2016; Bethesda, MD.

Professional membership

Member, Virginia Academy of Science
2017-2018

Member, Society for Neuroscience
2017-2018

Member, Neuroscience Interest Group at VCU
2017-2018

Member, International Association for the Study of Pain (IASP)
2018

Awards

Best Student Presentation Award - Poster presentation. Virginia Academy of Science,
Richmond, Virginia. May 2017

Cancer Research Retreat Award - Poster presentation. Massey Cancer Center, Virginia
Commonwealth University, Richmond, Virginia.
June 2017

Volunteering Service

Linwood Holton Elementary School Science Fair Judge, February 18, 2016. Richmond, VA.

Computer Skills

Microsoft office Word, Excel, Power Point; GraphPad Prism, SPSS.